AN APPROACH FOR MODELLING SNOWCOVER ABLATION AND SNOWMELT RUNOFF IN COLD REGION ENVIRONMENTS

A Thesis Submitted to the
College of Graduate Studies and Research
in Partial Fulfilment of the Requirements
for the Degree of Doctor of Philosophy
in the Department of Geography and Planning
(Centre for Hydrology)
University of Saskatchewan
Saskatoon, Canada

by

PABLO FERNANDO DORNES

Permission to use

In preparing this thesis in partial fulfillment of the requirements for a Postgraduate degree from the University of Saskatchewan, I agree that the Library of this University may make it freely available for inspection. I further agree that permission for copying of this thesis in any manner, in whole or part, for scholarly purposes may be granted by the professor or professors who supervised my thesis work or, in their absence, by the Head of the Department or the Dean of the College in which my thesis work was done. It is understood that any copying, publication, or the use of this thesis or parts thereof, for financial gain shall not be allowed without my written permission. It is also understood that due recognition shall be given to me and the University of Saskatchewan in any scholarly use which may be made of any material in my thesis.

Requests for permission to copy or to make other use of material in this thesis in whole or part should be addressed to:

Head of the Department of Geography and Planning

University of Saskatchewan

Saskatoon, Saskatchewan S7N 5A5

ABSTRACT

Reliable hydrological model simulations are the result of numerous complex interactions among hydrological inputs, landscape properties, and initial conditions. Determination of the effects of these factors is one of the main challenges in hydrological modelling. This situation becomes even more difficult in cold regions due to the ungauged nature of subarctic and arctic environments.

This research work is an attempt to apply a new approach for modelling snowcover ablation and snowmelt runoff in complex subarctic environments with limited data while retaining integrity in the process representations. The modelling strategy is based on the incorporation of both detailed process understanding and inputs along with information gained from observations of basin-wide streamflow phenomenon; essentially a combination of deductive and inductive approaches. The study was conducted in the Wolf Creek Research Basin, Yukon Territory, using three models, a small-scale physically based hydrological model, a land surface scheme, and a land surface hydrological model. The spatial representation was based on previous research studies and observations, and was accomplished by incorporating landscape units, defined according to topography and vegetation, as the spatial model elements.

Comparisons between distributed and aggregated modelling approaches showed that simulations incorporating distributed initial snowcover and corrected solar radiation were able to properly simulate snowcover ablation and snowmelt runoff whereas the aggregated modelling approaches were unable to represent the differential snowmelt rates and complex snowmelt runoff dynamics. Similarly, the inclusion of spatially distributed information in a land surface scheme clearly improved simulations of snowcover ablation. Application of the same modelling approach at a larger scale using the same landscape based parameterisation showed satisfactory results in simulating snowcover ablation and snowmelt runoff with minimal calibration. Verification of this approach in an arctic basin illustrated that landscape based parameters are a feasible regionalisation framework for distributed and physically based models. In summary, the proposed modelling philosophy, based on the combination of an inductive and deductive

reasoning, is a suitable strategy for reliable predictions of snowcover ablation and snowmelt runoff in cold regions and complex environments.

ACKNOWLEDGMENTS

In assembling this thesis I received invaluable assistance from several persons, but Dr. Alain Pietroniro and Dr. John Pomeroy my supervisors, deserve special mention for their guidance, support and encouragement throughout this project. Special gratitude is owned to my graduate advisory committee members, Dr. Dirk de Boer, Dr. Philip Marsh, Dr. Bing Si, and Dr. Lawrence Martz, and the external examiner Dr. David Tarboton, for their constructive criticisms, comments and suggestions.

For providing hospitality, friendship, information and sage advice, I am grateful to Rick Janowicz, Glenn Ford, and Glenn Carpenter of Yukon Environment.

I am indebted to the staff of the National Hydrology Research Centre of Saskatoon, and especially to Bruce Davison for his ongoing help, and to Brenda Toth, Newell Hedstrom, Dell Bayne, Raoul Granger, Jessika Töyrä, Jan Mydynski, and Kelly Best. I am thankful to Tom Brown from the Centre for Hydrology, University of Saskatchewan, for his invaluable and continuous help. Special thanks also to Bryan Tolson, Frank Seglenieks, Ric Soulis, and Nick Kouwen from University of Waterloo, to Diana Verseghy from Environment Canada, to Sean Carey from Carleton University, and to William Quinton from Wilfrid Laurier University.

I would also like to thank to all my friends and fellow graduate students who provided continuous support and encouragement.

I would also like to gratefully acknowledge the sources of funding I received in support of this research. In particular, Environment Canada, Canadian Foundation for Climate and Atmospheric Sciences, Research Council of Canada, Canada Research Chairs, and International Polar Year (IPY).

Finally, I wish to express my gratitude to my family for enduring years of erratic schedules and never ending tasks. Without their love and unrelenting support the completion of this thesis would not have been possible.

TABLE OF CONTENTS

LIST OF TABLES

LIST OF FIGURES

LIST OF SYMBOLS

B	Thermal capacity of snow or fraction of ice in unit mass of wet snow
C	Infiltration coefficient
C	Cloudiness index
D_d	Drainage density [km^{-1}]
d_e	Average effective depth at the stream edge [m]
DNR	Drainage index used to simulate soil drainage.
D_{100}	Minimum snow depth with a 100% of snow covered area
dT/dz	Rate of change of soil temperature with depth [°C]
dU/dt	Rate of change of internal energy of a snowcover with time [$W \cdot m^{-2}$]
$d\psi/dz$	Rate of change of suction head (matrix potential) with depth
E	Nash-Sutcliffe efficiency coefficient
e_a	Air vapour pressure [mbar]
H	Depth of the first soil layer [L]
INF	Cumulative snowmelt infiltration [mm]
K	Storage constant
K_h	Hydraulic conductivity [$cm \cdot d^{-1}$]
K_{ext}	Extraterrestrial solar radiation
K_{dif}	Calculated diffusive short-wave radiation
K_{dir}	Calculated incoming short-wave radiation
K_{ssr}	Horizontal soil leakage [$mm \cdot T^{-1}$]
K_{s0}	Horizontal saturated hydraulic conductivity at the surface
K_{theo}	Theoretical incoming clear sky short-wave radiation
$K\downarrow$	Observed incoming short-wave radiation [$W \cdot m^{-2}$]
K^*	Net short-wave radiation to snow [$W \cdot m^{-2}$]
L	Typical length of model grid [L]
LAI	Leaf area index
L_V	Stream length of model grid [L]
$L\downarrow$	Incoming long-wave radiation [$W \cdot m^{-2}$]
L^*	Net long-wave to snow [$W \cdot m^{-2}$]
M	Snowmelt depth [$cm \cdot d^{-1}$] or [$mm \cdot d^{-1}$]
MF	Melt factor or rate of melt per degree unit time [$mm \cdot °C^{-1} \cdot hr^{-1}$]
N	Maximum number of hours of sunshine in the day
n_s	Number of hours of sunshine in the day
N	Manning's roughness coefficient
P	Precipitation flux [$kg \cdot m^{-2} \cdot s^{-1}$]
P_{atm}	Atmospheric pressure [mb]

PAI	Ratio between total plant surface area and surface area
P_{snow}	Snowfall [mm]
P_{rain}	Rainfall [mm]
P_0	Atmospheric pressure at sea level (1013.25 hPa)
Q	Streamflow [$m^{-3} \cdot s^{-1}$]
Q_D	Vertical advection to snow from rain [$W \cdot m^{-2}$]
Q_E	Turbulent flux of latent heat to/from snow [$W \cdot m^{-2}$]
Q_G	Ground heat flux to from snow [$W \cdot m^{-2}$]
Q_H	Turbulent flux of sensible heat to snow [$W \cdot m^{-2}$]
Q_M	Energy available for the melting of snow [$W \cdot m^{-2}$] or [$kJ \cdot m^{-2} \cdot d^{-1}$]
Q_N	Net all-wave radiation over ground and snow [$W \cdot m^{-2}$]
Q_0	Daily clear sky short-wave radiation [$W \cdot m^{-2}$] or [$kJ \cdot m^{-2} \cdot d^{-1}$]
q_{int}	Interflow [$L^3 \cdot T^{-1}$]
q_{over}	Overland flow [$L^3 \cdot T^{-1}$]
q_s	Saturated interflow [$L^3 \cdot T^{-1}$]
q_u	Unsaturated interflow [$L^3 \cdot T^{-1}$]
$RMSE$	Root Mean Square Error
R_{ssr}	Recharge drainage factor [$mm \cdot T^{-1}$]
S	Saturation of first soil layer controlling interflow [$L^3 \cdot L^{-3}$]
SCA	Snow covered area
SH	Specific humidity [$g \cdot g^{-1}$]
S_I	Average soil saturation (water +ice) of 0-40 cm of soil [$mm^{-3} \cdot mm^{-3}$]
SM_i	Actual soil moisture content [mm]
SM_{max}	Maximum soil moisture content [mm]
SWE	Snow water equivalent [mm]
S_0	Surface soil saturation [$mm^{-3} \cdot mm^{-3}$]
T_a	Temperature of the air [°C]
T_b	Base temperature at which snow begins to melt (0°C) [°C]
T_c	Temperature of the canopy [°C]
t_c	Time after saturation at which interflow becomes unsaturated [T]
T_I	Average temperature of 0-40 cm of soil [K]
T_{max}	Daily maximum air temperature
T_{min}	Daily minimum air temperature
t_0	Infiltration opportunity time [hr]
U	Wind speed [$m \cdot s^{-1}$] or [$km \cdot hr^{-1}$]
Vx	Horizontal flow velocity [$L \cdot T^{-1}$]
$XSLP$	Average slope of GRU for overland and interflow calculations [$m \cdot m^{-1}$]

Greek Symbols

α	Albedo of a snow-covered area
ε	Surface emissivity
Λ_I	Average GRU slope
λ_f	Latent heat of fusion of water [0.3337 $MJ \cdot kg^{-1}$]
λ	Thermal conductivity of soil layer [$W \cdot m^{-1} \cdot K^{-1}$]
ρ_w	Density of water [$kg\ m^{-3}$]
σ	Stefan Boltzmann constant [4.9E9 $MJ \cdot m^{-2} \cdot K^{-4} \cdot d^{-1}$]
θ_I	Initial water (ice) content [%]
θ_p	Soil porosity values [%]
θ_s, θ_c	Average soil moisture values at for saturated and unsaturaded first soil layer

Abbreviations

ALP	Alpine meteorological and snow survey station
AGR	Aggregated modelling approach
BB	Back Brush meteorological and snow survey station
bg	Bare ground
CL	Cold Lake stream gauge station
CLASS	Canadian Land Surface Scheme
CRHM	Cold Regions Hydrological model
DDS	Dynamically Dimensioned Search optimisation algorithm
DIST	Distributed modelling approach
DEM	Digital Elevation Model
EBSM	Energy-Budget Snowmelt Model
EF	East facing slope
EVAP	Evaporation module of CRHM
F	Forest meteorological and snow survey station
GLA	Gap Light Analyser software
gr	Grasses
GB	Granger Basin
GC	Granger Creek stream gauge station
GCM	Global Climate Model or Global Circulation Model
GEM	Global Environmental Multi-scale model
GLUE	Generalised Likelihood Uncertainty Estimation
GRU	Group Response Unit
HBV	Hydrologiska Byråns Vattenbalansavdelning model.
HRU	Hydrological Response Unit
LSH	Land Surface Hydrological model
LSS	Land Surface Scheme
MEC	Modélisation Environmentale Communautaire
MESH	MEC- Surface Hydrology modelling system
MSC	Meteorological Service of Canada

NF	North facing slope
PILPS	Project for Intercomparison of Land Surface Parameterisation Schemes
PLT	Plateau area
REA	Representative Elementary Area
REV	Representative Elementary Volume
REW	Representative Elementary Watershed
sh	Shrubs
SDC	Snowcover depletion curve
SF	South facing slope
SHE	Système Hydrologique Européen model
SMR	Soil Moisture Routing model
SVATS	Soil Vegetation Atmospheric Transfer Schemes
SWAT	Soil Water Assessment Tool model
SWM	Stanford Watershed Model
TVC	Trail Valley Creek Basin
UB	Upper basin
UBC	University of British Columbia model
UEB	Utah Energy Balance model
UWC	Upper Wolf Creek stream gauge station
VB	Valley bottom
WATCLASS	Former MESH model (CLASS + WATFLOOD)
WATFLOOD	University of Waterloo Hydrological and Flood Forecasting System
WC	Wolf Creek Basin
WCAH	Wolf Creek Alaska Highway stream gauge station
WF	West facing slope

CHAPTER 1

INTRODUCTION AND OBJECTIVES

1.1 Background

Mathematical representations of basin response to rainfall and snowmelt are of critical importance to hydrology and remain a major challenge to hydrological research. These responses are characterised by basin heterogeneity and involve nonlinear interactions between various hydrological processes.

Since the development of the Stanford Watershed Model (SWM; Crawford and Linsley, 1966) numerous hydrological models have been developed that use the basin as the fundamental spatial unit to describe the various components of the hydrological cycle. The complexity of these models varies with user requirements and data availability. Thus, hydrological models vary from simple empirical and lumped conceptualisations to spatially distributed and physically based approaches. The typical representation of the land surface hydrological processes as conceptual buckets in spatially lumped models cannot capture the lateral or horizontal redistribution of moisture in soils and in the drainage network. They instead rely on calibration of empirical parameters to reproduce observations of hydrological processes over complex terrain. Therefore fully distributed and physically based models are needed to account for the partitioning of mass and energy inputs in runoff. However, adding more complexity such as detailed process descriptions or more spatially explicit parameters does not necessarily lead to better or less uncertain predictions.

More complex models have more parameters and initial conditions to be set and hence more degrees of freedom. Greater complexity can result in greater uncertainty in prediction (Beven, 2006). The main challenge for reliable hydrological predictions is the quantification of the different sources of uncertainties associated with the representation of model inputs, process descriptions, and model parameters respectively (Sivapalan et al., 2003a).

Input data uncertainty is usually related to the lack of adequate datasets at multiple space-time scales and the insufficient capability to measure or capture the landscape variability. Uncertainty in input or forcing data can have complex effects. It is not only propagated through the hydrological model contributing to the model predictive uncertainty but also has an effect on error estimation of model parameters given the propensity of model parameters to compensate for errors during the model calibration process (Kavetski et al., 2003). Furthermore, in arctic and subarctic environments a related source of uncertainty with substantial effects on snowmelt model predictions is the usual assumption of uniform initial snowcover conditions within the model grid in spite of the known high heterogeneity of the end-of-winter snowpack as a result of vegetation and redistribution of snow by wind.

Uncertainty in process description (i.e. model structure) is attributed to the lack of understanding of hydrological processes at different scales and to the nonlinear interactions and feedbacks between the atmosphere, landforms, soil, and vegetation. Hydrological models are generally focused to solve for the mass balance of the basin or model domain whereas the energy balance is not always considered. This is a fundamental issue for snowmelt modelling, where conservation of energy principles are critical for an appropriate description of snowcover ablation and generation of snowmelt runoff. In this context, the use of models that include conservation of energy equations

such as the land surface hydrological models may be helpful to reduce predictive uncertainty.

Parameter uncertainty in distributed physically based models is related to the scale of resolution of application and complicated by the nonlinearity of the hydrological processes (Beven, 2001b). Inferring physically-based parameters in a distributed model is not a trivial problem. Since physically-based parameters have a physical meaning which is independent of the model itself, it was initially assumed that it would be possible to measure or derive all parameters from field observations without the need of rescaling and calibration (Abbott et al., 1986; Refsgaard and Storm, 1996). However, a difficulty in estimating parameter values resides in that observations are often sparse and the scale of those measurements usually differs from the modelling scale (Blöschl and Sivapalan, 1995). Furthermore, all distributed hydrological models, regardless of how spatially explicit their landscape representation, are to some degree lumped, so that their equations and parameters describe the processes as aggregated in space and time (Gupta et al., 2003). This means that measured and model parameters cannot be defined exactly in the same way. As a result, model parameters become "effective parameters" that are related but not identical to the measurable values. Typically this discrepancy is solved by the process of parameter estimation or calibration. In this process models are calibrated by adjusting the parameter values to fit some observation of interest.

The effect of grid size on the performance of distributed and physically-based models has been extensively studied. The choice of a model resolution determines what variability can be explicitly and implicitly represented (Grayson and Blöschl, 2001). In sub-arctic alpine tundra environments, the natural variability of snowcover during melting is complex and multi-scale but there seems to be 'scale breaks' to variables and parameters that lead to apparent 'process scales'. For example, differential covariance

between melt rate and snow water equivalent (SWE) was observed at different scales (e.g. small, landscape and basin) (Pomeroy et al., 2004; McCartney et al., 2006), and greater melt rates were seen under shrubs canopies (Bewley et al., 2007; Pomeroy et al., 2006).

Two main strategies to model building have been applied. These methodologies can be related to the general deductive and inductive approaches to scientific inference (Young and Jarwis, 2002). In the deductive modelling approach the *a priori* conceptual model structure is a theory based on the perception of the scientist and is strongly conditioned by assumptions that derive from scientific paradigms. It is believed that the physical system can be described very well, if not exactly, by these deterministic mathematical equations (i.e. reductionist philosophy). This was first outlined in the proposed blueprint for a distributed physically based hydrological model by Freeze and Harlan (1969), based upon numerical solutions to the coupled partial differential equations that describe water movement at the surface and in the unsaturated and saturated subsurface. Conversely, in the inductive approach, theoretical preconceptions are avoided as much as possible in the initial stages of the analysis. In particular, the model structure is not pre-specified; rather it is inferred from the observational data. Challenges to both approaches are that processes important at one scale may not necessarily be important at other scales (Blöschl and Sivapalan, 1995) limiting thus the deductive reasoning, whereas the restrictions to the inductive modelling approach are its attempts to identify processes directly at the scales of interest and interpret these in terms of properties and processes occurring at finer scales. Also, as data are usually rather limited, only simple and often physically unrealistic models can be inferred solely from the data (Sivapalan et al., 2003b).

A current debate in hydrological modelling is how to produce accurate and reliable predictions in ungauged or poorly gauged basins. This issue had led to the

International Association of Hydrological Sciences (IAHS) initiative on Prediction in Ungauged Basins (PUB) which mainly focuses in the need of improved processes understanding as a framework to developed enhanced knowledge and modelling strategies. Prediction of snowcover depletion and spring melt runoff in arctic and subarctic basins is particularly challenging due to their remote location, winter inaccessibility, and importance of the winter processes (e.g. snow accumulation and redistribution) in the water balance. Streamflow in those regions is generally poorly-gauged or ungauged (Pomeroy et al., 2005).

Snowmelt and subsequent runoff generation are amongst the most important hydrological processes in arctic and subarctic mountain environments. Hillslopes, valley bottoms and upland plateaus dominate the physiography of these regions in Canada, and both vertical and lateral water fluxes exhibit large variability since topography, soil properties, and vegetation vary widely over short distances (Carey and Woo, 2001b). Additionally, redistribution of snow by wind during the winter accumulation season can drastically change the snowcover conditions prior to melt, resulting in deep snow accumulated in sheltered sites such as lee slopes and vegetated areas and thin snowpacks on exposed windswept areas (Pomeroy et al., 1997; Essery and Pomeroy, 2004a). During the melt season, these very heterogeneous snowpacks form a patchy snowcover as a result of variable snow accumulation, slope and aspect effects on snow energetics (Pomeroy et al., 2003), effects of shrubs in governing snow melt energy (Liston et al., 2002; Bewley et al., 2007; Pomeroy et al., 2006), and local advection from bare ground and shrub stems (Liston, 1995; Marsh and Pomeroy, 1996; Neumann and Marsh, 1998). This spatial heterogeneity results in spatially differential snowmelt rates which subsequently modify the meltwater fluxes, runoff contributing area, and the timing and peak of snowmelt runoff (Carey and Woo, 2001a; McCartney et al., 2006).

1.2 Objectives

The main objective of this thesis is the implementation of a new model philosophy for predicting snowcover depletion and snowmelt runoff in complex cold regions environments with limited input data whilst retaining physical integrity in the processes representation.

The sub-objectives of this research are:

1. Defining a modelling strategy that allows scaling of point scale observations to catchment scale models.
2. Defining an appropiate representation of the spatial heterogeneity for physically based hydrological models in complex subarctic environments for predicting snowcover depletion and snowmelt runoff.
3. Evaluation of the effect of initial snowcover conditions and forcing data on simulations of snowcover depletion and snowmelt runoff in these environments
4. Identification of stable hydrological model and land surface scheme parameterisations using a landscape-based approach.

The motivation for this study is to enhance physically based hydrological model predictions of snowmelt in complex terrain with limited data that also could potentially improve the feedback to atmospheric models. This study attempts to apply the knowledge in cold regions process descriptions acquired throughout comprehensive hydrological research in the arctic and subarctic regions of Canada. Reliable statements about modelling hydrological processes require an understanding of the scale at which the processes operate, in order to deal with the natural variability in catchment characteristics. Thus, this study tries to define an appropriate model complexity for the available data, detail of processes understanding, and with information gained from

observations of basin-wide snowmelt runoff response, essentially a new modelling methodology for complex arctic and subarctic environments.

The reasoning behind this study is that by including an explicit landscape representation of topography and vegetation, predictive uncertainty on snowmelt simulations will be reduced, and thus to contribute to the improvement of those numerical predictions based on conceptualisation of the model elements as uniform units.

CHAPTER 2

LITERATURE REVIEW

2.1 Introduction

Physically based hydrological modelling emphasises the prediction of hydrological processes in the different phases of the hydrological cycle based on the application of physical principles. This chapter reviews the literature pertinent to cold regions hydrology focusing on the description of the hydrological processes controlling snowcover ablation and snowmelt runoff, and on the simulation techniques to date.

2.2 Cold regions hydrology

The northern part of Canada and other high latitude regions are characterised by their extreme seasonal radiation regimes, with negative radiation balances in the winter period, that; combined with freezing temperatures and snowfall as the principal component of the annual precipitation, result in snowcovers that often last over half the year (Woo et al., 2005). These snow dominated environments have a strong influence on the generation and dynamics of snowmelt runoff and on atmospheric processes as a result of energy balance considerations. Therefore, an improved understanding of the processes governing melt, infiltration into frozen soils, runoff generation, and streamflow routing of snowmelt water is essential not only for scientific interests but also for practical aspects such as numerical weather prediction due to the hydrological

feedbacks to the atmosphere, water recourses management, and for the evaluation of anthropogenic impacts due to northern development or land-use change.

2.2.1 Snow accumulation processes

A detailed understanding of the seasonal and spatial variations of snow accumulation within a basin is critical for the winter water budget and is a key issue to reduce uncertainties in modelling snowcover ablation and snowmelt runoff. Snow accumulation is what remains after falling snow has been modified by interception in vegetation canopies, sublimation, redistribution as a result of wind transport, and melt. Consequently, it is incorrect to assume that an increase of the snow on the ground is equivalent to snowfall (Pomeroy and Gray, 1995). Estimation of snowfall is particularly challenging. The properties and characteristics of fallen snow change as a function of energy fluxes, temperature, wind, moisture, water vapour, and pressure (Gray and Male, 1981). Measurements of snowfall precipitation are strongly affected by wind since upward-moving air in eddies in the orifice of unshielded gauges prevents snow from entering the gauge. Therefore, windshields are usually set up around the snow gauges to reduce snow undercatch. The standard snow gauge used in Canada was the MSC (Meteorological Service of Canada) Nipher shielded snow gauge system. This gauge consists in a hollow metal cylinder, 560 mm long and 127 mm in diameter, surrounded by a solid shield with the shape of an inverted bell. This instrument, designed to collect solid and liquid precipitation, proved to be a very reliable gauge compared to unshielded gauges or Alter-type shields with a catch efficiency of 95 percent or more at wind speeds of less than $5 \cdot m\ s^{-1}$, decreasing to less than 80 percent at wind speed of $7\ m\ s^{-1}$ (Goodison, 1978). However, since it should be manually operated, its application in northern cold regions was restricted to locations with safe accessibility. The main source of errors in measuring snowfall are the manual errors in measurement of snow depth as a result of the highly variable fresh-snow density, the wetting loss in the snow

gauge that is poured out of the measurement, and the trace amounts of snow that is given a value of zero (Pomeroy and Goodison, 1997). The same errors are associated with automatic snow gauges. Additionally, because automatic snow gauges are usually not attended, snow build-up and icing effects can drastically modify the snowfall data.

Since the description of snow accumulation processes depends not only an a adequate determination of the precipitation but also on the assessment of the processes of redistribution and phase change resulting from melt and sublimation, the evaluation of the interaction of these processes with topography and vegetation is an essential factor in the calculation of the mass and energy balances for a given basin. Efforts to reduce the uncertainty in the spatial variability of the snow accumulation patters have been focused on the identification of land use or landscape units where basin snow surveys are conducted (Steppuhn and Dyck, 1974; Woo and Marsh, 1978). Similar approaches were used in the arctic and subarctic research programs such as those in Trail Valley Creek and Wolf Creek Research Basins where extensive snow transects in representative landscape units are regularly surveyed by measuring snow depth and density.

Snow accumulation is a scale dependent process. At large or regional scales the spatial variability of snowcover is affected by latitude, elevation, orography, and the presence of large water bodies. At mesoscales (100 m to 10 km), patterns in snow accumulation are governed by topography (i.e. relief features) and vegetation cover, whereas at microscales variations in air flow patterns and interception are responsible for the spatial variability in the accumulation patterns. Differences in snow accumulation are the result of interception, sublimation, and redistribution processes (Pomeroy and Gray, 1995).

In open environments such as alpine and tundra areas, thinner end-of-winter snowcovers are expected in sparsely vegetated and exposed, windswept areas as result of the redistribution of snow by wind, given the relatively low surface roughness of

these areas. Conversely, deeper snowcovers are observed in sheltered sites due to the presence of leeward slopes, topographic depressions and denser and taller shrub areas that reduce snow transport processes and facilitate the deposition of the blowing snow. Estimation of the blowing snow, transport, and sublimation effects over the accumulation period for open environments led to the development of the Prairie Blowing Snow Model (PBSM; Pomeroy et al., 1993). This model uses a physically-based approach to calculate transport and sublimation rates for blowing snow given measurements of air temperature, humidity and wind speed. Applications of this model are described in Pomeroy and Li (2000) and Fang and Pomeroy (2007). Distributed numerical simulations of snow transport and sublimation using a simplified version of PBSM at the landscape scale in a low-arctic tundra environment (Essery et al., 1999) showed the importance of the inclusion of sublimation to accurately simulate late-winter accumulations. Essery and Pomeroy (2004a) also showed for the same environment that distribution of vegetation was a key factor in describing snowcover patterns, as shrubs act to trap blowing snow from open areas. They found that the amount of snow held by shrubs was proportional to the shrub height until a given threshold determined by the supply of snow, after which less variable snowcovers were observed. Similarly, an increase in shrub density led to a decrease in the spatial variance of the snow accumulation pattern. Since topographic effects were less dominant, presumably due to the low relief, aggregated simulations successfully described the control of the vegetation on snow redistribution.

Forest environments on the other hand, show a spatially more spatially uniform snow accumulation pattern. Boreal forests mainly consist of evergreen coniferous trees that intercept a large proportion of annual snowfall. This intercepted snow may sublimate or fall to the ground. Field observations from boreal forests showed that 30% to 45% of annual snowfall sublimates as a result of its exposure as intercepted snow (Pomeroy and Gray, 1995; Pomeroy et al., 1998a; Lundberg and Halldin, 2001).

Sublimation reduces the snow available for accumulation. Compared with snow on the ground, snow sublimates more quickly in forest canopies because of greater absorption of short-wave radiation by the canopy and a higher exposure to turbulent-exchange forces (Lundberg et al., 2004). Forest canopy is important in controlling the interception-sublimation process (e.g. Kuz'min, 1960; Pomeroy and Gray, 1995; Pomeroy et al., 2002). Hedstrom and Pomeroy (1998) and Pomeroy et al. (1998a) showed that an increase in the leaf area index (LAI) resulted in decreasing snow accumulation. Observations showed that the interception efficiency of the canopy is particularly sensitive to snowfall amount, canopy density and time since snowfall. Thus, interception efficiency decreases with increasing snowfall, time since snowfall, and initial canopy snow load. Based on those observations, a physically based model was developed to calculate snowfall interception from meteorological data and forest properties (Hedstrom and Pomeroy, 1998).

These results also suggested that differences between forest stands and clear-cuts are due to interception and sublimation processes in the forest canopy rather than redistribution of the snow intercepted in the canopy. Results from several boreal forest stands (Pomeroy et al., 2002) showed that the ratio of forest to clearing snow accumulation declined from values near 1 to near 0.5 as LAI and canopy increased. Pomeroy et al. (1998b) and Faria et al. (2000) found that the snow accumulation mass follows a log normal distribution within forests stands and that pre-melt variance of SWE within boreal forest stands increases with increasing canopy density. In conclusion, since most of the forested catchments are covered by a mosaic of clearings and stands of varying density, the knowledge of the variations in the seasonal and spatial patterns of snow accumulation and the relation between distributions of forest properties, such as LAI and snow accumulation, are essential for catchment-scale predictions of snow accumulation and melt.

2.2.2 Snow ablation process

Snowmelt is the most significant hydrological event in arctic and subarctic environments, since the spring snowmelt freshet is usually the largest runoff event of the year. The snowmelt period is characterised by complex and dynamic processes resulting in rapid changes in albedo, turbulent fluxes, internal snow energy, and surface temperature as the snowcover is depleted. These changes have drastic effects on the surface-atmosphere exchanges (Pomeroy et al., 1998b). Most studies of arctic and subarctic snowmelt hydrology have focused upon process descriptions including dynamics of snowpack percolation (e.g. Marsh and Woo, 1984a and b), canopy interception and sublimation (e.g. Pomeroy et al., 1999), canopy effects on radiation (e.g. Sicart et al., 2004; Bewley et al., 2007), snow advection (e.g. Liston, 1995, Marsh et al., 1997; Neumann and Marsh, 1998), infiltration, soil storage and runoff (e.g. Woo, 1983; Kane et al., 1991; McNamara et al., 1998; Carey and Woo, 1999; Carey and Quinton, 2005). Recent research however, has been focusing on the substantial variability of the snow ablation processes and interactions with the landscape, and their effects on snowmelt runoff (e.g. Marsh and Pomeroy, 1996; Liston, 1999; Marks et al., 2001; Liston et al., 2002; Pomeroy et al., 2003; Pohl et al., 2005a and b; Pomeroy et al., 2006, McCartney et al., 2006).

Snow surfaces have unique energetics as a result of their physical properties and distinctive winter climate conditions (Pomeroy and Goodison, 1997). The more important properties of the snow include radiative properties such as the high albedo (i.e. reflectance of incoming short wave radiation), high emissivity (absorbed longwave radiation is almost entirely re-radiated as thermal radiation), and the ability to allow the partial transmission of solar energy (i.e. translucent medium). The thermal insulating properties of snow, as a result of its low thermal conductivity, protect the soil from rapid atmospheric temperature changes. The low aerodynamics surface roughness results in

larger wind speeds compared to vegetated surfaces. Because solid, liquid, and gaseous phases are coexisting components of snow, there is a latent heat transport by diffusive or advective process through the snowpack as a result of phase changes among the liquid water, ice, and air components of snow.

Seasonal snowcovers are developed from several winter storms and modified by wind transport, rain, melting, and refreezing at the surface. As a result, seasonal snowcovers show a very heterogeneous and layered structure with alternating ice and snow layers of different density. Energetic of a snow surface involves phase changes through melt, condensation, sublimation, evaporation, and refreezing. These processes are also influenced by changes in the mass balance of the snowpack as a result of wind erosion, infiltration, and runoff. The typical approach used to calculate snow melt energy of a snowpack at point scales is based on the reference to a unit control volume (Male, 1980). Thus, the energy available for melt, Q_M [W·m^2] is:

$$Q_M = K^* + L^* + Q_E + Q_H + Q_D + Q_G - \frac{dU}{dt} \qquad (2.1)$$

where K^* is the net shortwave radiation to snow [W·m^2], L^* the net longwave radiation to snow [W·m^2], Q_E the latent heat flux (sublimation, evaporation and condensation) to the surface [W·m^2], Q_H the sensible heat flux from the air at the snow-air interface [W·m^2], Q_D the energy as heat flux transported to the snowpack by precipitation [W·m^2], Q_G the conducted heat flux from the ground [W·m^2], and U the change of internal energy of the snowpack over time t. Downward fluxes are considered positive.

During the melt season, meltwater is released from the snowpack in a diurnal cycle in response to the energy inputs. This diurnal cycle of meltwater is also affected by the nighttime energy deficit that needs to be compensated for the next day before the

snowpack returns to 0°C. The daily amount of melt produced by a given value of Q_M can be calculated from the following expression:

$$M = \frac{Q_M}{\rho_w \lambda_f B} \tag{2.2}$$

where M is the snowmelt water equivalent [cm·d^{-1}], Q_M the energy available for melt [kJ·m^{-2}·d^{-1}], ρ the density of water [kg·m^{-3}], λ_f the latent heat of fusion [kJ·kg^{-1}], and B the thermal capacity of snow or the mass fraction of ice in a unit mass of wet snow. B usually ranges between 0.95 and 0.97 (Gray and Male, 1981).

As the melt season progresses, increasing energy inputs change the internal energy of the snowpack, inducing a rise of the temperature until the snowpack has warmed to 0°C, after which the internal energy change is small (Male 1980) and any additional energy will result in phase change from solid to liquid, and hence in meltwater production. However, melt can also occur before isothermal conditions are established when surface meltwater in cold snowpacks flows through the pack following preferential flow paths (Marsh and Woo, 1984a; Marsh and Pomeroy, 1996); hence dU/dt need not to be zero for Q_M to be positive (Pomeroy et al., 2003). When the snowcover is continuous, early in the melt season, advection is negligible and net radiation is the dominant flux, while the contribution of turbulent exchanges of sensible and latent heat increases though the melt. During the period when the snowcover is patchy, the bare ground warms as a result of its low albedo, and the positive net energy of the bare ground is advected onto the remaining snow patches, enhancing melt (Marsh and Pomeroy, 1996; Shook and Gray, 1997; Neumann and Marsh, 1998).

As discussed in the previous section, several studies described the importance of the snowcover conditions prior to the onset of melt in the dynamics of the snowcover ablation. Pomeroy et al. (2004) described the spatial distribution of snowcover and melt rates that need to be considered for an appropriate description of the snowcover

depletion in subarctic environments. In agreement with Faria et al. (2000), they found that the log-normal frequency distribution may be used to describe the pre-melt spatial distribution of SWE in a complex tundra terrain, and suggested a slope class differentiation. Within-class variability of pre-melt SWE was further grouped into windswept tundra and sheltered tundra-forest regimes. In all sites however, the log-normal fit of observed SWE degraded progressively during melt as a result of the spatially variable melt rate. Observations showed that the spatial variability and covariability between initial SWE and average melt rates is scale and landscape dependent. At small scales (<100 m), a negative correlation between initial SWE and melt rate was observed in those areas where shrubs were exposed above snow. This negative association was not observed in forest or deeply drifted snow over short vegetation. Similarly, at medium scales (> 500 m) in shrub tundra environments a negative correlation between initial SWE and average melt energy was also found between adjacent landscape units likely due to the differential insolation and accumulation regimes between plateaus and slopes. However, further research at this scale is needed to include all the possible associations between slope geometry and meteorology (Pomeroy et al. 2003 and 2004). At larger or basin scales, the association between landscape-class initial SWE and melt rate turned positive due to the variability in melt, snow redistribution, and interception processes amongst the different landscapes (i.e. forest, shrub tundra, and alpine). Thus, the combined effect of low SWE and melt rate in alpine areas, larger SWE and melt rates in shrub areas, and low SWE and melt rates in forest areas, resulted, in most of the studied years, in an positive association with an initial deceleration and later acceleration of snow covered area (SCA) depletion compared with a monotonic snow depletion.

Studies stressing the importance of the spatial variability of the available snow melt energy in arctic, subarctic, and prairie environments have highlighted the effects of topography, vegetation, local advection, and importance of the initial conditions on the

dynamic of the snowmelt processes (e.g. Shook, 1995; Neumann and Marsh, 1998; Essery and Pomeroy, 2004a and b). Pomeroy et al. (2003) re-examined the snowmelt calculations to slopes and found substantial differences in energetics and rates of snow ablation over shrub–tundra surfaces of varying slope and aspect. Incoming solar radiation on NF and SF slopes varied with cloudiness conditions. On sunny days, the values on the SF were substantially higher that on the NF, whereas smaller differences were observed on cloudy days, showing thus that cloudiness plays a dominant role driving the spatial variability of melt. These differences in solar radiation on NF and SF slopes initially caused small differences in net radiation in early melt. However, as shrubs and bare ground emerged due to faster melting on the SF slope, the albedo differences resulted in large positive values of net radiation to the SF, whilst the NF fluxes remained negative.

The presence of shrubs was demonstrated to have important influences in controlling both snow accumulation and ablation regimes (Liston et al., 2002). Observations and modelling results of blowing snow transport in arctic and subarctic environments showed that in general the greatest accumulations in shrub tundra areas were associated with the presence of nearby open areas, acting as a source of snow transport, and due to exposure of shrubs that reduced the aerodynamics roughness, rather than the density or height of the shrubs (Pomeroy and Gray, 1995; Essery and Pomeroy, 2004a). Pomeroy et al. (1997) found that shrub tundra accumulated four to five times more snow than sparsely vegetated tundra. Sturm et al. (2001b) showed that the presence and height of shrubs influences the snow albedo over the melt season and the subsequent shrub melt rates. Snow albedo is drastically decreased when buried shrubs become exposed in middle to late spring. Pomeroy et al. (2006) showed the importance of shrub exposure in governing snowmelt energy. In general, shrub exposure enhanced melt energy; however the shrubs-snow interaction was very complex. As shrubs emerged from the snowpack during melt, net radiation increased

mainly due to lower surface reflectance overwhelming the longwave emission from the shrubs. A similar but lest conspicuous situation was observed under the shrubs, but was still greater than that to snow surfaces with minimal shrub cover. Turbulent exchanges also showed a complex pattern. Shrub canopy reduced turbulent transfer and therefore under the canopy latent heat due to sublimation declined with increasing shrub exposure. Because of relatively warm branches, sensible heat to the shrubs surface became more negative whereas from the shrubs to the snow surface was more positive with increasing shrubs. McCartney et al. (2006) observed that the greatest snow accumulation in tall shrubs plays a key role in the snowmelt streamflow regime. The effects on snowmelt rates and extinction of solar radiation due to shrub canopy were examined by Bewley et al. (2007). They developed a model to simulate the effective transmission and reflectance of shortwave radiation from a discontinuous shrub canopy over a melting snowpack. The inclusion of shaded canopy gaps was believed to improve the diurnal simulation of shortwave transfer respect to simple radiative transfer models. Results were consistent with available observations while there are still uncertainties in the validity of the areal albedo and trasnmissivity values due to the lack of observation at larger scales.

2.3 Hydrological modelling

2.3.1 Classification of hydrological models

Although there are several ways of classifying hydrological models (Chow et al., 1988; Singh, 1995; Refsgaard, 1996), modelling approaches may be distinguished by three main characteristics (Grayson and Blöschl, 2001): (1) the nature of the basic algorithm (empirical, conceptual, and physical or process-based), (2) the approach to input or parameter specification (stochastic or deterministic), and (3) the spatial representation (lumped or distributed).

Empirical models are derived from data; therefore they are not based on scientific laws describing physical processes. Since the model structure relies on a given range of data, their applicability and validity is limited to this range of data. Conceptual models are based on a theoretical understanding of the hydrological processes. They generally use physical laws but in a highly simplified form. Sometimes they apply non-physical concept of basin response. Conceptual models contain parameters that may have physical significance; however most of the parameters are conceptual and hence the definition of their values relies primarily on calibration (e.g. UBC model; Quick and Pipes, 1977). Physically based models on the other hand use scientific laws to describe hydrological processes.

In deterministic hydrological models, variable state outputs are uniquely determined from the initial conditions, inputs, and model parameterisation. On the other hand, stochastic models include some random component that limits exact model prediction, therefore model results are often associated to a given probability and usually delimited by confidence intervals.

According to the spatial representation of the landscape heterogeneity, hydrological models can be classified as lumped or distributed. Spatially lumped models in their more simplified version deal with a catchment as a single unit. They relate precipitation inputs to discharge outputs without any consideration of the spatial patterns of the hydrological processes and basin characteristics. Therefore, they cannot capture the lateral or horizontal redistribution of moisture in soils and in the drainage network. Examples of lumped models are the SWM (Crawford and Linsley, 1996) and the original version of the SLURP model (Kite, 1975). Conversely, spatially distributed models explicitly account for the spatial patterns of processes response. However, according to the approach used for the processes representation, distributed models can be distinguished as semi-distributed or fully distributed models. Spatially semi-distributed hydrological models are those models that subdivide the basin in different

model elements within which lumped calculations are performed. Different examples of this approach are the UBC model (Quick and Pipes, 1977) based on elevation bands, the TOPMODEL (Beven and Kirkby, 1979; Beven et al., 1995) based on the conceptual definition of topographic units, the rainfall-runoff model applied by Kuchment et al. (1996) based on a finite-element schematisation of the basin that incorporated information of the drainage network, topography and soils, the SWAT model (Arnold et al., 1998) based on the identification of similar hydrologic units (HRUs; Hydrological Response Units), and the WATFLOOD model (Kouwen, 1988) based on grouping similar HRUs called Group Response Units (GRUs). On the other hand, fully distributed models make use of grids or finite-elements to represent the spatial landscape heterogeneity where numerical solutions to the governing physical equations are performed, such as the SHE (Système Hydrologique Européen) model (Abbot et al., 1986, Refsgaard and Storm, 1996) that integrates on a regular grid a 3D groundwater model, a 2D diffusive wave approximation for the overland flow, and a 1D full dynamic component of the river flow.

2.3.2 Snowmelt modelling

In the last 40 years, many snowmelt models have been developed with several purposes and applications such as global circulation models, snow monitoring, snow physics hydrology, and avalanche forecasting (Etchevers et al., 2004). Snowmelt models generally fall into two categories: temperature index models and energy balance models.

Temperature index models have been the most common approach for snowmelt modelling mainly due to their low input data requirement, the wide availability of air temperature data, and adequate model performance in some environments despite their simplicity (Beven, 2001a). The temperature index or degree-day approach assumes an

empirical relationship between air temperature and snowmelt. The basic formulation developed by Anderson et al. (1973) is given by:

$$\begin{aligned} M &= MF(T_a - T_b), && T_a > T_b \\ M &= 0, && T_a \leq T_b \end{aligned} \tag{2.3}$$

where M is the snowmelt depth [mm/hr], MF is the melt factor or rate of melt per degree unit time [$mm°C^{-1}hr^{-1}$], T_a is the air temperature [°C], and T_b is the base temperature at which snow begins to melt [°C].

Although the performance of temperature index models can be successful, their application is restricted to 'typical' or average conditions, based on historical data, where the definition of a consistent relationship between temperature and snowcover energy exchange is possible (Garen and Marks, 2005). Therefore, temperature index models are not suitable for complex situations such as rain on snow or where temperature is not a good estimator for energy input to the snowpack. Application of temperature index models in open environments with continuous snowcover did not show satisfactory results; however, better snowmelt predictions have been achieved in mountainous and forested areas (Pomeroy and Goodison, 1997). Another important limitation of the temperature index approach is the spatial and temporal variability of the degree-day factor, since it depend on the relative contributions of energy balance components affected by atmospheric conditions and surface type (Hock, 2003). Thus, the derivation of degree-day factors based on point scale measurements (e.g. from snow and water density ratio; Martinec, 1985) or basin characteristics is not a trivial problem, especially in mountain terrains due to large variability in melt energy, temperature, and snowpack characteristics (Martinec and Rango, 1986). Consequently, degree-day factors are often determined by calibration procedures (e.g. Walter et al., 2005). As a result, the classical degree-day method is restricted to applications using average spatial conditions (i.e. catchment scale) and to periods exceeding the daily basis. Examples of temperature index models are the HBV model (Bergström, 1976), the SRM model

(Martinec and Rango, 1986), the UBC model (Quick and Pipes, 1977), and the SWAT model (Fontaine et al., 2002). Further, Walter et al. (2005) showed that simple physically based models had better snowmelt performance than temperature index models with the advantage that sources of errors can be identified, and hence improvements can be meaningfully addressed.

Physically based snowmelt models are based on the energy balance of the snowpack (Equation 2.1). Since snowmelt involves phase change, the energy balance equation is the main physical framework for modelling snowmelt and implies the application of the energy equation to a 'control volume' of snow. There are several variants of this parametric energy balance approach (e.g. Kustas et al. 1994; Liston and Elder, 2006b). The main difficulties in predicting snowmelt are the variations of the terms in equation (2.1) over time and space (Ferguson, 1999). The snowmelt period is characterised as a period of rapid changes in land-atmosphere exchange since albedo, turbulent fluxes, internal snow energy and surface temperature undergo dramatic alteration as the snowcover becomes wet and is then depleted (Pomeroy et al., 1998b).

Shortwave radiation is generally the dominant source of energy, particularly on clear days and can largely exceed the longwave loss at night. It varies greatly according to sun angle, cloud cover, and topographic effects. Much of the incoming shortwave radiation on a snow surface is reflected as a result of its high albedo. Incoming longwave radiation depends on the temperature of the emitting surface such as upper atmosphere, cloud cover, or vegetation canopy. Over snow surfaces, outgoing longwave radiation is generally larger than incoming, resulting in a net loss of longwave radiative energy from the snow cover (Male and Granger, 1981). Cloud cover has a marked influence on both short and longwave radiation fluxes. Incoming and the outgoing shortwave radiation decreases with increasing cloud cover, whereas the incoming longwave radiation exhibits an opposite trend with unaffected changes in the outgoing

longwave radiation. As a result, the net all-wave radiation at the snow surface increases with increasing cloudiness (Male and Granger, 1981).

The turbulent fluxes to or from the snow surface depend strongly on atmospheric conditions, and especially on the temperature profile. Large scale parameters affecting turbulent transfers are topography, altitude, season, and air mass characteristics. The relative importance of turbulent energy as sources for snowmelt varies markedly with timing of snowmelt and geographical location (Male and Gray, 1981). Pomeroy et al. (1998b) found for a prairie environment that the turbulent contribution to melt of a continuous snowcover was insignificant in most conditions, however for a subarctic mountain basin Pomeroy et al. (2003) showed that the relative magnitude and direction of the sensible heat flux to melting snow can vary markedly as a result of differences in insolation, slope, aspect, and vegetation exposure. Sensible heat increases with wind speed and is particularly important when snowcover is patchy and heat is advected over the snowpack from warmer snow-free areas (Morris, 1989; Marsh and Pomeroy, 1996; Essery et al., 2006). For an Arctic basin, Pohl and Marsh (2006) found that the sensible heat input to the snowmelt energy balance can be up to twice the net radiation during cloudy, warm, and windy periods but is very often around 40% of net radiation. Latent heat contributions can be of the same order as net radiation but are typically around 10% (Morris, 1989). Latent heat can vary greatly at diurnal scales during melt, with both positive and negative values, as a result of evaporation events that are associated to relatively high wind speeds and low relative humidity, and condensation events associated with high humidity and air and surface temperatures below freezing respectively. Ground heat flux is small and usually negligible on a daily basis, even though its cumulative effect throughout the winter period can be important (Gray and Male, 1981). The contribution of ground heat flux to melting snow is more important with shallow snowcovers. Ground heat transfers are drastically affected by phase

change changes from freezing and thawing in frozen soils which in turn influences the infiltration rate at the time of melt.

Applications of point scale energy balance snow models began with the work of Anderson (1976) varying in the degree of complexity in the representation of internal snow processes and in the vertical discretisation of the snowpack. Detailed models include the multiphase and multilayer SNTHERM (Jordan, 1991) and the SNOWPACK model (Bartelt and Lehning, 2002) developed for operational avalanche forecasting. Snow models with a simpler representation of the snowpack include SNOBAL (Marks et al., 1998) with a two layer snowpack and the Utah Energy Balance (UEB; Tarboton, 1995; Tarboton and Luce, 1997) with a snowpack represented by a single layer. Difficulties in the application of the energy balance approach arise when distributed simulations of snowcover are needed. Differences in snow accumulation regimes between environments generate very heterogeneous snowpacks which result in a gradual depletion of the snowcover. This is even more manifest in mountain environments because the initial snowpack tends to be deeper at higher elevations whereas the melt energy tends to be lower, so that snow persists for a long time in the higher parts of the basin. Consequently, the use of a reductionist approach based on the application of a 'point' model at many points over a fine grid often becomes impractical due to the lack of distributed observations needed to capture the spatial landscape heterogeneity that affects the hydrological processes. Nevertheless, remote sensing offers a promising alternative for providing spatially distributed inputs to hydrological models.

Snowcover depletion curves (SDCs) are used as a way to describe the spatial distribution of the snowcover. They relate the areal coverage of the snowpack with the average snow depth at a given time. In this approach, the amount of melt is multiplied by the snow covered area to estimate the total input of water to a basin. Historically, SDCs were based on the temperature index approach (e.g. Anderson, 1973; Martinec, 1985; Brubaker et al., 1996) by relating snow covered area to accumulated melt or

degree days and usually applied to large areas such as elevation zones or entire watersheds. Examples of application of SDCs in physically based and distributed models includes the landscape based approach (Donald et al., 1995) and as way of parameterisation of subgrid variability (Luce et al., 1999).

The spatial distribution of snow covered area is a key input to atmospheric and hydrological models. During snowmelt, there is a significant change in snow albedo as snow cover ablates in vegetation, which leads to a large increase in net radiation and sensible heat flux to the atmosphere (Pomeroy et al., 2006). Therefore, when snow models are implemented as part of a land-surface scheme coupled to an atmospheric model for numerical weather prediction or climate modelling, they have to represent the influences of snow on the albedo of the surface and exchanges of heat and moisture between the surface and the atmosphere (Essery and Etchevers, 2004). Snow models and land-surface models have increased greatly in sophistication over recent years, and the number of parameters that have to be specified for their operation has increased accordingly. The Project for Intercomparison of Land Surface Parameterization Schemes (PILPS; Henderson-Sellers et al. 1995) had shown that different parameter set and model structures among LSS models give significantly different surfaces fluxes. Particularly, in Phase 2(d) of the PILPS project, the representation of the snow in LSS models was evaluated (Slater et al., 2001). PILPS 2(d) found that all LSS models were able to reproduce interannual variations of accumulation and ablation patterns, but that significant differences in timing of the complete ablation of snow between the models were observed. Problems in representing amounts of energy incident on the portion of the grid assigned as snow, especially during ablation events at early stages of the snow season, were the cause of substantive divergences during the snow season due to internal feedback processes. Similarly, the Snow Model Intercomparison Project (SnowMIP) found a wide range of capabilities in simulating snow water equivalent (SWE) at a point during the accumulation and melt periods between the models (Etchevers et al., 2004).

Modelling approaches in arctic environments includes the derivation snowcover areal depletion curves from satellite observations to distribute the SWE (Déry et al., 2004 and 2005). Despite its simplicity this method is limited by the spatial and temporal resolution of the satellite images. Such images are better suited for larger scale studies. Physically based modelling studies showed the effects of the spatial variability of the incident solar radiation and turbulent fluxes in controlling snowmelt even in relatively low relief areas (Pohl et al., 2005a and 2006). Comparison between simulations using uniform and distributed snow accumulation and melt showed that the uniform approach was unable to reproduce the observed snowcover depletion whereas the distributed approach provided a more realistic and gradual snowcover ablation (Pohl and Marsh, 2006). Pohl et al. (2005b), using a distributed land surface hydrological model with a vegetation-based spatial representation, were able to simulate mean SWE and basin runoff in a open tundra environment, whereas less satisfactory results were seen in a energetically more complex shrub tundra environment. Improvement to the landscape representation was conducted by Davison et al. (2006) by incorporating topographic effects such as wind-swept tundra and drift snow accumulation classes.

2.3.3 Scaling issues

In this study and following the definitions proposed by Blöschl and Sivapalan (1995), the term ‘scale’ refers to a characteristics length or time, and the term ‘scaling’ denotes a change in scale. Moreover, upscaling means transferring information from smaller to larger scales (i.e. aggregating) whereas downscaling refers to the opposite transference of information, where the information is disaggregated from large to small scales.

In general the scale at which the data is collected is different from the scale at which predictions are needed. Measurements are made to get information about the natural processes; however, these data will not exactly reproduce the natural variability

of the processes mainly due to instrument error and the spatial dimensions of the instruments. Hence, patterns of the data will differ from the true natural patterns. Precipitation, for example, is measured at widely space points typically with fine resolution. Even at an experimental watershed, spacing between gauges may be on the order of 5 to 10 km. In order to capture the diurnal pattern of heating and cooling on the surface temperature, which can be a strongly nonlinear process, climate information is needed on time scales of at least one to a few hours. Interpolation of monthly precipitation appears reasonable in some studies, but hourly or even daily precipitation cannot be reasonably interpolated from widely spaced precipitation gages (Johnson and Handson, 1995). Similar problems almost certainly exist for temperature and longwave radiation. Wind data, so critical to blowing snow and turbulent heat transfers, is even rarer than precipitation data.

Typically, the modelling or working scale is a compromise between the process representation and the model application. Since more often than not the modelling scale is different from the process scale (i.e. scale that the natural phenomena exhibit) and much larger than the observation scale (i.e. scale at which observations are sampled), scaling techniques are needed to bridge this gap (Blöschl and Sivapalan, 1995). Thus, interpolation and aggregation/disaggregation techniques are the more common methods used. Interpolation techniques estimate patterns from points (i.e. changes of scale in terms of spacing) whereas aggregation methods involve the combination of a number of point values in space to form one average value (i.e. change of scale in terms of support) which correspond to an increase in support scale. Disagregation methods on the other hand, are the opposite transformation and estimate patterns from spatial average values.

Hydrological models are sensitive to scaling issues (Klemeš, 1983; Gupta et al., 1986; Beven, 2001a). At small scales, basin response is dominated by specific features (e.g. macropore distribution, variation of saturated hydraulic conductivity with depth, canopy influences in snowmelt) whereas at larger scales basin response is largely

controlled by the spatial distribution of meteorological and hydrologic inputs (e.g. precipitation, SWE), topography and landcover types. As a result, application of models at large scales should include some transference of information or adjustment of model parameters to account for the difference in scales between the process description and the model application. The typical modelling approach is to apply the same model structure in several basins whereas the parameters, empirical or not, are varied in the calibration process. This means that the model structure is general but not the parameters. Therefore, a change in scale might involve a change in the parameter values, in particular if these parameters are related to local conditions such as climate and physiography (Bergström and Graham, 1998). Moreover, due to the data is combined (i.e. aggregated and/or disaggregated) in the models, predictions will, in general, be different from the apparent variance of the data (Blöschl, 1999).

A particular scaling issue is the coupling between atmospheric and hydrological models using the LSS as the common link. In general, LSSs, also known as soil-vegetation atmospheric transfer schemes (SVATS), are meant to provide the lower boundary conditions to Global Climate Models (GCM). Because the grid scale of GCMs is typically 2.5° x 2.5° or 15 km x 15 km like in the regional configuration of the Global Environmental Multiscale (GEM) model of Canada, landcover will be strongly heterogeneous within a model grid (De Boer 2001). Reliable representation of the landscape heterogeneity requires the application of upscaling techniques to transfer information from small to larger scales. This had been performed by assuming that the landcover of the model grid is represented by the dominant landcover type within the grid. This approach has serious limitations since it can not capture the natural variability and the different spatial scales that hydrological processes exhibit. An alternative method for representing the landscape heterogeneity is the mosaic approach, in which each grid cell is subdivided into a number of tiles and the LSS is run on each

tile independently to calculate the energy and water fluxes to the atmosphere. Soulis et at. (2000) combined the Canadian Land Surface Scheme (CLASS; Verseghy, 1991; Verseghy et al., 1993) with a hydrological streamflow model (WATFLOOD; Kouwen, 1988; Kouwen et al., 1993) to provide a stand-alone land surface hydrological (LSH) model known as WATCLASS. This model evolved later into the MESH modelling system (Pietroniro et al., 2007) which allows running the LSH coupled to the atmospheric model (online version) or as a stand-alone (offline) version. This coupling system has the flexibility to run the LSH model at different time and space scales relative to the atmospheric model, but more appropriate for hydrological simulation, while still providing two-way water and energy feedback between the atmosphere and the land surface (Soulis et al., 2005).

2.3.4 Aggregation methodologies

Heterogeneity in the landscape has forced hydrologists to conceptualise the physics and seek effective parameter values (Pietroniro and Soulis, 2003). Distributed hydrological models use aggregation methods to account for landscape variability and processes representation; however, a critical point in the application of these models is the choice of element size. In general, increasing the level of discretisation increases the accuracy of the simulation, but there should be a level beyond which the model performance can not be increased (Wood et al., 1988). In addition, the smaller the grid size in which the catchment is divided, the larger the volume of information needed and the associated computational time.

A typical method for representing landscape heterogeneity is the grid-based approach (e.g. SHE model). In this case, the basin is split into a number of usually square elements linked to channel reaches. Each grid is the computational element and has a specific surface elevation given by a digital elevation map. This approach has the potential to assign distributed field of meteorological data and the capability to predict a

variety of distributed processes at each element grid. However, predictions are grid-scale dependent. Refsgaard (1997) concluded, after comparing finer and coarser grids that simulations based on 1000 m or larger grid size, while still accurate, may require recalibration of the parameters. In distributed hydrological models the assumption of areas with similar hydrological behaviour is a common method for reducing model complexity. The Representative Elementary Area (REA) approach defined by Wood et al. (1988) assumes that the size of the areal elements is defined by considering that the processes at smaller scales are hydrologically insignificant for modeling purposes. Wood et al. (1988) carried out an empirical averaging experiment to assess the impact of scale. They averaged simulated runoff over small subcatchments, aggregating the subcatchments into larger catchments, and repeating the averaging process. After ranking the runoff volumes and plotting the average runoff versus area, they found that after approximately 1 km^2 the curves flatted out with increasing area. Since different correlation lengths and spatially invariant precipitation did not significantly change this result, they concluded that the REA was strongly influenced by topography. Even though the concept of universal REA is attractive for modelling purposes (e.g. grid based models), it had been demonstrated that the size for a model element is dependent on the processes being represented and the type of climate, terrain and vegetation where the model is being applied (Blöschl at al., 1995, Woods et al., 1995). These results show that there is no evidence for one universal size of REA and that the size of REA depends on many factors, including storm duration and variability, flow routing and infiltration characteristics. It is therefore apparent that the size of the REA will be specific to a particular catchment and particular application.

The complexity of the environment and data availability have seen many researchers favour lumped or aggregated computational units. The main reason for that is to limit the increasing computational time, especially for larger basins and finer spatial resolution, and the number of parameters to be determined. Hydrological

Response Unit (HRU) is one of the more common aggregation approaches where the model units are defined according to the hydrological behaviour. These units can be related to landscape types and are characterised from an understanding of the hydrological processes and land use point of view. Therefore HRUs are usually defined by overlapping maps of different characteristics, such as soils, slope, aspect, vegetation cover, etc. (Flügel, 1995; Beven, 2001a). Similarly, Grouped Response Units (GRUs; Kouwen et al., 1993) is an alternative for describing spatial variability, where areas with similar land cover, soils, etc., are grouped with no requirement for grids or sub-basins to be hydrologically homogenous. For a detailed description of HRUs and GRUs see Chapter 4. The major disadvantage in models using aggregation methods based in similarities (e.g. HRUs, GRUs), is the way in which each unit is considered to be spatially homogeneous. In general, within a computational element the physics is conceptualised and effective parameter values are used to account for subgrid variability. The representative elementary watershed (REW; Reggiani, 2000; Reggiani and Schellekens, 2003) is another approach to represent spatial heterogeneity. The basis of the REW approach is that it is the smallest elementary unit into which a basin can be discretised for any given time scale of interest and that the governing equations derived from the REW approach are applicable directly at the catchment scale, as opposed to at the point or representative elementary volume (REV) scale as in current models. The REW unit is composed of five sub-regions: the unsaturated zone, saturated zone, concentrated overland flow zone, saturated overland flow zone and channel zone. Recent efforts have focused on the closure of the governing equations at the REW scale (Zehe et al., 2006).

There are several methods currently used to attempt to include subgrid heterogeneity into distributed modelling efforts. One includes replacement of the most important dependent variables in the governing equations by probability distribution functions (pdfs). Becker and Braun (1999) applied areal distribution functions of soil

water holding capacity to represent spatial heterogeneities distinguishing between agricultural and forested HRUs. However, they concluded that additional scaling laws are required for describing lateral flows between landscapes. Faria et al. (2000) examined the forest canopy influence on snow-cover depletion. They found that the frequency distribution of SWE under boreal canopies fit a log-normal distribution; and the highest canopy density had the most variable snow water equivalent. The relationships between the spatial distributions of SWE and melt energy promoted earlier depletion of the snow cover than if the melt energy were uniform, with the strongest effect in heterogeneous or medium density canopies. Another example is the explicit incorporation of parameterisation of subgrid variability through the use of a depletion curve into the snowmelt model by Luce et al. (1999) and Luce and Tarboton (2004). Analogous conclusions were reported by Pomeroy et al. (2004), where one of the major scaling problems in applying point-scale equations over large areas is the spatial association between driving variables and/or parameters, which can result in spatial correlations and covariance amongst the terms of a physically based equation. A different approach is the up-scaling of point-scale hydrological conservation equations to the computational grid areas. This mainly seeks to scale the governing equations so that they accurately represent the phenomena at the larger modelling scale. It is based on the 'coarse-graining' approach which states that mechanisms important in one scale are not important in either a much larger or much smaller scale (e.g. Kavvas et al., 1998; Kavvas, 1999).

2.3.5 Parameter estimation

One of the consequences of using sophisticated hydrological models or a detailed spatial model discretisation is the increase in the number of unknown model parameters with their associated uncertainties that when propagated through the model, increase the predictive uncertainty (Atkinson et al., 2003). Applicability of physically

based modelling approaches, which in theory would enable the parameters to be derived from field measurements, has been restrained by data availability, heterogeneity of process responses, and unknown scale-dependence of parameters. Prior information is thus limited and it is recognised that models and/or parameters must be identified through inverse modelling (Kavetski et al., 2003). Kuchment and Gelfan (1996) concluded that to improve the representation of the spatially average values of the snowmelt and the snowpack outflow, empirical parameters, used in a point model or for spatial averaging, need to be calibrated.

Calibration of hydrological models is meant to estimate the model parameters so that the model can closely match observed behaviour of the real system (Gupta et al., 1998). Traditionally the calibration of hydrological models has been performed manually by trial-and-error. The trial-and-error method implies a manual parameter adjustment by running a number of model simulations. Due to its limitations (e.g. subjectivity and time consuming processes), research into automatic calibration procedures based on the increasing computer power has led to the use of different automatic parameter optimisation approaches. These approaches are based in general on optimise (i.e. minimise or maximise) the value of one or several objective functions, used to measure the difference between observed and simulated data (Sorooshian and Gupta, 1995). Automatic parameter optimisation has the advantage, compared with manual calibration, that it is faster since it is computer based, is less subjective and the confidence of the model simulation can be explicitly stated. On the other hand, the difficulty in defining the best objective function or criterion to be optimised, the difficulty in finding the global optimum when many parameters are involved, the mutually dependency of, and the impossibility to distinguish between the different error sources are the main disadvantages of automatic calibration methods (Refsgaard and Storm, 1996).

Sources of uncertainty can be due to (1) random or systematic errors in the input data and recorded data used for comparison with the simulated output, and in the definition of the initial conditions, (2) errors associated with the values and conceptualisation of model parameters such as those used for landscape representation, and (3) errors due to an incomplete or inappropriate model structure. In addition, Duan et al. (1992) illustrated that, despite simple model structures and absence of input data error, the parameter estimation problem is not trivial. The estimation of optimum or reliable parameters is sometimes constrained by many regions of attraction (i.e. many local optima) in the parameter space, a rough response surface with discontinuous derivatives, a poor and varying sensitivity of response surface of objective functions, and non linear parameter interaction.

Research into automatic model calibration, with an increasing degree of sophistication generally linked with corresponding increases in computer power, has led to the understanding that there are no clear 'best' optimisation criteria and 'best' optimisation algorithms. (e.g. Duan et al. 1994; Boyle et al. 2000). Furthermore, Beven and Binley (1992) introduced the term of 'equifinality' which indicates that many parameters sets are capable of producing model outputs with similar performance statistics. They developed the Generalised Likelihood Uncertainty Estimation (GLUE) approach, where parameter sets are evaluated in terms of likelihood measurements. Definition of behavioural parameters is usually performed using a threshold criterion. Model outputs for these parameters are ranked using a weighted likelihood measure to form a cumulative distribution function from which predictive bounds can be calculated. There are a variety of methods to combine likelihood measurements. In general, a GLUE application for a given model requires the definition of parameter ranges, selection of the sampling strategy in the parameter space (e.g. uniform, latin hypercube), and the choice of the likelihood measures for model evaluation and parameter rejection.

For models with significant run times and a large number of parameters, the GLUE approach is not suitable.

Part of the lack of uniqueness of parameter sets lies in the use of a single criterion for model performance, and recently the automatic calibration procedures have focussed on the use of multiple performance criteria. The multi-criteria approach addresses the optimisation problem by performing automatic search of the feasible parameter space using several optimisation criteria or objective functions (e.g. Gupta et al., 1998; Yapo et al., 1998; Madsen, 2000 and 2003). Thus, there are several parameter sets that are 'equally good', which are commonly referred to as Pareto optimum solutions (i.e. non dominated solutions).

2.3.6 Regionalisation of model parameters

Regionalisation methods imply the transference of model parameters from a basin that is expected to behave similarly to the basin of interest. The similarity measure can be based on spatial proximity, basin attributes, or similarity indices (Blöschl, 2005). There are several regionalisation techniques, and nearly all studies follow the same approach (e.g. Blöschl and Sivapalan, 1995; Abdulla and Lettenmaier, 1997; Fernandez et al., 2000; Littlewood, 2003). Typically, regionalisation techniques involve the definition of relationships between calibrated model parameters and basin attributes. The most common methods are the bivariate and multivariate regression methods between parameters and basin attributes, and the definition of clusters or groups of basins in hydrologically homogeneous areas where apriori defined parameters can be applied. These relationships can be derived either from the calibrated model parameters (direct calibration method) or by calibrating the functional function (regional calibration method). The main factors that make the transfer of model parameters difficult are that optimal parameters sets, found through calibration, depend on the models and objective functions used to measure their performance (Gupta et al., 1998;

Madsen, 2003), that parameters are uncertain, and that parameters are not unique (equifinality), since many parameter sets might produce similar simulations (Beven and Binley, 1992; Kuczera and Mroczkowski, 1998).

Hydrological regionalisation studies have so far shown limited success and in general depend on the degree of similarity between the basins and on the type of the data used in the regional analysis (Littlewood, 2003). Merz and Blöschl (2004), using a lumped model, suggested that more stable relationships between parameters and basin attributes can be found using multi-objective calibration procedures. They found that spatial proximity was the better spatial indicator of runoff dynamics compared to regression methods, and it was not clear whether this was due to the basin attributes being poor hydrological indicators at the regional scale or due to problems with the linearity assumption of the multiple linear regressions used. Examples of regionalisation of distributed conceptual models includes the study performed by Götzinger and Bárdossy (2007), however fewer studies address the transference of physically based model parameters. Chapter 7 further explores this analysis and describes the transference of landcover based parameters.

CHAPTER 3

STUDY AREA

3.1 Introduction

The selection of the Wolf Creek Research Basin (WC) as a study site was based on the substantial amount of research conducted in this basin, the corresponding availability of meteorological and field data, and its representativeness as a headwater basin of the subarctic cordilleran landscape of northern Canada. Research began in 1992 as part of Indian and Northern Affairs Canada's Arctic Environmental Strategy, in partnership with National Hydrology Research Institute (NHRI) of Environment Canada, designed to improve knowledge of Yukon waters. Additionally, the basin was the subject of several research projects of the University of Saskatchewan and other Canadian universities, including studies of snow accumulation and ablation process, runoff generation, and infiltration and subsurface drainage in organic and frozen soils. Furthermore, the basin was selected as a program site of the Global Energy and Water Cycle Experiment (GEWEX) following the initiative of the World Climate Research Programme to improve the ability to model energy and water balance processes and assess the sensitivity of these processes to climate change.

Similarly, the Trail Valley Creek Research Basin (TVC) was also selected as a study site as a result of the substantial research conducted in this basin and its corresponding data availability. The basin, located just outside of the lower Mackenzie Valley, is representative of the subarctic-arctic tundra transition zone. Numerous

hydrological studies have been conducted since 1992 by NHRI, most of them focussing on snow accumulation, snowmelt and snowmelt runoff processes. In 1994 the basin was also selected as a site of the Mackenzie GEWEX study (MAGS), focussing on the description of snow accumulation and ablation processes and on modelling prediction.

3.2 Wolf Creek Research Basin

3.2.1 Description

The Wolf Creek Research Basin (WC) encompasses an area of 195 km^2 in the southern part of the Yukon Territory, Canada. It is located 15 km south of Whitehorse and lies in the interior edge of the Coast Mountains at approximately 61° N latitude, 155° W longitude (Figure 3.1). The basin is part of the southern mountainous headwaters of the Yukon River Basin and is situated within the Boreal Cordillera ecozone and between the "Southern Yukon Lakes" and "Yukon-Stikine Highlands Ecoregions" (Environment Canada, 1995). It is drained by Wolf Creek and has a general north-easterly aspect with elevations range from 800 to 2035 m a.s.l. and a median elevation of 1325 m a.s.l. The geological framework consists of bedrocks covering 50-60% of the basin area, whereas the remaining 40-50% of the area is covered by deposits of glacial, glaciofluvial, alluvial, lacustrine, and windblown material (Seguin et al., 1999). This mantle of glacial till ranges from a thin veneer to depths of one to 10 metres. Upper elevations present frequent bedrock outcrops with shallow glacial deposits of colluvial material, whereas the valleys are extensively scoured and covered with fine textured alluvium (Mougeot and Smith, 1994).

The WC basin is within the sporadic discontinuous permafrost zone (Heginbottom et al., 1995) underlying approximately 25-32% of the basin (Seguin et al., 1999). Lewkowicz and Ednie (2004), using the basal temperature of the snow to predict the distribution of the permafrost, determined that continuous permafrost (permafrost probabilities, p>0.9) was found above 1800 m a.s.l. but that these areas cover only 5% of the basin. Most of the area between 1400 and 1700 m a.s.l. showed discontinuous permafrost (p= 0.5-0.9), whereas the lower area (800-1400 m a.s.l) presented sporadic discontinuous permafrost (p= 0.1–0.5). Permafrost is present in NF slopes, poorly drained areas, or areas with significant organic layers which provide insulation. In permafrost areas and the riparian zones, soils are capped by an organic layer up to 0.4 m thick consisting of peat, lichens, mosses, sedges and grasses (Carey and Quinton, 2005).

The WC basin spans three major ecosystems based primarily on a gradient of elevation. The boreal forest (spruce, pine, aspen) is found in lower areas (800-1300 m a.s.l.), subalpine taiga (shrub tundra) is found at mid-elevations (1300-1800 m a.s.l.), while alpine tundra (short shrubs, forbs and bare rock) dominates high elevation areas (1800-2035 m a.s.l.). These ecological zones cover 22, 58 and 20% of the basin area respectively (Francis, 1997).

The climate is sub-arctic continental which is characterized by a large variation in temperature, low relative humidity and relatively low precipitation. Mean annual temperature is in the order of -3°C, with summer and winter monthly mean temperatures ranging from 5° to 15°C, and -10° to -20°C, respectively. Summer and winter extremes of 25° and -40°C are not uncommon. An Arctic inversion develops during the winter months when air temperature can increase with elevation. Mean annual precipitation is 300 to 400 mm with approximately 40 percent falling as snow (Pomeroy et al., 1999).

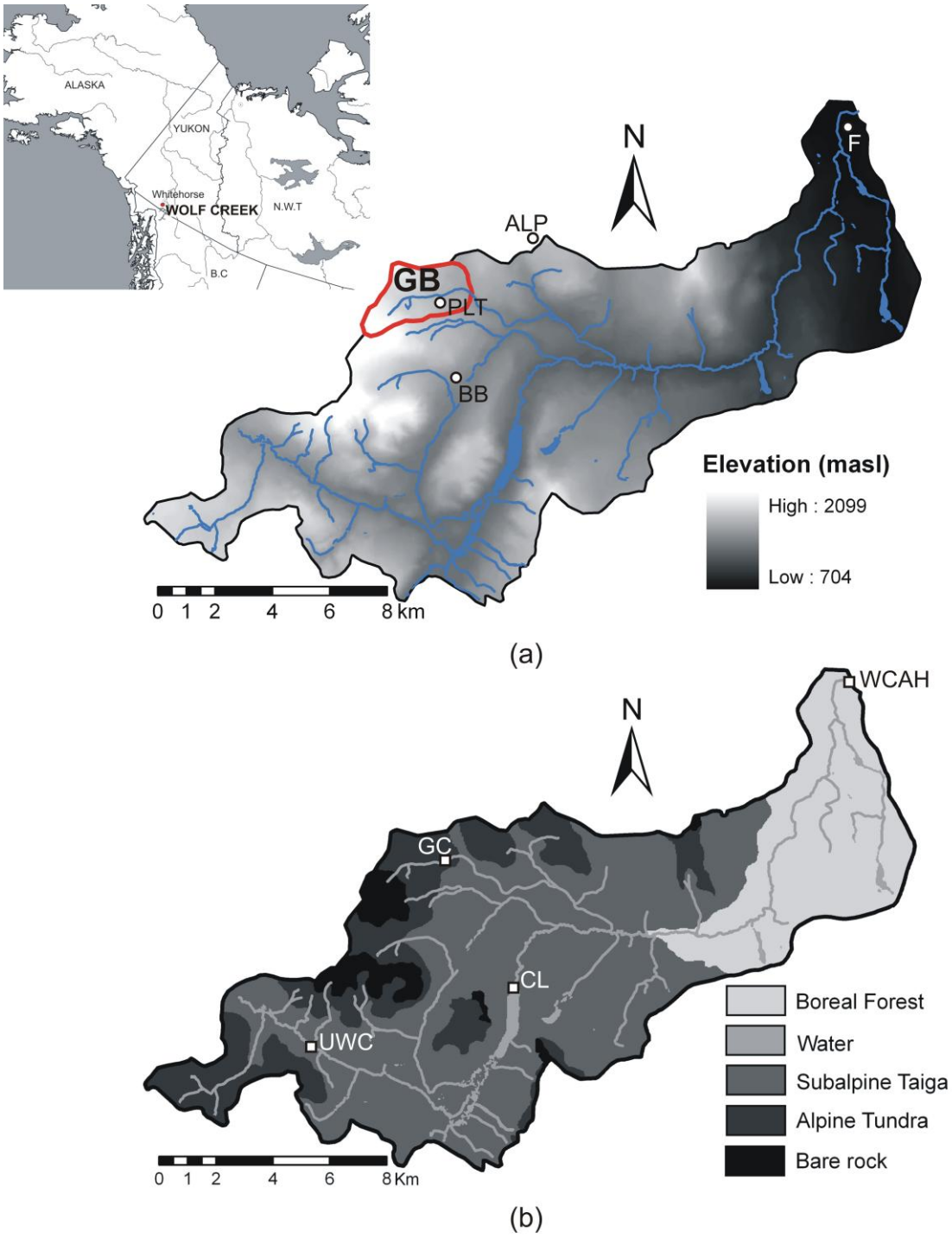

Figure 3.1: Wolf Creek Research Basin (WC). a) Topographic map. GB: Granger Basin. Circles indicate meteorological stations (PLT: Plateau, ALP: Alpine, BB: Back-brush, and F: Forest), b) Land-cover map. Squares indicate streamflow gauge stations. (UWC: Upper Wolf Creek, GC: Granger Creek, CL: Coal Lake, and WCAH: Wolf Creek Alaska Highway). Inset shows location in Canada

The snowmelt period extends up to two months starting approximately in mid April to the end of May or early June, depending on aspect and other slope characteristics. A study in the shrub area showed that snowmelt runoff is limited to slopes with ice-rich substrates with reduced infiltration (Carey and Woo, 2001a and b). Summer runoff (interflow) dominates in slopes with porous organic layers overlying mineral soil, with differences in flow determined by the location of the water table. Snowmelt is responsible for much of the annual basin runoff and most of the peak discharges in subarctic mountainous regions. Basin streamflow response is characterized by peak flows of 10 to 20 $m^3 \cdot s^{-1}$ in late May or early June due to snowmelt with low flows occurring in March. Winter flows are relatively high, in the order of 0.4 $m^3 \cdot s^{-1}$, presumably due to the substantial lake storage within the basin and groundwater contribution. Interannual variability is very important due to differences in snowfall and subsequent wind redistribution resulting in different spring melt rates, and also as a result of frequent and intense summer rainstorm events which produce secondary peaks (Janowicz, 1986).

3.2.2 Granger Basin

Granger Basin (GB) is a small 8 km^2 sub-basin located in the north-west fringe of WC basin (see Figure 3.1). It is drained by the Granger Creek which with a length of approximately 3 km flows from the base of Mount Granger following a north-easterly direction. Physiographically, the basin is characterised by a north-easterly aspect and ranges in elevation from 1310 to 2035 m a.s.l. Five main distinct landscapes were identified according to both field observations of vegetation cover, soils and permafrost, slope, and exposure, and the basin units described by McCartney (2006). Figure 3.2 illustrates the location of the landscapes units in GB whereas Table 3.1 summarises the characteristics of the identified landscapes. The upper basin (UB), located between 1600 and 2035 m a.s.l. in the lee side of Mount Granger, has a northeast oriented 15°

slope. Colder climate conditions and exposure result in a very sparse vegetation cover where grasses, lichens and mosses prevail. No organic layer is observed and the mineral soil is generally exposed. A small perennial snowpack in the upper reaches of the UB is evidence of the climate and snow drift inputs from upwind catchments. The plateau (PLT) area expands over an area of 1 km^2 at an elevation of 1500 m a.s.l. and its vegetation cover is characterised by short shrubs (<0.3 m). Mineral soil prevails with a thin organic layer. The NF slope is where the organic layer is more significant and continuous permafrost is observed. It is located near the basin outlet and comprises an area of approximately 1 km^2. Vegetation cover is composed by a mix of tall (1 m) and short (0.3 m) shrubs. The SF slope, with similar vegetation cover to the NF slope, expands on the north fringe of the basin covering an area of approximately 3 km^2. The organic layer is less significant, whereas discontinuous permafrost with a patchy structure is observed at the beginning of the melt season. The valley bottom (VB) includes the lower reach of Granger Creek near the basin outlet. It is characterized by a significant presence of organic layer and by tall shrubs (1-2 m).

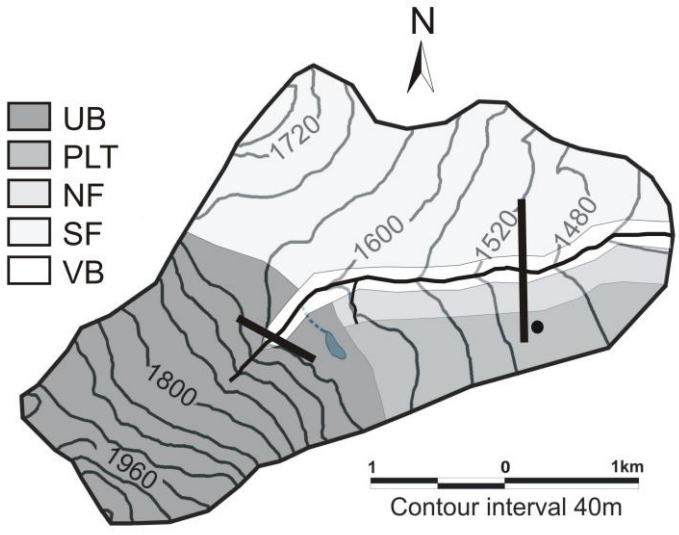

Figure 3.2: Landscape units of Granger Basin. UB: Upper basin, PLT: Plateau area, NF: North facing slope, SF: South facing slope, and VB: valley bottom. Back lines indicate snow survey transects. Circle: meteorological station.

Table 3.1: Physiographic characteristics of the landscapes units at Granger Basin. Vegetation cover and soil type were adapted from McCartney (2006) and Bewley (2006). sh: shrubs, gr: grasses (also lichens, mosses, peat), and bg: bare-ground (also rocks).

Landscape unit	Area (km^2)	Elevation Type (m)	Vegetation Type	Vegetation cover (%)			Soil type
				sh	gr	bg	
Upper basin (UP)	2.5	1600 - 2035	bare-ground	35	45	20	mineral/rocks
Plateau area (PLT)	1	1460 - 1520	short-shrubs (<0.3m)	80	15	5	mineral + thin organic layer (< 0.1m)
North facing slope (NF)	1	1350 - 1460	mix-shrubs (0.3-1m)	78	17	5	thick organic layer (0.25m) + mineral
South facing slope (SF)	3	1350 - 1760	mix-shrubs (0.3-1m)	74	20	6	organic layer (0.12m) + mineral
Valley bottom (VB)	0.5	1310 - 1350	tall-shrubs (> 1 m)	71	19	10	organic layer (0.14m) + mineral

3.2.3 Observations

The study period includes the snowmelt seasons of 2002, 2003, and 2004. The selection of these periods was based on data availability. Meteorological observations consisted of measurements of air temperature, relative humidity, incoming short and long wave radiation, atmospheric pressure, precipitation, and both wind speed and direction. Observations were made on the PLT area of GB, buck-brush station, alpine station, and forest station (McCartney, 2006; Yukon Environment).

Snow surveys were typically conducted on a daily basis from mid-April to early June in each of the landscape units of GB. These surveys consisted of transects where both snow depth and density were measured every 5 and 10 metres respectively. Length of the transects varied as a function of the landscape heterogeneity, thus when the snow cover was continuous a total of approximately 50 and 25 points were measured in the UB, and the PLT area, whereas 20, and 6 points were measured in the NF and SF slopes, and the VB respectively (for more details see McCartney, 2006). Table 3.2

illustrates the available snow survey transects and their corresponding initial SWE values.

Table 3.2: Initial SWE in mm for each landscape unit of GB. The aggregated values (AGR) were calculated from the spatially weighted basin-average using NF, SF, and VB landscape units.

year	UB	PLT	NF	SF	VB	AGR
2002			303.6	114.6	150.1	160.9
2003	187.8	138.9	218.4	275.2	172.0	251.1
2004		94.8	239.6	229.6	180.8	226.6

Because of random measurement errors such as difficulties in sampling snowdrifts due to compacted snow, the use of different snow samplers (ESC-30 and Mount Rose for shallow and deeper snowcovers respectively), ice crusts, or keeping loose granular snow in the corer, corrections to the estimated SWE were conducted in those locations where highly variable snow density were measured. Appendix A shows the corrections performed in the observations of snow cover ablation. Additional pre-melt snow surveys conducted on the forest area, alpine and buck-brush stations were used to determine the initial conditions at these locations. Figure 3.3 illustrates the estimation of SWE at the NF in 2002. The linear relationship between snow depth and snow density showed a weak association mainly at early stages of melt with a large scatter around the straight line (see Appendix A). Since an important snow drift was seen that likely made the snow density measurements difficult, the density was held constant around the highest observed value (300 kg m^{-3}) corresponding to drifted snow till 10 May, whereas for the remaining period a linear fitting of the observed density values was used in order to reduce their variability.

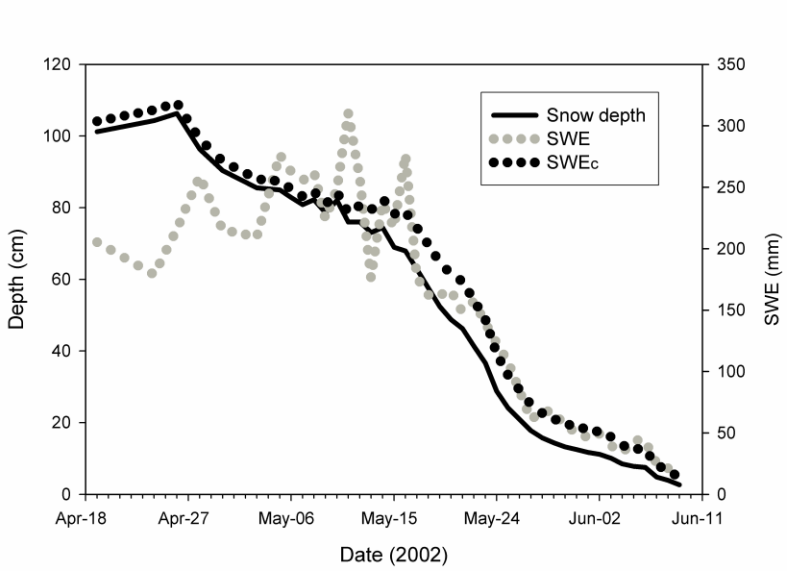

Figure 3.3: Observed and calculated snow ablation at the NF slope of GB in 2002. SWE: snow water equivalent calculated from observations, SWE_C: corrected snow water equivalent.

Canopy structure measurements such as shrub cover, vegetation height, and plant area index (PAI) were taken along the NF, VB, SF and PLT snow survey transects, and in a 30 m x 30 m grid (GB-grid) located in the VB beside the snow survey transect (Bewley, 2006). Observations of shrub cover included the use of aerial photographs from a camera mounted on a remote controlled model helicopter, whereas PAI, defined as the ratio between the total plant surface area and the surface area of ground covered by plants was calculated using two methods, a LAI-2000 Canopy Analyzer and an upward-looking hemispherical (fish-eye) camera using GLA software (Frazer et al. 1999). Values of fraction of the landscape covered by shrubs (Fs) at the VB varied from 0.20 % to 0.71 % at early and late stages of the snowmelt season respectively. Average LAI (i.e., plant area index) values were obtained using upward-looking hemispherical (fish-eye) photographs taken at 5 m intervals across the GB-grid and a LAI-2000 Canopy Analyzer along the PLT snow transect for late melt stages. Average LAI values were 0.43 for tall shrubs exposed above the snow in the VB and 0.31 in the PLT area at the end of April of 2004, whereas LAI values above 2 were measured in summer time in

different points of the basin. Values of Fs and LAI for the remaining landscape units were estimated by comparing their canopy structure such as vegetation height and density with the measured sites and from previous LAI measurements in similar sites of WC basin.

Measurements of areal albedo (flux-weighted by wavelength) above the canopy were conducted in 2003 and 2004 at the PLT area and the VB. Initial pre-melt albedo values for the tall and short shrubs (short shrubs were essentially an unvegetated snow field at this time) were 0.39 and 0.89 respectively. Larger and faster albedo decays were observed on the PLT area due to the abrupt change in snow covered area as bare patches emerged when the shallow snow melted; in contrast tall shrubs areas showed a gradual albedo decay along the snowmelt season as shrubs potentially emerged from the snow during melt of a much deeper snowpack.

Runoff data expressed as daily mean flow values were collected at a permanent stream gauge at the GB and WC basin outlets by the Yukon Territorial Government and Water Survey of Canada respectively.

3.3 Trail Valley Creek Basin

3.3.1 Description

The Trail Valley Creek Research Basin (TVC) is an arctic basin with an area of 57 km^2. It lies approximately 55 km north-east of Inuvik in the Northwest Territories, Canada, at 68° 45'N, 133° 30'W (Figure 3.4). The basin is located at the northern edge of the subartic-tundra transition zone. The area has a low relief characterized by gently rolling hills with some deeply incised river valleys. Elevation ranges from 48 to 205 m a.s.l. The landscape is dominated by open tundra in the upland areas, whereas shrub tundra is along streams, lake edges, and river valleys, as well as some upland areas. Vegetation in the upland open tundra areas consists mostly of grasses, lichens (*Lecidea*)

and mosses (*Sphagnum*), while tall shrubs (*Alnus, Betula, Salix*), with height ranging from 0.5 to 3m, dominates in moister hillslopes and valley bottoms, and sparse pockets of black spruce (*Picea*) forest.

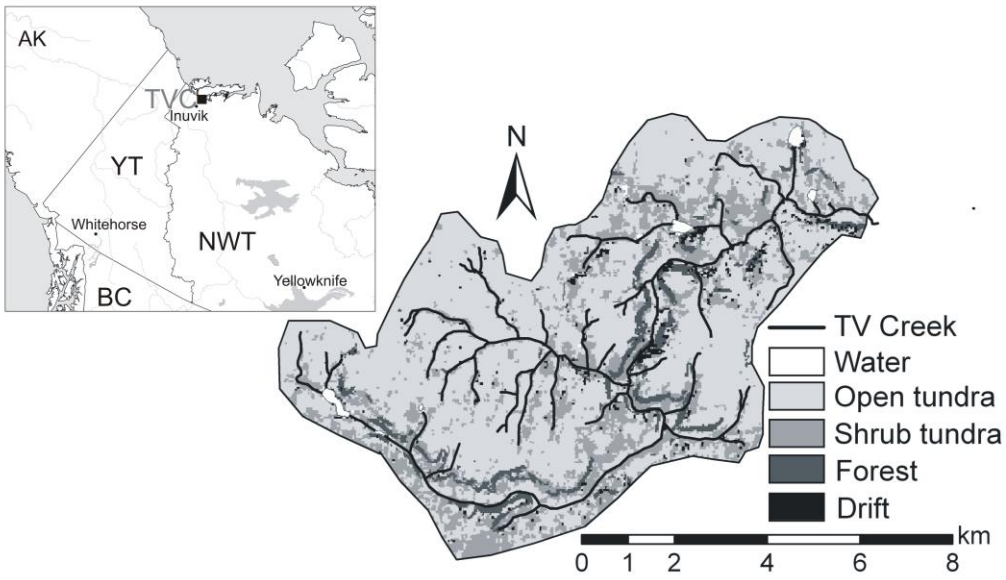

Figure 3.4: Trail Valley Creek Research Basin (TVC). Inlet illustrates its location in Canada

The basin is underlain by continuous permafrost. Ground surface is characterised by numerous periglacial features such as ice wedges, earth hummocks and thermokarst phenomena, while maximum observed active layer depths range between 0.4 and 0.8 m depending on aspect and soil type (Marsh and Pomeroy, 1996). Soils are organic cryosols, consisting of an upper peat layer over a silty clay mineral soil (Quinton and Marsh, 1999). The peat, depending in the stages of developments, varies from scarcely decomposed and little compacted to highly humified and dense and ranges in thickness from 0.2 to 0.5 m (Quinton et al., 2000).

The climate of the region is characterized by short summers and long cold winters, with an eight month snow-covered period. The snowmelt period is short and extends approximately one month, from mid May to early June. Timing and magnitude of snowmelt runoff volumes are also frequently affected by snow-ice dams in the creek.

Landscapes types were classified using a midsummer Landsat Thematic Mapper image (Marsh and Pomeroy, 1996). The resulting landscape classification map is shown in Figure 3.4, and the percentage cover of each landscape type is given in Table 3.3. Drift are defined as the areas including a slope greater than 9°, stream channels and lake shorelines.

Table 3.3: Physiographic characteristics of the landscapes units at Trail Valley Creek Research Basin. Vegetation cover was adapted from Marsh and Pomeroy (1996).

Landscape unit	Area (km^2)	Vegetion-Landscape Type
Open tundra	69.8	Tundra Sparse shrubs
Shrub tundra	21.5	Open shrubs Closed shrubs
Drift	8.2	Slope drift Channel and lake shortlines
Forest	0.5	Sparse forest

3.3.2 Observations

Simulations in TVC basin were performed in the snowmelt seasons of 1996 and 1999, respectively. Meteorological observations were conducted in the study basin at two permanent measurement stations on a half-hourly basis. Given the lack of observations of incoming long wave radiation in TVC, the same forcing data used by Pohl et al. (2005b) and Pohl and Marsh (2006) were applied. Therefore, outputs from the numerical weather model (GEM, Global Environmental Multiescale) model of Environment Canada were used in 1996, whereas calculated empirical values with the Satterlund (1979) equation that were found to match fairly closely the GEM outputs, were used in the 1999 snowmelt season.

Simulations of snowcover depletion were contrasted to the observed basin average snow covered area (SCA) in TVC. Observed values were determined from

SPOT satellite images by aggregating the 20 m resolution images to 1 km grid squares corresponding to the model grid. Six images were obtained during the snowmelt period of 1996 (23 May, 25 May, 28 May, 1 June, 5 June, and 8 June) (Neumann and Marsh, 1998), whereas three SPOT images (23 May, 28 May, and 10 June) were used in the 1999 snowmelt seasons (Pohl and Marsh, 2006). Runoff data expressed as daily mean flow values were collected at a permanent stream gauge at the TVC basin outlet by the Water Survey of Canada.

CHAPTER 4

METHODOLOGY

4.1 Introduction

The purpose of this chapter is to present the methodology used to simulate snowcover ablation and snowmelt runoff in complex subarctic environments. The modelling strategy is centred on the research and observation evidence of the processes controlling snowmelt and runoff generation conducted in research northern basins in the last 20 years. The main focus of this section is on the reasoning used for modelling which includes an evaluation of the uncertainties related to the representation of the landscape heterogeneity, the effects of initial conditions and forcing data, and the identification of landscape based parameter sets. Application of this modelling approach was presented in Dornes et al. (2006), Dornes et al. (2008a), and Dornes et al. (2008b).

4.2 Modelling approach

Traditionally, either deductive or inductive strategies to model building have been applied. In the deductive or hypothetical approach there is 'a priori' conceptualisation of the model structure based on the perception of the scientist-modeller. As a result, the model structure is strongly conditioned by observations and assumptions that derive from scientific hypotheses. In the inductive approach,

theoretical preconceptions are avoided as much as possible in the initial stages of the analysis. In particular, the model structure is not pre-specified; rather it is inferred from the observational data. In the context of hydrological modelling these approaches are also identified as 'bottom up' or 'upward' and 'top down' or 'downward' respectively.

The deductive approach assumes that a detailed understanding and conceptualisation of the processes at smaller scales is needed to develop process descriptions at larger scales. In this approach, spatial distributions of processes and their spatial limits are specified from what is understood and limited by physics of the coupled energy and mass system. Typically, this means that physically based equations developed at laboratory or point-scale are usually applied to describe hydrological processes at larger scales (i.e. basin models). The deductive approach is based on a deterministic reductionism where it is believed that the physical system can be described very well, if not exactly, by these deterministic mathematical equations (Young, 2003). Thus, the model building process using a deductive approach focuses on what we know in a hydrological model using mathematical equations and physical laws and then sees how this fits to generate runoff. Examples of deductive hydrological applications include the SHE model. Conversely, the inductive approach has a model structure which is inferred from the data (e.g. streamflow data) whereas the model conceptualisation is based on the dominant processes at the catchment scale (Sivapalan et al., 2003b). The inductive approach was described by Klemeš (1983) who defined it as the "route that starts with trying to find a distinct conceptual node directly at the level of interest (or higher) and then looks for the steps that could have led it from a lower level". In other words, information or model complexity is added when the prior conceptualisation was not able to describe the processes of interest. Inductive

hydrological models range from the rational method, unit hydrograph, to many conceptual models like the SWM.

The deductive approach can have important limitations because of the change of dominant processes with changing scales, where it can be argued that at a large scale not all the complexity embedded in small-scale is actually necessary. Another related problem is the excessive model complexity relative to data availability. The inductive approach on the other hand, also has some limitations. Since it attempts to identify conceptual relationships, to represent the process, directly at the scale of interest (e.g. basin) and interprets these as properties and processes occurring at finer scales, small-scale process interactions are usually ignored (Sivapalan et al., 2003b) which often violate continuity laws.

The conceptual methodology of this study is based on the combination of the strength of the two main reasoning approaches used in hydrological modelling. Thus, the inductive (i.e. top-down) and deductive (i.e. bottom up) modelling approaches are combined to cope with the main uncertainties for reliable snowmelt model predictions in subarctic mountain environments such as the landscape heterogeneity, model parameterisation, and the lack of distributed data. The inductive approach was used for the identification of these units (i.e., basin segmentation) based on a basin-wide understanding of the main hydrological responses, whereas a deductive modelling approach, based on a detailed process description, was applied in each of the model units to generate the physically based forcing data and process representations. The modelling methodology of this study includes different modelling techniques that involve up-scaling and regionalisation exercises. The goal is to define an appropriate modelling strategy in cold regions environments that would allow the scaling from point scale observations to catchment scale models and the identification of stable landscape-based model parameterisations in order to reduce the predictive uncertainty in ungauged basins. The methodology is summarised in the following and in Figure 4.1.

1. A hydrological model (CRHM, Cold Regions Hydrological Model) was used to simulate snowcover ablation and basin runoff in a small-scale subarctic mountain basin (GB) using detailed process descriptions such as correction of the incoming solar radiation due to topography and infiltration into frozen soils.

2. A land surface scheme (CLASS, Canadian Land Surface Scheme) was run independently in each of the landscape units of the same basin using the corrected solar forcing provided by CRHM. The numerical exercise included the analysis of simulations of snowcover ablation using distributed initial snow conditions and solar forcing with respect to the traditional approach where grid uniform snowcover conditions and solar forcing are assumed.

3. A land surface hydrological model (MESH, Modélisation Environnementale-Surface and Hydrology) was then applied to a larger basin (WC) where distributed simulations of snowcover ablation and snowmelt runoff were performed using the snowmelt parameterisation defined in point 2.

4. Finally, a regionalisation exercise was applied in order to test the landscape based parameter defined in point 2 in TVC basin using MESH.

As a result, the philosophical basis of the modelling approach is the desire to describe the processes in as physically-realistic manner as possible given the availability of data and parameters to run the models.

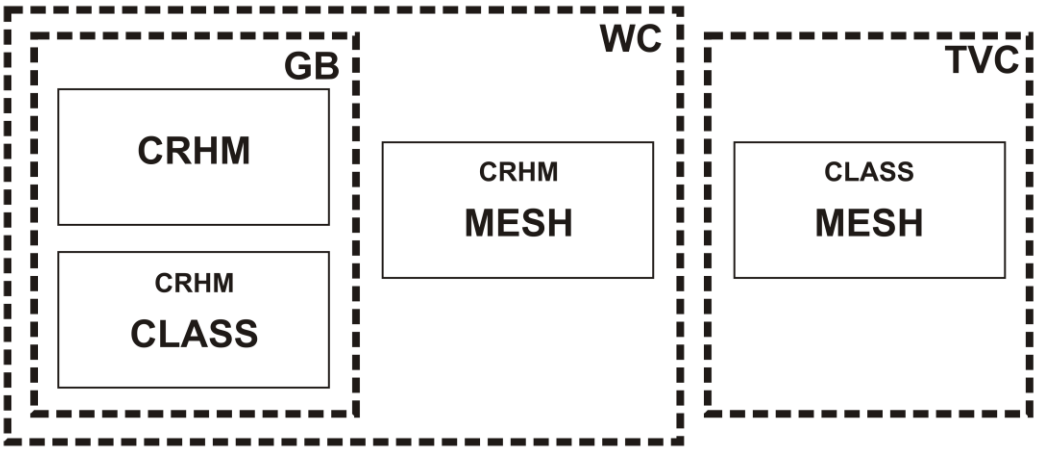

Figure 4.1: Illustration of the modelling strategy. CRHM: Cold Regions Hydrological Model, CLASS: Canadian Land Surface Scheme, MESH: Modélisation Environnementale-Surface and Hydrology model, GB: Granger Basin, WC: Wolf Creek Basin, and TVC: Trail Valley Creek Basin.

4.3 Model descriptions

Three models were used in this study. The selection of these models was based on their physically based description of cold region processes. The analysis included a hydrological model (CRHM), a land surface scheme (LSS) (CLASS) and a LSS-hydrological model (MESH).

4.3.1 Cold Regions Hydrological Model

The Cold Regions Hydrological Model (CRHM; Pomeroy et al., 2007) is a distributed and physically based hydrological model which is the result of extensive research in cold regions environments (e.g., Gray and Landine, 1988; Pomeroy et al., 1998a; Gray et al., 2001; Sicart et al., 2006). It has a modular structure that allows for different process representations. Physically based algorithms are integrated in the model through different modules such as radiation, infiltration into frozen soils, snow interception, snow transport, snowmelt, etc., that finally route the water via different pathways. This model platform offers a great flexibility in the selection and combination of cold region hydrological processes, where a wide range of process

descriptions from conceptual to physically-based approaches can be linked to simulate a hydrological response of a given area. The spatial representation is based on the Hydrological Response Unit (HRU) concept.

Figure 4.2 depicts the relevant CRHM modules and the forcing data used in this application. Two main subdivisions can be identified: (1) physically-based modules, which include algorithms developed using the physical principles governing processes, such as energy balance snowmelt, evaporation and infiltration into frozen soils; and (2) conceptual modules, which represent processes that are less well understood, such as the soil moisture balance and flow routing. Modules describing blowing and intercepted snow are considered not outside of the scope of this research. Instead, initial SWE values from filed observations, were used to initialise the model at each model unit. Forcing of the data is handled in the OBSERVATION module. The main features of this module include the use of a threshold temperature parameter (0°C) to distinguish between snowfall and rainfall events, and a lapse-rate correction (6.5°C/1000 m) to account for elevation effects. The GLOBAL module accomplishes the partitioning of the incoming solar radiation according to slope and aspect, and cloudiness effects. Direct shortwave radiation (K_{dir}), diffuse shortwave radiation (K_{dif}), and a cloudiness index (c) are calculated using expressions proposed by Garnier and Ohmura (1970). The determination of c is based on the comparison between the observed incoming shortwave radiation ($K\downarrow$) and the theoretical clear sky direct-beam component of solar radiation (K_{theo}) over flat areas, and is then used to calculate K_{dir} on slopes having some aspect. The contribution of diffusive sky radiation, K_{dif}, is first estimated for flat areas (List, 1968) using the extra-terrestrial solar irradiation on a horizontal surface at the outer limit of the atmosphere K_{ext}, and then corrected by slope and aspect following Garnier and Ohmura (1970). Net radiation and ground heat flux are calculated in the NETALL module using the algorithm presented by Satterlund (1979) for estimating

daily net longwave radiation and presuming that ground heat flux is proportional to net radiation. Net radiation calculated in the NETALL module is not used for snowmelt calculations, but for evapotranspiration.

Snowcover albedo is estimated in the ALBEDO module, which assumes that the albedo depletion of a shallow snow cover, not subject to frequent snowfall events, can be approximated by three line segments of different slope describing the periods: pre-melt, melt and post-melt (the period immediately following disappearance of the snow cover). This approach was based on several years of point and areal measurements of reflected shortwave radiation during the snowmelt period (Gray and Landine, 1987). Snow-cover ablation is estimated using the Energy-Budget Snowmelt Model (EBSM module; Gray and Landine, 1988). The model uses the snowmelt energy equation (equation 4.1) as its physical framework, and physically-based procedures for evaluating radiative, convective, advective, and internal-energy terms from standard climatological measurements:

$$Q_M + Q_N + Q_H + Q_E + Q_G + Q_D = \frac{\mathrm{d}U}{\mathrm{d}t} \tag{4.1}$$

where Q_M is the energy available for snowmelt, Q_N is the net radiation, Q_H is the turbulent flux of sensible heat, Q_E is the turbulent flux of latent energy, Q_G is the ground heat flux, Q_D is the advection energy from external sources, and $\mathrm{d}U/\mathrm{d}t$ is the flux rate of change of internal energy in the snowpack. All units are in W m^{-2}.

Daily estimates of net radiation, maximum and minimum air temperature, threshold air temperature for melt initiation, and snow-cover and snowfall depths to establish the "start" of the melt and albedo depletion rate are used to drive the EBSM. The net radiation is calculated for pre-melt as follows:

$$Q_N = -0.04 + 0.76\left\{\underbrace{Q_0\left(0.52 + 0.52\frac{n_s}{N}\right)(-\alpha)}_{\text{net short - wave term}} + \underbrace{0.97\sigma T_a^4\left[(-0.39 + 0.093e_a^{0.5})\left(0.26 + 0.81\frac{n_s}{N}\right)\right]}_{\text{net long - wave term}}\right\} \tag{4.2}$$

and for the melt period:

$$Q_N = -0.53 + 0.47 Q_0 \left[0.52 + 0.52 \frac{n_s}{N} \right] (1 - \alpha) \qquad (4.3)$$

where Q_0 is the daily clear-sky shortwave radiation incident to the surface [MJ m^{-2} d^{-1}], n_s is the number of hours of bright sunshine in the day, N is the maximum possible number of hours of bright sunshine in the day, α is the mean surface albedo, σ is the Stefan-Boltzmann constant (4.9×10^{-9} MJ m^{-2} K^{-4} d^{-1}), T_a is the mean daily air temperature [K], and e_a is the mean daily vapour pressure of the air [mbar]. The ratio n/N can be estimated from c, the cloudiness index, using shortwave radiation measurements if sunshine hours are unavailable (as in this application).

Turbulent transfer of sensible and latent heat is derived from boundary layer–flux–profile relationships, whereas the amount of melt, M, is calculated from Q_M (Equation 4.1). Daily melt [mm·d^{-1}] can be approximated by $M = 0.270 \cdot Q_M$ when Q_M is in W·m^{-2}. The fluxes directed towards the snowpack are taken as positive whereas those directed away are negative:

$$M = \frac{Q_M}{\rho_w \lambda_f B} \qquad (4.4)$$

where ρ_w is the density of water (1000 kg·m^{-3}), B is the thermal quality of the snow or fraction of ice in a unit mass of wet snow (B usually ranges from 0.95 to 0.97) and λ_f is the latent heat of fusion of ice (3.335×10^5 J kg^{-1}).

The change in internal energy (dU/dt) of the snowpack is estimated using an algorithm that assumes a minimum state of internal energy determined by the minimum daily temperature, a maximum state equal to zero, a maximum liquid-water-holding content of the snowcover equal to 5% by weight, a snowcover density of 250 kg·m^{-3}, and no melt unless indicated by the model.

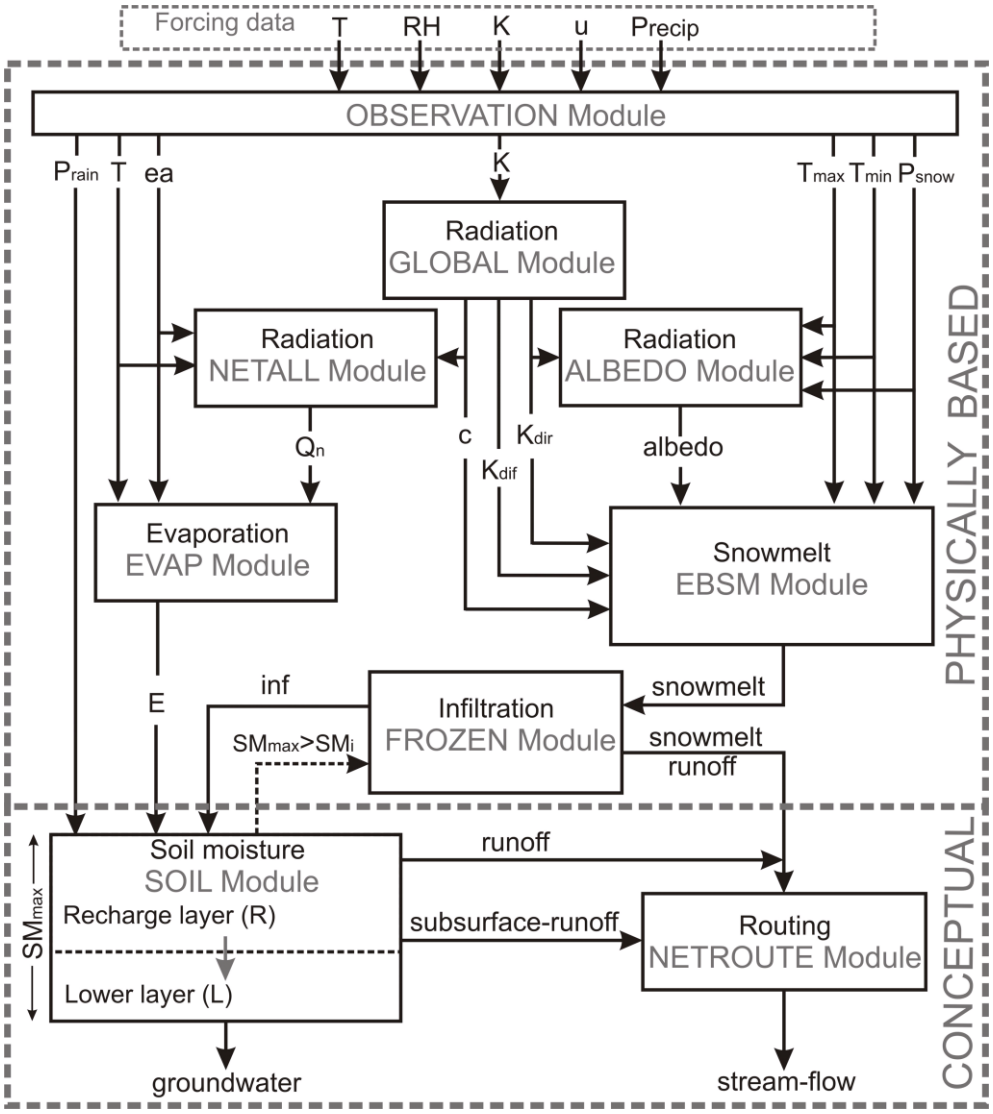

Figure 4.2: Outline of the modular structure of the CRHM model used. Solid arrows indicate module input/outputs. Dashed arrow indicates module feedback. *T*a: air temperature [°C], RH: relative humidity [%], *K*↓: incoming shortwave radiation [Wm^{-2}], *u*: wind speed [$m \cdot s^{-1}$], Precip: precipitation (mm), ea: water vapour pressure (Pa), T_{max}: daily maximum air temperature [°C], T_{min}: daily minimum air temperature [°C], K_{dir}: direct shortwave radiation [$W \cdot m^{-2}$], K_{dif}: diffuse shortwave radiation [$W \cdot m^{-2}$], *c*: cloudiness index, Q_n: net radiation [$W \cdot m^{-2}$], P_{snow}: snowfall [mm], P_{rain}: rainfall [mm], *E*: evapotranspiration [mm], SM_{max}: maximum soil moisture content [mm], SMi: actual soil moisture content [mm], inf: infiltration.

During the spring snowmelt, infiltration into frozen soils is estimated in the FROZEN module using the approach proposed by Zhao and Gray (1999) and Gray et al. (2001). This module divides the soil into restricted, limited and unlimited classes

according to its infiltration characteristics. When limited, infiltration is governed primarily by the snowcover water equivalent (SWE) and the frozen water content of the top 40 cm of soil. The frozen infiltration routine is disabled when the SWE of the snowpack is less than 5 mm. The cumulative snowmelt infiltration [mm] into frozen soils is computed as:

$$\mathrm{INF} = CS_0^{2.92}(1-S_I)^{1.64}\left(\frac{273.15-T_I}{273.15}\right)^{-0.45} t_0^{\,0.44} \tag{4.5}$$

where C is a coefficient, S_0 is the surface saturation [$mm^3 \cdot mm^{-3}$], S_I is the average soil saturation (water + ice) of 0–40 cm soil at the start of infiltration [$mm^3 \cdot mm^{-3}$], T_I is the average temperature of the 0–40 soil layer at the start of infiltration [K], and t_0 is the infiltration opportunity time [hr]. Infiltration opportunity time is estimated as the time required to melt a snowcover assuming continuous melting and small storages and evaporation. Thus, t_0 is calculated by cumulating the hours when there is snowmelt according to the EBSM module.

Actual evapotranspiration is estimated in the EVAP module using the algorithm proposed by Granger and Gray (1989). This algorithm is an extension of the Penman equation to unsaturated conditions. The ability to supply water for evaporation is indexed using only the atmosphere aridity, so no knowledge of soil moisture status is required for this module. To ensure continuity, however, evaporation is taken first from any intercepted rainfall store, then from the upper soil layer and then from the lower soil layer and restricted by water supply in the following module (see Pomeroy et al., 2007).

Variations in the soil moisture balance are conceptually represented as a two-layer soil profile in the SOIL module. The upper layer or recharge layer represents the topsoil and is where infiltration and evaporation occur. Transpiration is withdrawn from the entire soil profile. Snowmelt infiltration computed using the FROZEN module occurs when soil moisture capacity is available in the soil profile, otherwise snowmelt runoff is generated. Excess water from both soil layers constitutes runoff. Runoff is

generated when rainfall events exceed the soil moisture capacity and when the groundwater recharge has been satisfied. Snowmelt runoff and runoff are added together in the term that represents the overland flow. Furthermore, a horizontal soil leakage, subsurface runoff, continuously diminishes the amount of water in the soil and follows an exponential or linear reservoir decay:

$$K_{\text{ssr}} = \frac{R_i}{R_{\max}} R_{ssr} \tag{4.6}$$

where K_{ssr} is horizontal soil leakage [mm·T^{-1}], and R_i [mm] and R_{max} [mm] are the actual and maximum soil moisture capacity in the recharge or top layer, respectively, and R_{ssr} is a recharge drainage factor [mm·T^{-1}].

Outflow from an HRU, constituted by runoff and subsurface runoff flows, and eventually inflow from another HRU, are independently routed in the NETROUTE module using a hydraulic routing approach. Each flow is calculated by lagging its inflow by the travel time through the HRU, then routing it through an amount of linear storage defined by the storage constant, *K*. For a given HRU, the upstream inflow is conceptualised as the outflow from the upstream HRU, whereas runoff accounts for overland flow, and soil storage effects are considered in the subsurface runoff component.

4.3.2 Canadian Land Surface Scheme

The Canadian Land Surface Scheme (CLASS), introduced by Verseghy (1991) and Verseghy et al. (1993), has been widely used in Canada as the LSS for the Canadian General Circulation Model (GCM) and also coupled to a hydrological routing model WATCLASS (Soulis et al. 2000). In this study, CLASS version 3.3 was used. CLASS includes a physically based treatment of energy and moisture fluxes between the vegetation canopy, the snow cover and soil layers. Vegetation canopies in CLASS can be represented by four main vegetation types, needleleaf, broadleaf, crops, and grass.

Each vegetation type is treated separately and composite canopy values (e.g., albedo, roughness length, standing mass) used for subsequent energy balance calculations are obtained by averaging them.

Energy fluxes are determined by summing component contributions along a flat horizontal plane that is assumed to have zero thickness and therefore no heat storage capacity. The energy balance equation is given by:

$$K^* + L^* + Q_E + Q_H = G(0) \tag{4.7}$$

where K^* and L^* are the net shortwave and longwave radiation respectively, Q_E and Q_H are the latent and sensible heat fluxes, and $G(0)$ is the surface flux either to ground, to the snow pack, or to the canopy. Each term is related to the surface temperature and is solved iteratively until the left half side is equal to zero.

CLASS has a three layer soil representation of thicknesses 0.10 m, 0.25 m and 3.75 m, and thus of bottom depths 0.10, 0.35 and 4.10 m respectively. For each of the mosaic tiles, texture data such as percentage of sand, clay, organic matter contents are explicitly set with the possibility of distinguishing between mineral and organic layers. Additionally, surface parameters for each model tile such as soil drainage index, DNR, and soil permeable depth, SDEP [m], control the drainage through the bottom of the soil profile, and the depth of the soil when the bedrock occurs within a soil layer rather than at the interface between two layers, respectively.

The flux of energy across each soil layer boundary is evaluated using the flux-gradient relation for heat conduction in one dimension, given by:

$$G(z) = -\lambda(z)\frac{dT}{dz} \tag{4.8}$$

where the flux (G) across each layer boundary is controlled by thermal conductivity for each soil layer, λ, and the gradient of temperature, dT/dz. The condition is that dT/dz at the lowest soil boundary is equal to zero, therefore knowing the surface and the layer temperatures, the flux terms can be evaluated.

Moisture fluxes through the soil layers are calculated using one-dimensional unsaturated Darcian flow in the case of gravitational drainage, and using the Green-Ampt method in the case of infiltration. Similarly to the energy flux equation, the moisture flux across each layer boundary is controlled by the gradient of suction head, $d\psi/dz$, and the hydraulic conductivity of each soil layer, K_h. The condition s that $d\psi/dz$ at the lowest soil boundary is assumed to be a zero, therefore the soil flux is set equal to K_h. When the infiltration capacity is exceeded, water is allowed to pond on the surface up to a maximum surface detention capacity which varies according to land cover. Ponded water is retained on the surface until it either infiltrates or evaporates. The soil albedo, and the soil thermal and hydrological properties, vary according to texture and moisture content (Verseghy, 2000).

The snow model uses a coupled energy and mass balance at the top and bottom of the snow pack to calculate an internal energy state. When the surface temperature or the average layer temperature rises above 0°C, this excess energy is used to melt part of the snowpack and the temperature is set back to 0°C. Snow albedo and density vary with time according to exponential functions. Snowcover is assumed to be complete above a limiting depth of 0.10 m (D_{100}); otherwise fractional snow coverage is calculated through the employment of a snow cover depletion curve (Donald et al., 1995). Meltwater from the surface percolates through the snowpack and refreezes until the temperature of the snowpack reaches the freezing point, upon which any further melt reaches the base of the snowpack.

4.3.3 MESH Modelling System

As part of the MEC (Modélisation Environmentale Communautaire) developed by Environment Canada, MESH (MEC - Surface and Hydrology; Pietroniro et al., 2007) is a stand-alone LSH model configuration of MEC that couples CLASS with hydrological routing schemes. Representation of spatial heterogeneity is based on a

mosaic approach using the GRU concept. The GRU approach is described in section 4.4.2.3. The routing scheme was developed by Soulis et al. (2000, 2005). It includes the adaptation of CLASS to sloped terrain drainage functions and its coupling to the routing scheme of the WATFLOOD model (Kouwen, 1993). This involved the inclusion of physically based transfer functions between the soil column and the micro-drainage system within each GRU. The fundamental drainage element is conceptualised by an assembly of sloped blocks connected to a stream and with the drainage system. Each block has a typical length (L) perpendicular to receiving stream of length L_V. The L_s is the distance between the divide of the element (GRU) and the stream and is equal to the ½ of the drainage density, D_d, defined as $\Sigma L_V/A$ where A is the element area. Thus, a GRU is viewed as a mosaic of slope tiles, with average dimensions L and L_V and average slope Λ_I, drained by a system of micro channels.

Excess surface water drains to the micro-drainage system as overland flow, q_{over}. It is represented by Manning's equation.

$$q_{over} = \frac{D_d}{n} d_e^{5/3} \Lambda_I^{1/2} \tag{4.9}$$

where d_e is the average effective depth at the stream edge and n is Manning's roughness coefficient.

The horizontal near-surface flow, called interflow, q_{int}, occurs through the soil matrix and the macropore structure, leaving the control volume through the seepage face (Figure 4.3).

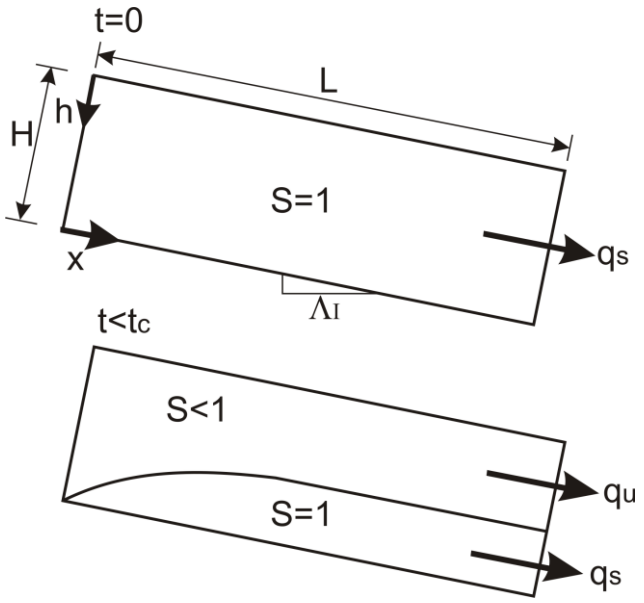

Figure 4.3: Sloped shallow aquifer model for interflow generation. Adapted from Soulis et al. (2000). *H*: depth of the soil layer, *S*: saturation, q_s and q_u are the saturated and unsaturated interflow respectively.

The conceptualisation of q_{int} was introduced by Soulis et al (2000) and uses shallow aquifer flow model assuming that q_{int} occurs almost entirely when soil moisture is between saturation and field capacity. However, rather than solving the Richard's equations with the adding complexity of highly variable hydraulic conductivities in the upper soil layer, the shallow aquifer was forced to fit a simpler power law that relates the total outflow at the seepage face, *q*, and the average moisture stored in a control volume, *u*.

This approach assumes that at $t = 0$, flow from the seepage face is fully saturated. After $t = t_c$, the water table drops below the surface of the face and the interflow becomes a mixture of saturated and unsaturated flow. Behind and above the water table, saturation (*S*) declines in both time and space (Figure 4.3).

The flow at the seepage face (x = *L*) and the average depth of water remaining in the aquifer is given by the following equations:

$$q(t) = \int_0^H Vx(L,h,t)dh \tag{4.10}$$

$$u(t) = \frac{1}{L}\int_0^L\int_0^H \theta_s S(x,h,t)dhdx \tag{4.11}$$

where V_x: horizontal flow velocity, θ_s: porosity, S: saturation, q_s and q_u are the saturated and unsaturated interflow respectively.

Finally the parameterised interflow equation is obtained by:

$$q_{\text{int}} = 2D_D K_{s0}(\theta_s)\left(\frac{\theta_1 - a\theta_s}{\theta_c - a\theta_s}\right)^f \frac{H}{e+1}\Lambda_I \tag{4.12}$$

where K_{s0} is the horizontal saturated hydraulic conductivity at the surface, θ_1, θ_c θ_s are the average soil values for layer one, a is the fraction of saturation at which effective interflow is zero, f is and exponent that may be obtained as $f = a \cdot c \cdot g(e)$ with $g(e) = \frac{(e+1)(e+2)}{(5e+2)}$, and with e normally between 0 and 3.

Figure 4.4 illustrates the soil moisture representation in the MESH modelling system. Gravitational movement of water between the soil layers is governed by a finite difference solution of Richard's equation for unsaturated flow in porous media. The relation between horizontal and vertical hydraulic conductivity in slopes is assumed to be less than 10%, so the Dupuit-Forscheimer approximation is valid and the V_x can be calculated using a one-dimension Richard's equation. Variation of the hydraulic conductivity with depth follows an exponential form similar to TOPMODEL, whereas the variation of hydraulic conductivity in unsaturated conditions uses the Clapp-Hornberger soil physics. However, determination of reliable values of parameters such as c, e and θ_s for each land-cover is highly uncertain.

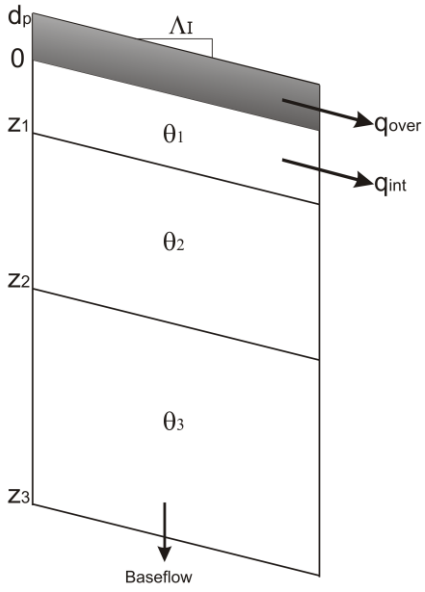

Figure 4.4: Representation of the soil moisturise budget in MESH modelling system. Adapted from Soulis et al. (2000).

River routing in MESH is based on a storage routing method originally implemented in the WATFLOOD model (Kouwen, 1988). This is a simple yet reliable technique since storage is calculated as a function of the outflow alone. The implementation is based on the continuity equation for each river reach where the inflow consist of overland flow, interflow, baseflow, and channel flow from all contributing upstream basin elements, whereas outflow is related to the storage through the Manning formula. Channel cross-section area is related to storage by dividing the storage by the channel length, and channel storage is calculated using a relation such that the channel cross-section area is given as a function of drainage area. The roughness coefficient incorporates a channel shape and width to depth ratio as well as Manning's *n*.

4.4 Spatial model representation

Reliable hydrological modelling at small to medium scales is very difficult. At these scales, models require incorporation of both detailed process understanding and inputs along with information gained from observations of basin-wide streamflow

phenomenon; essentially a combination of inductive and deductive approaches. Several years of research in WC and TVC allowed for the identification of landscape units as key factors in the dynamics of snow accumulation and snow depletion processes (Marsh and Pomeroy, 1996; Pomeroy et al., 2003). Specifically, landscape characteristics such as vegetation type and exposure, and the location of the landscape units in the basin were described as essential elements to properly describe snow accumulation processes, energy and mass balance calculations, resulting meltwater fluxes, runoff contributing area, and routing processes.

Incorporating basin heterogeneity to better describe hydrological process within a hydrological model has led to a number of methods of basin segmentation. Distributed hydrological models use spatial aggregation methods to account for landscape variability and processes representation; however, a critical point in the application of these models is the selection of a model element size. As a result, the spatial model representation was based on landscape units. Thus, an inductive approach was used for the identification of these units based on a basin-wide understanding of the main hydrological responses, whereas a deductive modelling approach was applied in each of the model units to physically describe the hydrological processes.

4.4.1 Lumped scale-basin aggregation approaches

Simulations using spatially lumped aggregation approaches at the basin scale were tested and compared with spatially distributed aggregation approaches. This approach involved the use of either model grid (i.e. landscape unit) or homogeneous snowcover initial conditions and solar inputs. The main objective of this approach was to evaluate the effect of not incorporating an explicit representation of the spatial heterogeneity of snow accumulation and snowmelt on model performance.

4.4.2 Distributed aggregation approaches

In order to incorporate an explicit landscape representation, several spatially distributed aggregation approaches were tested. Each of the following aggregation methods was set to match the landscape units based on the identification of these units as essential elements to adequately describe snow accumulation, snowcover ablation, and snowmelt runoff processes.

4.4.2.1 Hydrological response units

The definition of areas with similar hydrological behaviour is a common method for reducing model complexity in distributed models. Thus, similar hydrological areas are explicitly defined as Hydrological Response Units (HRUs), which comprise landscape parcels with similar water balance and runoff generation processes. These units are characterized from an understanding of the hydrological processes and land use point of view, and they are usually defined by overlapping maps of different characteristics, such as soils slope, aspect, and vegetation cover. Therefore, an HRU is usually a physical location within the basin which has implications in the stream routing scheme, since the location of each HRU within the basin may play an important role in the water exchange to the downstream HRUs. A common approach is to define HRUs as sub-basins embracing a drainage area and organized by a river network typology such as the Aggregated Simulated Areas (ASAs). This concept presumes that streamflow at the sub-basin outlet is comprised of surface, interflow and groundwater runoff, where each HRU is parameterised for all three runoff components. It is assumed that the parameterisation process incorporates the spatial variability of the landscape to approximate the runoff mechanisms in each HRU. However, besides the convenience of this approach, it is inappropriate for large basins since a large number of HRUs could lead to a very complex parameterisation process. Also, landscape heterogeneity driving hydrological exchanges within or between sub-basins (e.g. blowing snow) can compromise the HRU concept if they are defined as sub-basins. Figure 4.5 illustrates a

simple conceptual example where a basin with only three land-cover types leads to a fairly complex spatial discretisation. Figure 4.5b shows that when a land-cover type is also considered in the definition of the HRU, a large number of HRUs is generated. This approach can challenge the routing scheme in most of the models, resulting in a basin response the may not necessarily reflect the processes involved (Figure 4.5c).

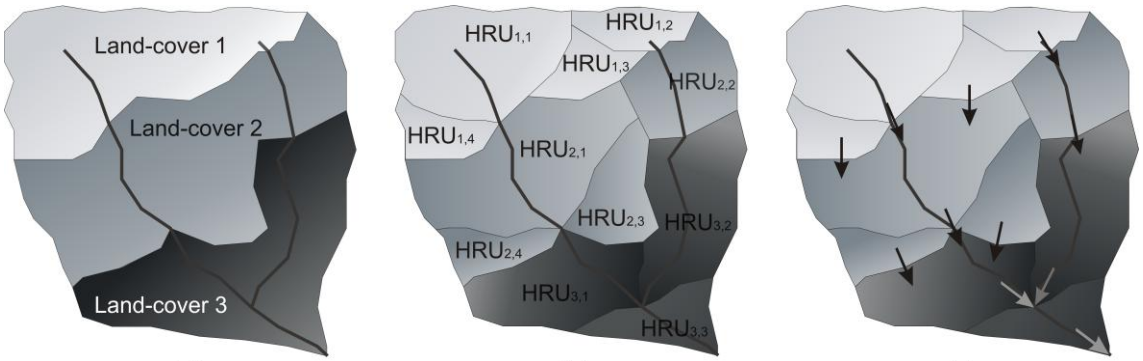

Figure 4.5: Conceptual illustration of the delineation of HRUs using the sub-basin approach and land-cover type. Arrows represent flow direction.

To evaluate the benefits of explicit landscape representation on modelling snowmelt ablation and snowmelt runoff generation in a mountainous arctic environment, distributed tiles using the HRU approach were compared with a basin aggregated approach (i.e. lumped) in GB (Figure 4.6). In the aggregated model, all the landscape units were aggregated in a single, flat HRU. In this case, initial conditions (mean SWE, mean soil moisture) and forcing data (mean radiation and mean air temperature) were weight-averaged according to the landscape unit area (Figure 4.6a). For the distributed analysis, the basin was divided into different HRUs according to the landscape units (Figure 10b). Exposure, and subsequently vegetation and soil types, were the main criteria used to define the landscape units. Five main landscape units (i.e. UB, PLT area, NF and SF slopes, and VB) which are presumed to approximate HRUs, were used for basin segmentation.

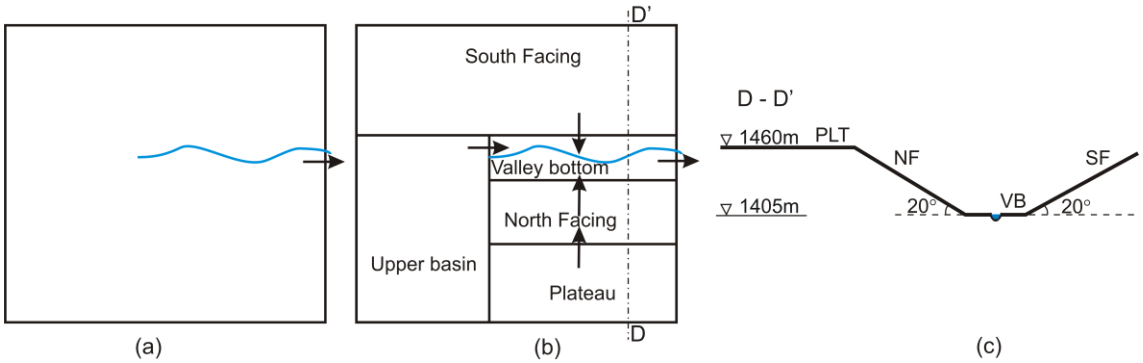

Figure 4.6: Schematic representation of Granger Basin. a) Aggregation of the different landscapes in one single and flat HRU, b) Distribution of the HRUs according to landscape units, and c) profile exhibiting differences in elevation and exposure among HRUs. Arrows indicate flow direction.

4.4.2.2 Land-based approach

Land surface schemes (LSSs) are usually applied as means to provide reliable large scale surface states and vertical fluxes to atmospheric models. In general they are applied as a column model and therefore no explicit representation of the landscape heterogeneity is included. This approach has meant that small scale horizontal processes and landscape heterogeneity are either ignored or aggregated. To evaluate the LSS performance for different landscapes, distributed and independent model runs (i.e. point mode) were conducted in each of the landscape units of GB (see Figure 3.2) and compared with simulations using a basin wide aggregated approach.

4.4.2.3 Grouped response units

The Grouped Response Unit (GRU; Kouven et al., 1993) is an alternative method for describing spatial variability, where areas with similar land cover, soils, etc., are grouped with no requirement for grids or sub-basins to be hydrologically homogenous. This approach is based on the identification of land surface covers, usually one or a combination of land cover types, with similar physical characteristics. The implicit assumption is that each individual component of the land surface mosaic has the same response for given inputs of energy and water. Based on that similarity

criteria, GRUs are grouped together into predefined square model grids where only one calculation is needed to describe its response. Energy and mass balances are calculated at the GRU level within the grid, whereas the runoff generated from the different groups of GRUs is summed together and then routed to the stream and river system. This approach has the advantage that the location of the GRU within a grid is not longer important in the routing scheme and that the parameters are landscape dependent rather than sub-basins based. Since the location of the landscape element within the calculation unit is not important, the size of the area of each of this element is controlled by only the input data heterogeneity. Thus, this spatial aggregation methodology is very suitable for combining the needs of LSS and hydrological models because it facilitates the inclusion of large areas but still keeps and adequate representation of the landscape heterogeneity. Figure 4.7 depicts the GRU approach using the same example proposed in Figure 4.5. In this case, each of the three land-cover types are assumed to behave as an independent GRU, then energy and mass balances are performed for each GRU within the predefined model grid where the area-weighted runoff components are summed (Figure 4.7b), and finally routed to the streamflow network (Figure 4.7c). Applications of the GRU approach based on landcover types defined from satellite information include Pietroniro et al. (1996), Pohl et al. (2005a), Pohl and Marsh (2006) and Davison et al (2006).

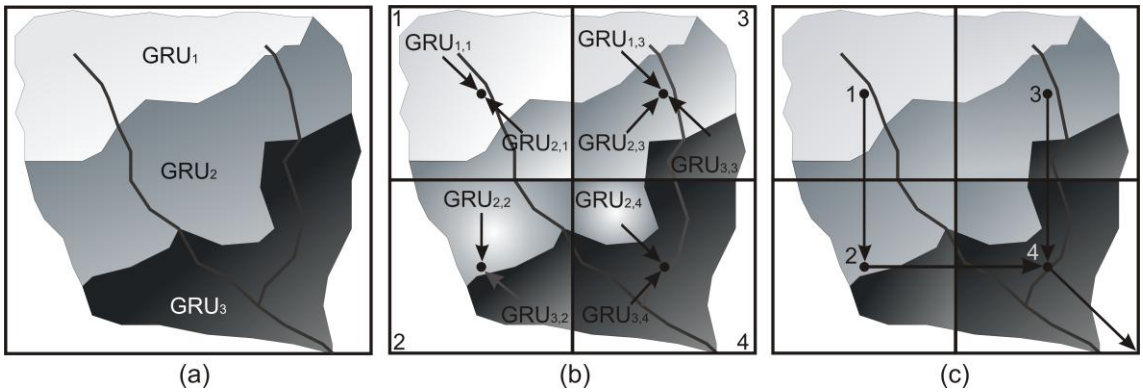

Figure 4.7: Schematisation of the Group Response Unit (GRU) aggregation approach. a) GRUs are assumed to represent land-cover types, b) energy and mass balances are

calculated at the GRU level whereas all the runoff components are added at the grid level, and c) runoff components are routed to the streamflow network.

Process studies in mountain subarctic environments have shown the importance of blowing snow redistribution, shortwave radiation, topography and vegetation in governing snow accumulation and ablation, and runoff generation processes. However, spatially uniform incoming solar radiation and initial snowcovers are still used to force and initialise hydrological models and sometimes over complex terrains. To evaluate the inclusion of explicit landscape heterogeneity, the GRU approach was used represent the spatial landscape heterogeneity of WC. A 3 km x 3 km model grid was used to aggregate runoff calculations (Figure 4.8). As a result the 195 km^2 basin was dived in a 10 by 7 square grid. The grid size was selected to approximate the area of GB in order to compare the distributed results of one grid of 9 km^2 with the observations at GB.

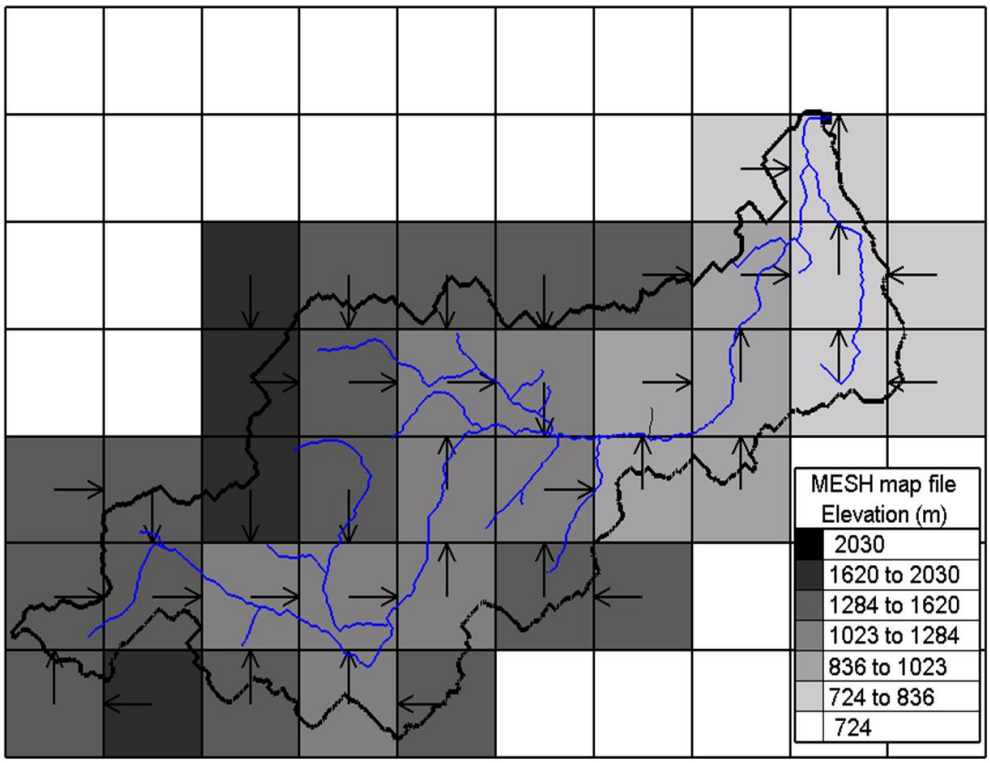

Figure 4.8: Illustration of the grid model used in the GRU approach for WC. Arrows represent flow direction and blue lines the drainage network.

In order to account for topographic and vegetation effects in snowcover ablation and snowmelt runoff at the WC scale, the GRU delimitation was based on landscape tiles defined by land-cover types (i.e. alpine, shrubs, and forest), and slope and exposure controlling snow accumulation and snow energetics. Slopes with angles lower than 20° were assumed to be equivalent to horizontal terrain. The exposures explicitly considered were those relevant to both snow accumulation and ablation processes. Therefore, NF and SF slopes were included due to their distinct energy and snow accumulation regimes as a result of redistribution of snow by wind, whereas the EF slopes were explicitly included due to their characteristic snow drift formations as a result of its the lee locations respect to the dominant western wind direction (McCartney, 2006). Figure 4.9 shows the resulting thirteen GRUs for WC.

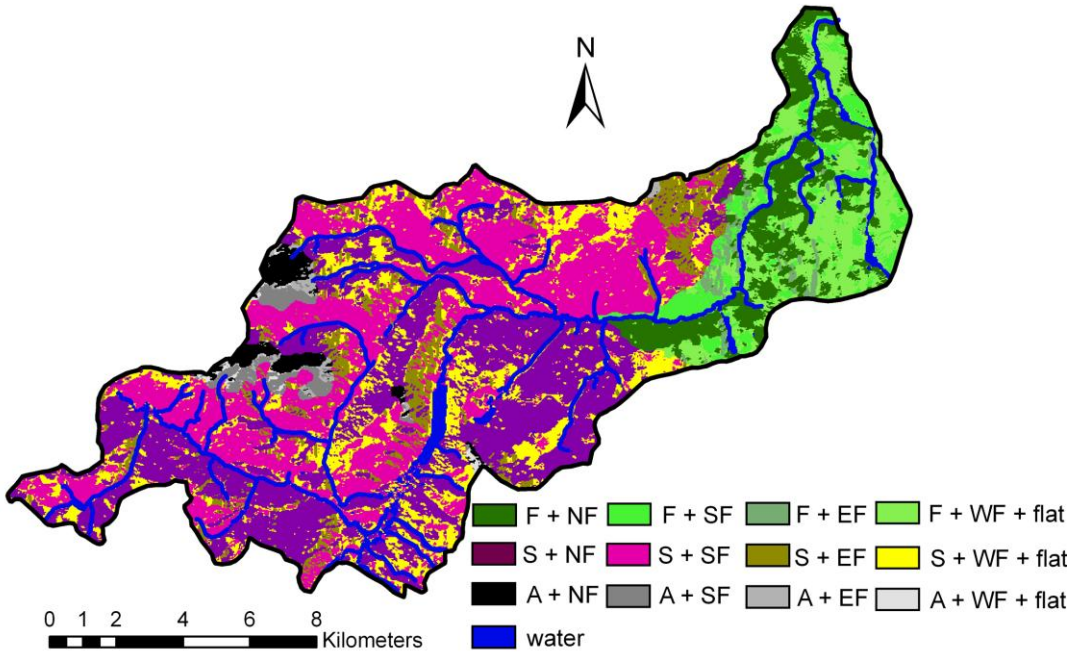

Figure 4.9: Illustration of the GRUs used for landscape model representation of WC in the MESH model. F: Forest, S: Shrub, A: Alpine, NF: North facing slope, SF: South facing slope, EF: East facing slope, and WF: West facing slope.

4.5 Effects of initial conditions and forcing data

Most LSSs include a detailed description of energy and water exchanges between soil layers and an explicit representation of canopy effects and snow-cover. However, given that LSSs are usually applied as means to provide the lower boundary conditions to global climate models (GCMs) or numerical weather prediction (NWP) models LSSs are regarded as one-dimensional vertical models while the horizontal processes and landscape heterogeneity are either ignored or aggregated. In subarctic environments, spatial variability of snow cover due to topographic effects, presence of vegetation, and redistribution by wind, has been found to be a key factor for describing snow-cover energetics and snowmelt runoff generation in small scale basins. Here, the importance of including distributed initial conditions (SWE) and slope and aspect effects on solar forcing, in predicting snow-cover ablation and snowmelt runoff is examined. Figure 4.10 depicts the model comparisons that were conducted using distributed observations of initial snow-cover (SWE) and corrected incoming solar radiation (K) due topographic effects with simulations using uniform snowcover and topography.

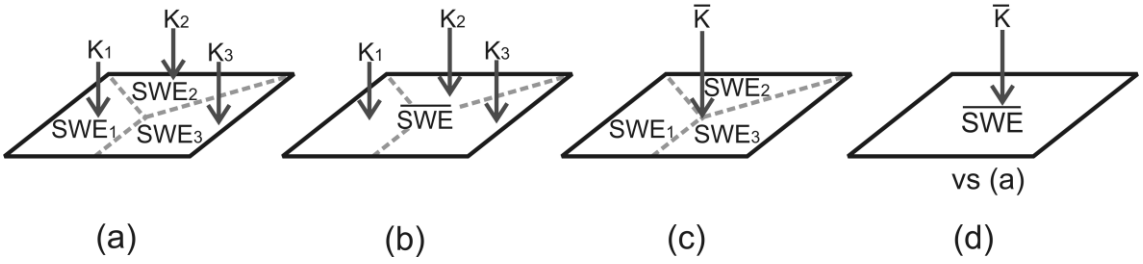

Figure 4.10: Schematic illustration of the modelling approaches used to simulate snowcover ablation showing a basin with three hypothetical landscape units. a) Distributed initial conditions (SWE) and solar forcing (K), b) Basin average initial SWE and distributed K., c) Distributed SWE and basin-average K, and d) Aggregated (basin-average) SWE and K.

4.6 Model parameterisation

Distributed models typically use physically based equations to describe hydrological process. A major challenge is the representation of landscape heterogeneity in the model parameterisations. Physical descriptions of the land surface processes were generally developed at the point scale; hence the application of these parameters at different and usually larger scales involves either rescaling the universal conservation laws which essentially means that model parameters must be measurable quantities, or some relaxation in the model parameterisation. Therefore, the definition of effective parameters is a common approach used to solve this scaling issue. However, given the difficulty in defining these parameters from observations, the lack of adequate process descriptions at larger scales, and the non linear nature of the hydrological processes; the determination of these effective parameters is not a trivial problem.

4.6.1 Calibration approaches

Traditionally, calibration of hydrological models has been performed manually using a trail-an-error parameter adjustment procedure. This process may be very tedious and time-consuming depending on the number of parameters and their interaction. Furthermore due to the subjectivity involved, it is difficult to assess the confidence of the model simulations. Consequently, a great deal of research has been directed to the development of more efficient and more objective automatic calibration procedures.

In order to retain the physical meaning of parameter and model, multi-objective functions based on different processes (e.g. snowcover ablation and streamflow) were used when possible, and calibration was always constrained to ill-defined parameters. Consequently, it was performed for conceptual parameters (e.g. routing parameters in CRHM) or when it was not possible to set the value of the parameters from observations (e.g. D100 parameter in CLASS). Manual calibration was suitable when simple

conceptual modules were used; whereas automatic calibration procedures were applied where a large number of parameters were involved.

4.6.2 Optimisation algorithm

Automatic calibration procedures were applied to define effective parameters of CLASS and MESH for each landscape unit. Parameter sets were found using the Dynamically Dimensioned Search (DDS; Tolson and Shoemaker, 2007) global optimisation algorithm. DDS was implemented using MATLAB software. Parameter sets of CLASS describing snowmelt in GB were obtained after performing 500 independent model simulations with the DDS algorithm using a single objective function, the root mean square error (RMSE) with respect to the SWE observations during melt. Calibration of the MESH model in WC was performed for the parameters controlling streamflow routing and the SCD parameter using single objective function to evaluate model performance, the Nash Sutcliffe Efficiency coefficient, (*E*; Nash and Sutcliffe, 1970). Calibration of MESH model in TVC was formulated using a multi-objective calibration approach that aggregated the model performance calculated with the *E* coefficient of the average basin snow covered area (SCA) and basin streamflow simulations.

CHAPTER 5

IMPORTANCE OF AGGREGATION APPROACHES, INITIAL CONDITIONS AND FORCING DATA IN HYDROLOGICAL AND LAND SURFACE MODELLING

5.1 Introduction

This chapter presents the numerical experiments used to evaluate the predictive uncertainty in snowmelt modelling using a hydrological model and a LSS in a subarctic mountain environment. The analysis centres on the comparison between basin-aggregated and distributed landscape representations and on the effects of the initial conditions and forcing data in snowmelt simulations. In particular, it evaluates the effects on modelling performance of lumped and distributed aggregation approaches and the consequences of using distributed information of initial snowcover and solar forcing corrected by topography. The results were previously published in Dornes et al. (2008a) and Dornes et al. (2008b).

5.2 Background

A major limitation for hydrological predictions is the quantification of the different uncertainties associated with the representation of model inputs, process descriptions and model parameters (Sivapalan et al., 2003a). Catchment models are usually conceptualised based on different aggregation approaches and are therefore simplified representations of the real world (Blöschl and Sivapalan, 1995).

Incorporating basin heterogeneity to better describe and predict hydrological processes within numerical models has led to a number of methods of basin segmentation. However, given the heterogeneity in the landscape, hydrologists are forced to conceptualise the physics to some degree and seek effective parameter values (Pietroniro and Soulis, 2003). This is especially important in remote regions such as northern Canada, where soils, vegetation and topography are not well inventoried. Distributed hydrological models use aggregation methods to account for landscape variability and process representation; and a critical point in the application of these models is the selection of a landscape element size. Most snow energetics, snow hydrology and snow–atmosphere interaction models still do not account for slope and aspect, solar angle and sky-view effects, and their respective scales of influence (Pomeroy et al., 2003). However, those that include these effects show substantial impact on the timing, area and duration of snowmelt (e.g. Marks et al., 2002). This issue is especially important in LSSs because they are typically applied as a means to provide the lower boundary condition to general circulation models (GCMs) or numerical weather prediction (NWPs) models and therefore they have been focused on providing reliable large scale surface states and vertical fluxes to the atmosphere and hydrological inputs to continental-scale river forecasts. This approach has meant that the representation of small scale horizontal processes and landscape heterogeneity in LSS has been either ignored or aggregated.

Small scale heterogeneity is especially important in arctic and subarctic mountain environments during the spring snowmelt season. Over the winter, snow is blown from areas of high wind exposure to sheltered sites, and ablates in an uneven manner (Pomeroy et al. 1997; Liston and Sturm, 2002; Essery et al. 1999). This generates a highly non-uniform distribution of snow cover in the spring which usually leads to a mosaic of snow, bare ground, and emergent vegetation as melt progresses. Additionally, topographic and vegetation effects on snow accumulation and ablation

regimes contributes to the heterogeneity of the snow covers during melt. Explicit representations of landscape heterogeneity in LSSs and land surface hydrological (LSH) models, including slope and aspect effects at small to medium basin scales in arctic and mountainous environments, have been shown to significantly improve simulations of snowcover ablation and basin runoff compared with aggregated approaches (Déry et al. 2004; Pohl et al., 2005, Davison et al. 2006; Pohl and Marsh, 2006). Effects included a more accurate description of differential snowmelt rates and an improved timing and magnitude of spring snowmelt runoff. However, fewer studies have evaluated the effects of landscape heterogeneity on melt model performance, at the landscape and basin scale, in mountain tundra environments during the snowmelt season. Therefore, the objectives of this study are two-fold:

a) To examine the implications for the simulations of snowcover ablation and snowmelt runoff for a small basin in a mountain tundra environment of different spatial model aggregations and parameterisations in describing the main hydrological processes affecting snowmelt, using a small scale and physically based hydrological model. In addition, to assess the suitability of a simple and conceptual soil moisture balance and flow routine for runoff generation during snowmelt in a permafrost environment.

b) To evaluate the effects of including an explicit landscape representation of snow distribution and slope and aspect in a Land Surface Scheme for the simulations of snowcover ablation for a small basin in a mountain tundra environment. The evaluation is conducted by comparing the effects on model performance of using aggregated initial conditions and forcing data in distributed field observations of snowcover and contrasting spatially aggregated and distributed model results at basin scale.

5.3 Modelling strategy

Two models, a small-scale hydrological model and a land surface scheme, were used to simulate the effects of including explicit landscape representation on the prediction of snowmelt. The Cold Regions Hydrological Model (CRHM) was used to evaluate the effects of different spatial aggregations on simulations of snowcover ablation and snowmelt runoff, and to generate the distributed solar forcing for an offline version of the Canadian Land Surface Scheme (CLASS) model. Therefore, incoming solar radiation corrected by slope and aspect was precalculated using CRHM.

5.3.1 Distributed versus aggregated approaches

The selected study site for this analysis was Granger Basin (GB) (see Figure 3.2) due to the availability of distributed measurements of snowcover ablation and meteorological data. Importance of the spatial aggregation approaches in simulations of both snowcover ablation and basin snowmelt runoff was evaluated using CRHM (see Figure 4.2). Meteorological measurements of air temperature, relative humidity, incoming solar radiation, and both wind speed and direction for two snowmelt periods from 17 April to 10 June 2002 and from 17 April to 31 May 2003 were used to force the modules within CRHM. Observations were made on the PLT area, with the exception of precipitation data obtained at the BB station using an automatic precipitation gauge. This precipitation gauge consists of a storage bin filled with antifreeze used to convert snow to liquid water. As snow melts, the change of the level in the antifreeze reservoir is recorded and converted to millimeters of precipitation. The precipitation data were corrected by wind-induced undercatch according to Pomeroy and Li (2000). Snowcover ablation was evaluated by estimating the SWE from snow surveys in each landscape unit of GB. SWE was calculated in each point of the snow survey transects by multiplying the snow depth by the snow density and dividing by the density of water. The areal SWE represents the average SWE along the snow survey transect.

Measurements of snow depth and density along the snow survey transect were conducted every 5 and 10 m, respectively. Length of the transects varied as a function of the landscape heterogeneity; thus, when the snow cover was continuous, approximately 25 points were measured in the PLT area, whereas 20 were measured in the NF and SF slopes, and six points in the VB (for more details see McCartney et al., 2006).

The aggregated model was initialised by computing the spatially-weighted average values from each landscape. Therefore, basin average values of elevation, SWE, albedo and soil moisture were estimated. The distributed model was initialised using calculated SWE values from available snow surveys at the different HRUs. Average SWE values from the PLT area and NF slope in 2002 were assigned to the UB, assuming that the UB compromises characteristics of the NF slope and the PLT area because of its northeast orientation. Since no substantial differences in the snow cover were seen prior to the snowmelt, all HRUs were initialised with the same albedo value of 0.83, determined using radiometric measurements in GB (Bewley et al., 2007). Liquid water content measured in the previous autumn prior to freeze-back (Carey and Quinton, 2005; Quinton et al., 2005) was used as the pre-melt soil frozen moisture content.

Typically, the definition of the spatial model elements is an arbitrary criterion given the difficulty, or impossibility, of finding an optimum element size that can represent measurements, processes and modelling scales (Blöschl, 1999). The criterion for spatial representation of the landscape heterogeneity used in this study was based on the assumption that nature self organises into distinct units. Therefore, natural landscape units were selected based on their distinct parameters that are relevant for snowmelt. The spatial model representation was based on the HRU concept. Delineation of the modelling units was based on the understanding of the main processes that govern snowmelt (i.e. snow accumulation, snow redistribution, and snow energetics) in sub-tundra mountainous environments. As a result, five main landscape

units (i.e. UB, PLT area, NF and SF slopes, and VB), which are presumed from field observations to approximate HRUs (McCartney et al.,2006), were identified and used for basin segmentation according to their vegetation cover, soils and permafrost, slope and exposure (see Figure 4.10). For example, NF slopes and shrub-tundra areas act as accumulation zones, while spring melt rates are much higher on SF slopes due to increased incident solar radiation. The present approach for basin segmentation (i.e. inductive) balances data availability with the desired resolution of the predictions (i.e. identification of differential snowmelt rates between landscape units). In the aggregated model, all the landscape units were aggregated in a single, flat HRU (Figure 4.6a). In this case, initial conditions (mean SWE, mean soil moisture) and forcing data (mean radiation and mean air temperature) were weight-averaged according to the area of the landscape unit. For the distributed analysis, the basin was divided into five different HRUs according to the landscape units (Figure 4.6b). Exposure and, subsequently, vegetation and soil types, were the main criteria used to define landscape units.

5.3.2 Initial conditions and forcing data

The importance of the initial conditions and forcing data on model performance were evaluated using CLASS. The analysis was founded on the recognition of the necessity to include the heterogeneity of the snowpack, as a result of topographic and vegetation effects in the snow redistribution processes, to reduce predictive uncertainties. This was achieved by incorporating distributed (i.e. landscape based) information of SWE. The evaluation of the effects of forcing data on simulations of snow-cover ablation included the explicit estimation of the differential solar forcings (i.e. incoming solar radiation) as a result of slope and aspect effects. Snowcover ablation was evaluated using CLASS in a point mode (i.e., as a vertical column) for each landscape unit of GB where simulations using distributed initial snow-cover conditions

and solar forcing were contrasted to simulations assuming a uniform snowcover and solar forcing. Four modelling approaches were tested and compared (see Figure 4.10),

a) Distributed simulations of SWE using both distributed initial conditions and forcing data,

b) Distributed simulations of SWE using aggregated (i.e. basin-average) initial conditions but distributed forcing data,

c) Distributed simulations of SWE using distributed initial conditions but aggregated forcing data; and

d) Comparison of simulations of SWE using aggregated (i.e. initial conditions and forcing data) and distributed (i.e. re-aggregated values of point 1) modelling approaches.

In order to consider the topographic effects on the forcing data, slope corrected incoming solar radiation was calculated using CRHM for the UB, and NF and SF slopes, whereas observations of solar radiation (without correction) were applied to in the level landscape units such as the PLT and VB. These data along with the complementary meteorological observations were used as forcing data for CLASS (Figure 5.1).

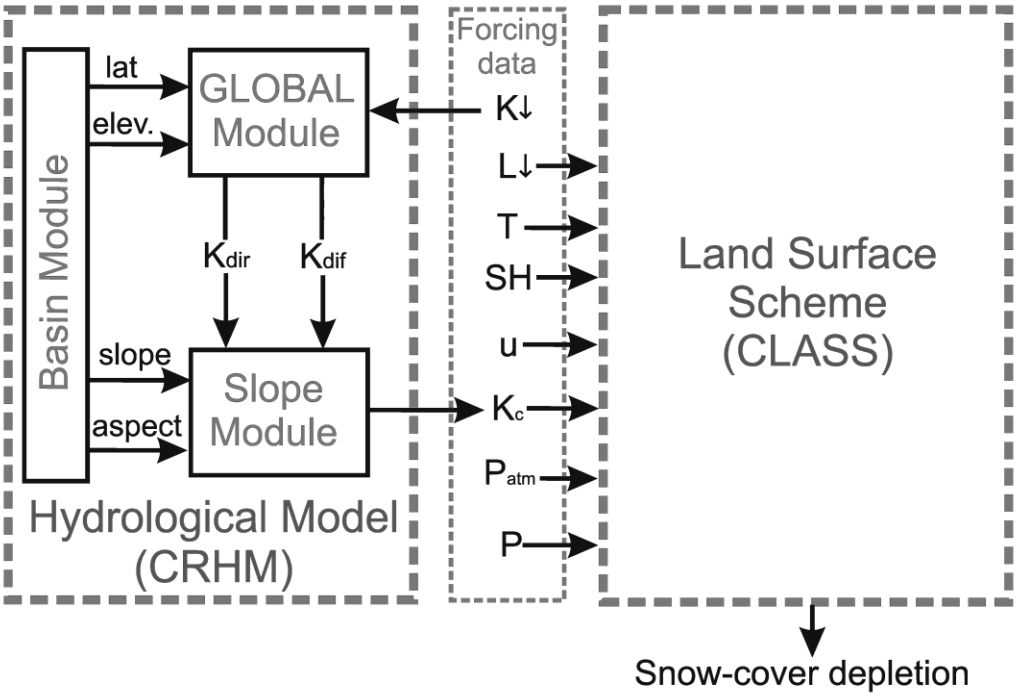

Figure 5.1: Outline of the coupled modelling strategy applied. *CRHM*: Cold Regions Hydrological Model. *CLASS*: Canadian Land Surface Scheme (version 3.3). Solid arrows indicate module and model input/outputs. *K*: incoming short wave radiation [W·m^{-2}], *L*: incoming long wave radiation [W·m^{-2}], *T*: air temperature [ºC], *SH*: specific humidity [g g^{-1}], *u*: wind speed [m s^{-1}], K_c: corrected incoming short wave radiation [W·m^{-2}], P_{atm}: atmospheric pressure [hPa], *P*: precipitation flux [kg m^2 s^{-1}], K_{dir}: direct short wave radiation [W·m^{-2}], K_{dif}: diffuse short wave radiation [W·m^{-2}].

Three CRHM modules were used in this application. The BASIN module where all the basin specifications such as HRU elevation, slope and aspect, soil type and vegetation cover characteristics were set, the GLOBAL module where partitioning of the incoming solar radiation into direct beam and diffusive components for clear skies was accomplished, and the SLOPE module where the correction of the incoming solar radiation due to slope and aspect effects and calculation of cloudiness conditions were performed.

The snowmelt seasons of 2002, 2003 and 2004 were used in this analysis. The same meteorological observations used in the CRHM for 2002 and 2003 were used to force CLASS, whereas observations at the VB were applied in the 2004 snowmelt

season. Atmospheric pressure was measured at the Alpine (A) station located at a similar elevation (1616 m a.s.l.). Initial conditions such as snow density and snow mass needed for CLASS were extracted from snow survey observations. Soil temperatures were obtained from observations in all the landscape units using buried thermocouples. Temperatures of the canopy were set to match the air temperature. As for pre-melt conditions, no ponded water was considered and minimal liquid water content (0.04) was assumed for the entire soil column.

5.3.3 Model calibration

Calibration of the CRHM model was performed on the conceptual modules, whereas the parameter values of the physically-based modules were derived experimentally. Therefore, calibration was only performed on discharge data by tuning the parameters of both the SOIL and NETROUTE modules to fit the observed hydrograph shape.

In order to adjust for the start of melt, a melt delay parameter was set in the EBSM module, since no winter model runs were performed to compute the internal energy of the snow pack prior to melt. Parameter values describing infiltration into frozen soils were set in consideration of the results of field studies (e.g. McCartney et al., 2006; Zhao and Gray, 1999). Thus, C = 2 and S_0 = 1, were assumed to have the same value for all HRUs based on rapid melt. Table 5.1 shows the S_I and the calculated t_0 values for each HRU.

The water storage potential for each HRUs comprises water stored in both the organic and mineral soils, and in depression storage. Field observations demonstrate that surface depression storage is very important towards the end of the melt season in the PLT area, NF slope and VB. While the limits of depression storage values are uncertain, a 300 mm water storage potential was defined for each HRU, regardless of the presence of an organic layer, permafrost, or the dissimilar proportion of unfrozen

and frozen soil moisture. This value was estimated considering previous calculations, which included an estimation for the NF slope of about 230 mm of total moisture (water + ice) in the upper 40 cm of soil (Quinton et al., 2005), while initial basin storage of 180 mm was estimated for the same depth in the NF and SF slopes based upon soil moisture profiles at three soil moisture probes (TDR) by Carey and Quinton (2005). Soil parameter calibration was undertaken manually and was based on previous basin knowledge. Since percolation to groundwater in the SOIL module is only active when there is soil water excess, subsurface runoff values (K_{ssr}) were lagged in the NETROUTE module to account for groundwater losses due to macropore flow and through other mechanisms not properly represented in the SOIL module. As a result, the PLT area and NF slope had the HRUs with the largest amounts of lagged subsurface runoff, followed by the SF slope. Both the Lag parameter and an additional *K* storage parameter were adjusted for each flow in the NETROUTE module to account for different travel times between HRUs (see Figure 4.2). Due to the late and continuous snowmelt season of 2002, K storage values were assigned only to the NF slope. However, for 2003, with discontinuous snowmelt events, large K storage values for the UB and the PLT area were needed to account for differences in timing.

CLASS was automatically calibrated in 2003 and the results were validated in 2002 and 2004 respectively. The selection of 2003 as the calibration period was based on data availability since 2003 was the year with snow surveys in each of the landscape units (see Table 4.2), also 2003 represents an average year for the basin in terms of snow accumulation and redistribution with larger snow drifts on the NF slope as a result of the dominant south and south-west wind directions (McCartney et al. 2006).

Table 5.1: Model parameter values for each landscape unit for the FROZEN, SOIL and NETROUTE modules of CRHM. S_I: average soil saturation (water + ice) of 0–40 cm soil at the start of infiltration, t_0: calculated infiltration opportunity time, R_{ssr}: recharge drainage factor, K_{ssr}: horizontal soil leakage, and K: linear storage constant.

Parameter	UB	PLT	NF	SF	VB
S_I [$mm^{-3} \cdot mm^{-3}$]	0.25	0.20	0.34	0.25	0.25
t_0 for 2002 [hr]	504	408	432	408	480
t_0 for 2003 [hr]	360	312	528	504	360
Initial soil moisture for 2000 [mm]	270	200	300	190	260
Initial soil moisture for 2003 [mm]	200	200	200	260	300
R_{ssr} for 2002-2003 [$mm \cdot d^{-1}$]	0.50	0.50	0.50	0.50	0.50
K_{ssr} for 2002 [$mm \cdot d^{-1}$]	0	20	4	1	1
K_{ssr} for 2003 [$mm \cdot d^{-1}$]	0	0.5	0	0.5	0
K for 2002 [d]	0	0	1	0	0
K for 2003 [d]	12	4	0	1	0

Effective parameter sets for each landscape unit were found using the DDS global optimisation algorithm and were used as model parameterisation for testing the effects of aggregating both initial conditions and forcing data. Calibration was performed over 13 parameters that control snowmelt in CLASS (Table 5.2) and implemented using MATLAB software. Parameters of the two dominant vegetations types, shrub and grass (see Table 3.1), were allowed to vary, whereas parameters for bare ground or rock were maintained constant. The calibration problem was formulated using as a single objective function, the root mean square error (RMSE) with respect to the SWE observations during melt. Independent calibration was performed in each of the landscape units, and optimum parameter sets were obtained after performing 500 model simulations using the DDS algorithm. The selection of the number of simulations was based on the algorithm efficiency. After 100 model simulations DDS was generally able to find good and steady solutions. Since the simulation time was not a limitation (~20 sec), the number of simulations was increased to 500 to ensure that a

global minimum with respect to the objective function in the parameter space was found.

Table 5.2: Optimised parameter values for the different landscape units. Parentheses indicate parameter bounds. STL: stomatal, STO: stomata, SC: snowcover.

Parameter	UB		PLT		NF		SF		VB	
	Shrub	Grass	Shrub	Grass	Shrub	Grass	Shrub	Grass	Shrub	Grass
Max. LAI (LAMX)	1.5 (1,1.5)	1.9 (0.5,2)	2.17 (2, 2.5)	0.53 (0.5, 2)	2.81 (2, 3)	1.95 (0.5, 2.5)	2.73 (2, 3)	2.0 (0.5, 2.5)	2.98 (2.5, 3)	0.64 (0.5, 3)
Min. LAI (LAMN)	0.50 (0.4, 0.5	0.31 (0.1, 0.4)	0.50 (0.4, 0.5)	0.28 (0.5, 3)	0.99 (0.4, 1)	0.29 (0.5, 3)	0.60 (0.4, 1)	0.24 (0.5, 3)	0.80 (0.4, 1)	0.29 (0.5, 3)
LN roughness length (LNZ0) (m)	-3.65 (-3.7,-3.2)	-3.69 (-5.3, -3.7)	-3.66 (-3.7, -2.3)	-4.09 (-4.8, -3.5)	-2.42 (-3.7, -1.8)	-3.72 (-4.8, -3.5)	-1.87 (-3.7, -1.8)	-3.12 (-4.8, -3.5)	-1.89 (-1.9, -1.3)	-3.08 (-4.8, -3.5)
Visible albedo (ALVC)	0.031 (0.03, 0.2)	0.081 (0.02, 0.2)	0.032 (0.03, 0.2)	0.183 (0.02, 0.2)	0.087 (0.03, 0.2)	0.178 (0.02, 0.2)	0.033 (0.03, 0.2)	0.199 (0.02, 0.2)	0.030 (0.03, 0.2)	0.025 (0.02, 0.2)
Near-infrared albedo (ALIC)	0.303 (0.3, 0.5)	0.310 (0.2,0.5)	0.302 (0.3, 0.5)	0.424 (0.2, 0.4)	0.464 (0.3, 0.5)	0.446 (0.2, 0.5)	0.326 (0.3, 0.5)	0.448 (0.2, 0.5)	0.301 (0.3, 0.5)	0.250 (0.2, 0.5)
Biomass Den. (CMAS) ($Kg \cdot m^{-2}$)	1.74 (1, 5)	0.08 (.05, .35)	3.06 (3, 7)	0.11 (.05,.35)	6.13 (6, 10)	0.19 (.05, .35)	7.08 (6, 10)	0.07 (.05,.35)	8.53 (7, 11)	0.19 (.05, .35)
Min. stl. resist. (RSMN)	175.0 (50, 300)	91.6 (50, 300)	145.1 (50, 300)	251.5 (50, 300)	51.9 (50, 300)	140.5 (50, 300)	115.8 (50, 300)	214.9 (50, 300)	104.9 (50, 300)	268.4 (50, 300)
Coef. sto. resp. to light (QA50) ($W \cdot m^{-2}$)	40.6 (20, 60)	27.3 (20, 60)	58.3 (20, 60)	46.1 (20, 60)	21.1 (20, 60)	37.6 (20, 60)	38.4 (20, 60)	35.3 (20, 60)	47.2 (20, 60)	49.9 (20, 60)
Coef. stl. resist. to VP deficit (VPDA)	1.13 (0.2, 1.5)	1.47 (0.2, 1.5)	1.19 (0.2, 1.5)	1.31 (0.2, 1.5)	1.08 (0.2, 1.5)	0.87 (0.2, 1.5)	1.28 (0.2, 1.5)	0.63 (0.2, 1.5)	0.32 (0.2, 1.5)	1.42 (0.2, 1.5)
Coef. stl. resist. to VP deficit (VPDB)	0.61 (0.2, 1.5)	0.70 (0.2, 1.5)	0.61 (0.2, 1.5)	0.61 (0.2, 1.5)	0.93 (0.2, 1.5)	0.23 (0.2, 1.5)	0.78 (0.2, 1.5)	0.89 (0.2, 1.5)	1.21 (0.2, 1.5)	0.46 (0.2, 1.5)
Coef. stl. resist. to soil WS (PSGA)	96.8 (50, 150)	130.0 (50, 150)	81.6 (50, 150)	146.7 (50, 150)	93.5 (50, 150)	135.6 (50, 150)	87.7 (50, 150)	141.1 (50, 150)	71.8 (50, 150)	76.3 (50, 150)
Coef. stl. resist. to soil WS (PSGB)	2.08 (1-10)	6.01 (1, 10)	2.57 (1-10)	4.92 (1, 10)	1.09 (1-10)	1.15 (1, 10)	1.23 (1-10)	5.09 (1, 10)	4.30 (1,10)	2.18 (1, 10)
Min. avg. depth 100% SC (D100) (m)	0.90 (0.01, 1)		0.42 (0.01, 0.5)		0.81 (0.01, 1)		0.86 (0.01, 1)		0.44 (0.01, 0.5)	

Parameter ranges were restricted according to both distributed observations at GB (e.g. McCartney, 2006; Bewley et al., 2007) and prior information (e.g. Verseghy, et al., 1993; Davison et al., 2006) for northern and mountainous environments. Table 5.2 shows the optimised parameter values and their corresponding ranges for the two dominant land covers (i.e. shrubs, grass) in each landscape unit. Although optimum parameter sets varied among the landscape units, these variations showed consistent values with respect to the observations.

5.4 Results and discussion

5.4.1 Distributed versus aggregated

5.4.1.1 Ablation

Distributed SWE simulations during the ablation of the snowcover using CRHM are shown in Figures 5.2 and 5.3 for 2002 and 2003, respectively. In general, they illustrate a very good representation of both the evolution and the differential melt rates observed for each of the landscape units considered, although differences from the observations are usually seen towards the end of the melt season. Table 5.3 displays the efficiency criteria, the RMSE and the Nash Sutcliffe Efficiency coefficient (*E*; Nash Sutcliffe 1970) used for evaluating the model performance.

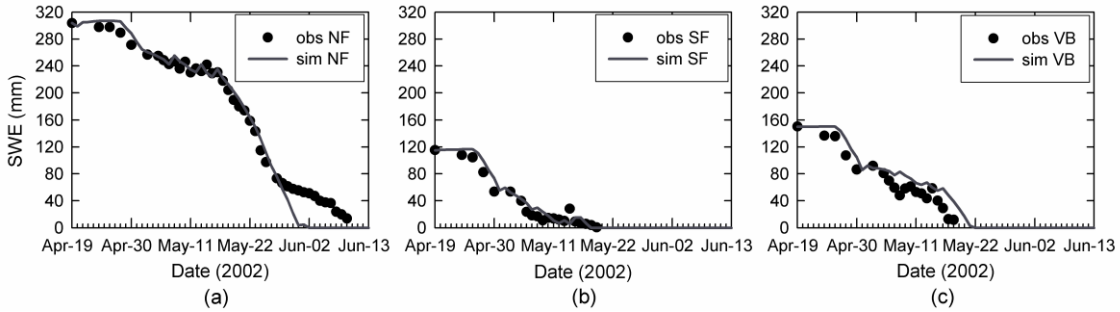

Figure 5.2: Distributed observed and simulated areal SWE values using CRHM at different landscape units of GB for 2002. a) NF: North facing slope, b) SF: South facing slope, and c) VB: Valley bottom.

SWE values at the NF slope (Figure 5.2a and 5.3a) showed close agreement with observed values during the main melt event in the middle of the melt season that resulted in *E* values of 0.95 and 0.84 for 2002 and 2003 respectively. However, differences were observed at the end of the melt seasons. This is attributed to episodic inputs of blowing snow in this HRU throughout the melt period, with substantial accumulation becoming apparent by the end of melt phenomena that could not be represented at the scale used. This HRU is fed by blowing snow, even when other HRUs are ablating (Pomeroy et al., 2003), for simplicity blowing snow was not represented in this CRHM configuration. Simulated values for the SF slope showed an accurate description of the observed evolution of the snow-cover ablation for the entire melt season for 2002 (Figure 5.2b) with a E value of 0.93. In 2003, differences in the late stage simulations (Figure 5.3b) due to the persistence of a snow drift that melted approximately 10 days later than predicted by the model, reduced the model performance to an *E* value 0.75 resulting in a difference of RMSE values of 22.9 mm between both seasons.

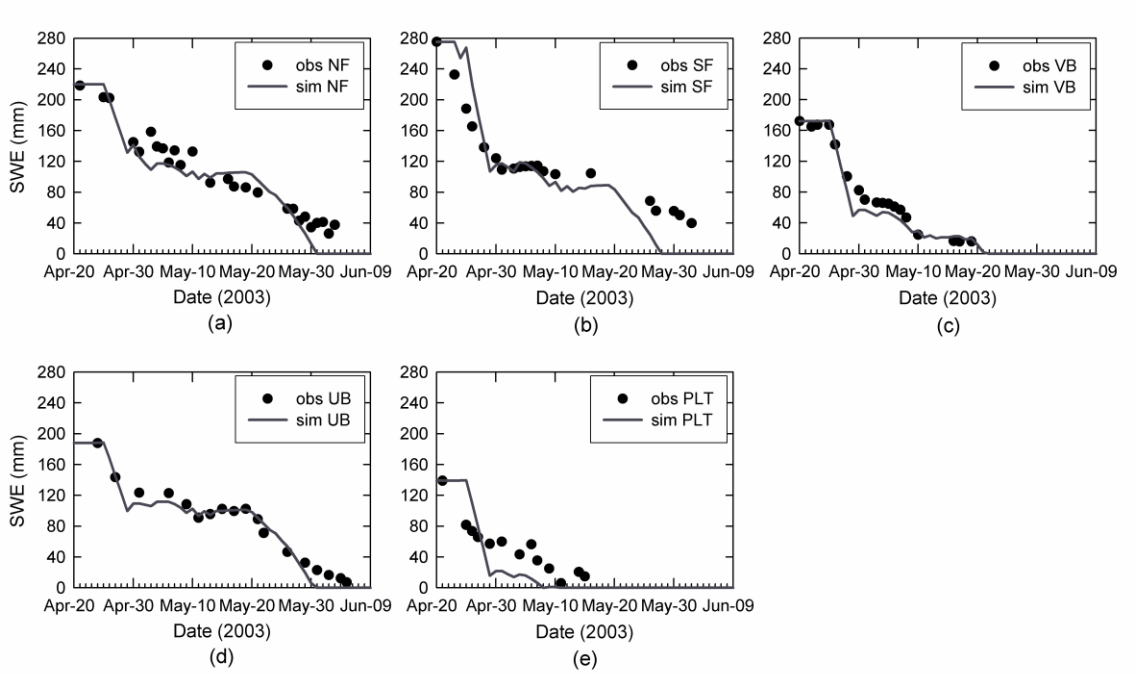

Figure 5.3: Distributed observed and simulated areal SWE values using CRHM at different landscape units of Granger Basin for 2003. a) NF: North facing slope, b) SF: South facing slope, c) VB: Valley bottom, d) UB: Upper basin, and e) PLT: Plateau area.

In the VB, simulation results for the studied years were dissimilar; a good description (*E*: 0.96) of the observed SWE values was modelled in 2003 (Figure 5.3c), whereas in 2002, modelled melt rates on average were lower than the observed values throughout the melt period, particularly at later stages (Figure 5.2c), which reduced the model efficiency to a *E* of 0.90 (RMSE: 19.7 mm). This is attributed to the progressive exposure of tall shrubs (2-3 m) which affects radiation to snow (Bewley, 2006). Simulations for the UB in 2003 (Figure 5.3d) showed an accurate representation of the observed values with only small differences with observations at late stages of melt (*E* value of 0.96). Simulated snowmelt rates at the PLT area (Figure 5.3e) were faster than the observed in 2003, with larger differences at both early and late stages of the snowmelt season. This lack of agreement resulted from the inclusion of at least two points of the snow transect with tall shrubs that affected the overall SWE calculation, as

a consequence of large snow accumulation amounts and drastic changes in albedo due to sudden branching emerging.

Table 5.3: Comparison of model performances in describing snow-cover ablation using CRHM in the different landscape units of GB. E: Nash-Sutcliffe efficiency coefficient.

	UB		**PLT**		**NF**		**SF**		**VB**	
	RMSE (mm)	E	RMSE (mm)	E	RMSE (mm)	E	RMSE (mm)	E	RMSE (mm)	E
2002					21.69	0.95	10.14	0.93	19.67	0.90
2003	9.99	0.96	31.39	0.14	21.82	0.84	33.00	0.75	11.52	0.96

Figure 5.4 and Table 5.4 illustrate the comparison between observed and simulated snowpack ablation with CRHM using the aggregated and distributed modelling approaches. Observations represent the spatially-weighted average of those landscape units where snow survey data were available. Thus, only the NF and SF slopes and VB were considered. In order to compare both modelling approaches, outputs from the distributed model for the considered HRUs were re-aggregated using a spatially-weighted average. For the 2002 snowmelt season, modelled and observed snow ablation rates were similar at the early stages of the snowmelt season for both the aggregated and the distributed models, respectively. However, more substantial differences between modelled and observed values were seen during the late stages. The aggregated model showed more rapid depletion than the re-aggregated distributed model or the observed data that resulted in *E* values of 0.88 and 0.96 respectively (Table 5.4). In contrast, the aggregated model dramatically failed to predict the observed snow ablation rates for 2003 (*E*= -0.09), while the distributed results showed a similar performance to that for 2002 (*E*: 0.78), with some differences at the late stages of the snowmelt season.

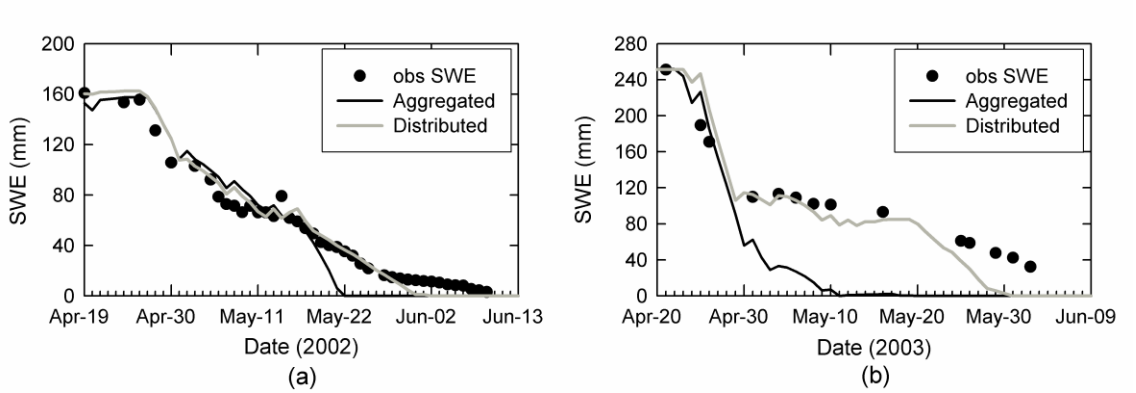

Figure 5.4: Comparison between observed and the simulated SWE values using the aggregated and distributed models. Values represent the spatially-weighted basin-averages using NF and SF slopes, and VB observations. (a) 2002 and (b) 2003.

Table 5.4: Comparison of model performances in describing snow-cover ablation (SWE) and basin runoff (Q) using CRHM in Granger Basin. E: Nash-Sutcliffe efficiency coefficient. AGR and DIST: aggregated and distributed simulations.

	SWE_{AGR}		**SWE_{DIST}**		**Q_{AGR}**		**Q_{DIST}**	
	RMSE (mm)	E	RMSE (mm)	E	RMSE (mm)	E	RMSE (mm)	E
2002	14.82	0.88	8.26	0.96	0.13	0.63	0.09	0.84
2003	62.06	-0.09	27.76	0.78	0.15	-3.26	0.07	0.12

5.4.1.2 Snowmelt runoff

Snowmelt runoff response in GB proved to be very sensitive to differential snowmelt rates (Figure 5.5 and Table 5.4). An uninterrupted snowmelt event resulting in a single peak hydrograph was observed for 2002, whereas a multi-peak hydrograph showed the effect of discontinuous melt due to a sequence of warmer and colder periods in 2003 (McCartney et al. 2006; Quinton et al. 2005). Moreover, since snowmelt discharge volumes represented only 50% and 35% of the winter snowpack for 2002 and 2003 respectively, and the presence of a relatively constant base flow (~ 7 $l \cdot s^{-1}$) before melt, indicate that either not all the snowmelt immediately contribute to spring runoff due to soil water storage effects or it goes into groundwater and reach the stream at a downstream location of the gauge station in Granger Creek. Carey and Woo (2000) for

example, found that snowmelt runoff represents 80% of the winter snowpack in WC for a NF slope with an open forest (black and white spruce) and continuous permafrost. The organic layer transmitted 21% of the runoff while 53% and 26% came from rill and matrix flows in the mineral soil, respectively. This runoff deficit made it difficult to properly close the basin water balance during the spring snowmelt season. Figure 5.5a illustrates that for 2002, both modelling approaches had good overall performance in terms of runoff volumes and peak runoff with *E* values of 0.63 and 0.84 for the aggregated and distributed approaches respectively. However, the aggregated model deviated from observed in timing of the rising and falling limbs of the observed hydrograph, whereas the distributed model accurately described the hydrograph shape. Similar results were found by Dornes et al. (2006) using a simplified version of the infiltration into frozen soil and soil moisture modules, which suggest that parsimonious models can provide an accurate description of single and continuous snowmelt events.

On the other hand, a dissimilar performance amongst the models was observed for 2003 (Figure 5.5b). Although some differences were seen, the distributed model was able to reproduce the timing of the three observed snowmelt peaks, though over predicting the magnitude of the last peak (*E*: 0.12). Conversely, the aggregated model was unable to replicate multiple peaks in the observed hydrograph that resulted in a *E* value of -3.26 and a RMSE (0.15 m^3 seg^{-1}) twice that of the distributed simulation.

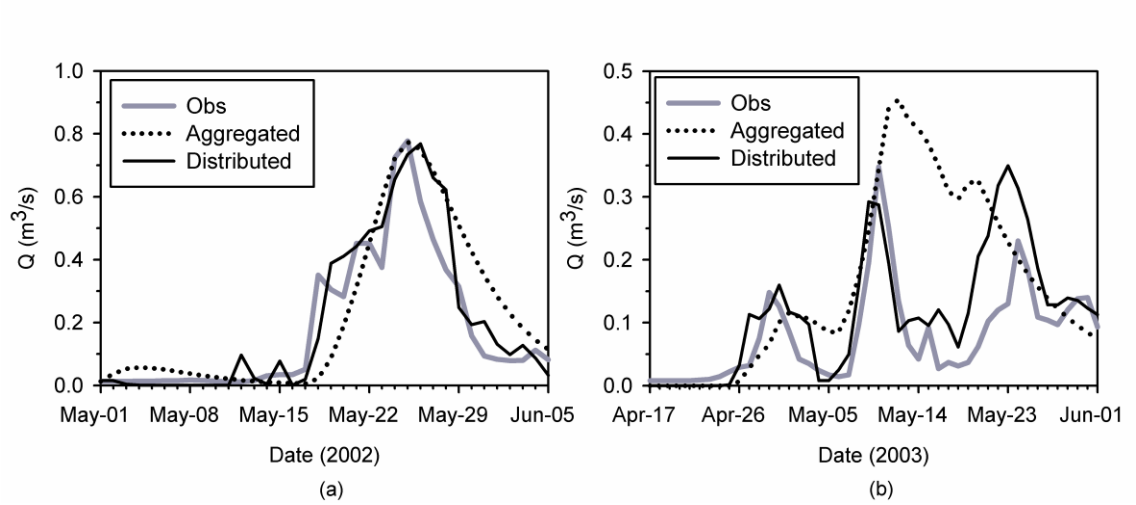

Figure 5.5: Observed and simulated basin discharge using aggregated and distributed configurations of CRHM in Granger Basin.

5.4.2 Effect of initial conditions and forcing data

In order to facilitate the interpretation of the effects the initial conditions and forcing data on modelling performance, simulations results (Figures 5.6 to 5.9) were grouped according to both landscape unit, except for the Figure 5.6 which combines results of the UB and the PLT area with fewer years of observations, and modelling approach. Thus, the first row in the figures illustrates the simulations using distributed initial conditions and forcing data, the second row shows the simulations using aggregated initial conditions and distributed forcing data, and the last row displays the simulations using distributed initial conditions and aggregated forcing data. Table 5.5 displays the modelling performance, the RMSE and *E*, for each modelling strategy. The four modelling approaches tested are described in the following:

a) Simulations using distributed initial conditions and forcing data

Distributed simulations of SWE and available observations are shown in Figures 5.6a-5.9a for 2003. Simulations represent the model performance of the optimum parameter set for each landscape unit obtained from the DDS algorithm. An accurate simulation of the snowcover ablation during the melt period was realised for most of the landscape units analysed. This shows that CLASS could be successfully optimised to

describe the different snowmelt rates, timing and duration of the melt amongst the landscape units if fully distributed inputs and parameters were used. The slow, uniform, snowmelt rates in the UB and NF slope were accurately simulated in 2003 (Figures 5.6a and 5.7a) as were the more variable melt rates on the PLT area (Figure 5.6b) and in an area covered by tall shrubs such as the VB (Figure 5.9a) with a NS coefficient value of 0.98. However, an unsatisfactory performance was observed for the SF slope. While the rapid ablation at early stages of the snowmelt period was adequately simulated, the observed low melt rates at late stages were not properly simulated (Figure 5.8a and c). The high sub-grid variability of SWE due to the presence of an unusual drift in the SF slope (McCartney, 2006) not properly considered in the spatial discretisation of the model may explain why unsatisfactory simulations were observed on the SF slope for 2003 and 2004.

Figures 5.6c, 5.7b-c, 5.8b-c, and 5.9b-c display the validated SWE simulations for the different landscape units, using the parameter set calibrated in 2003, for 2002 and 2004 when data was available. In general, similar results as in the calibration period were observed for all the landscape units analyzed. Higher performance criteria with *E* values of 0.86, 0.89, and 0.94 that matched both timing and duration of the melt were seen in the PLT in 2004 (Figure 5.6c), in the SF slope in 2002 (Figure 5.8b), and in the VB in 2004 (Figure 5.9c) respectively. Despite the faster melt rate simulated in the late stages of the melt in the NF slope (Figures 5.7b-c) for 2002 and 2004, in the SF slope for 2004 (Figure 5.8c), and in the VB for 2002 (Figure 5.9b); reasonable performance criteria with *E* values of 0.92, 0.72, 0.73, and 0.78 were respectively seen.

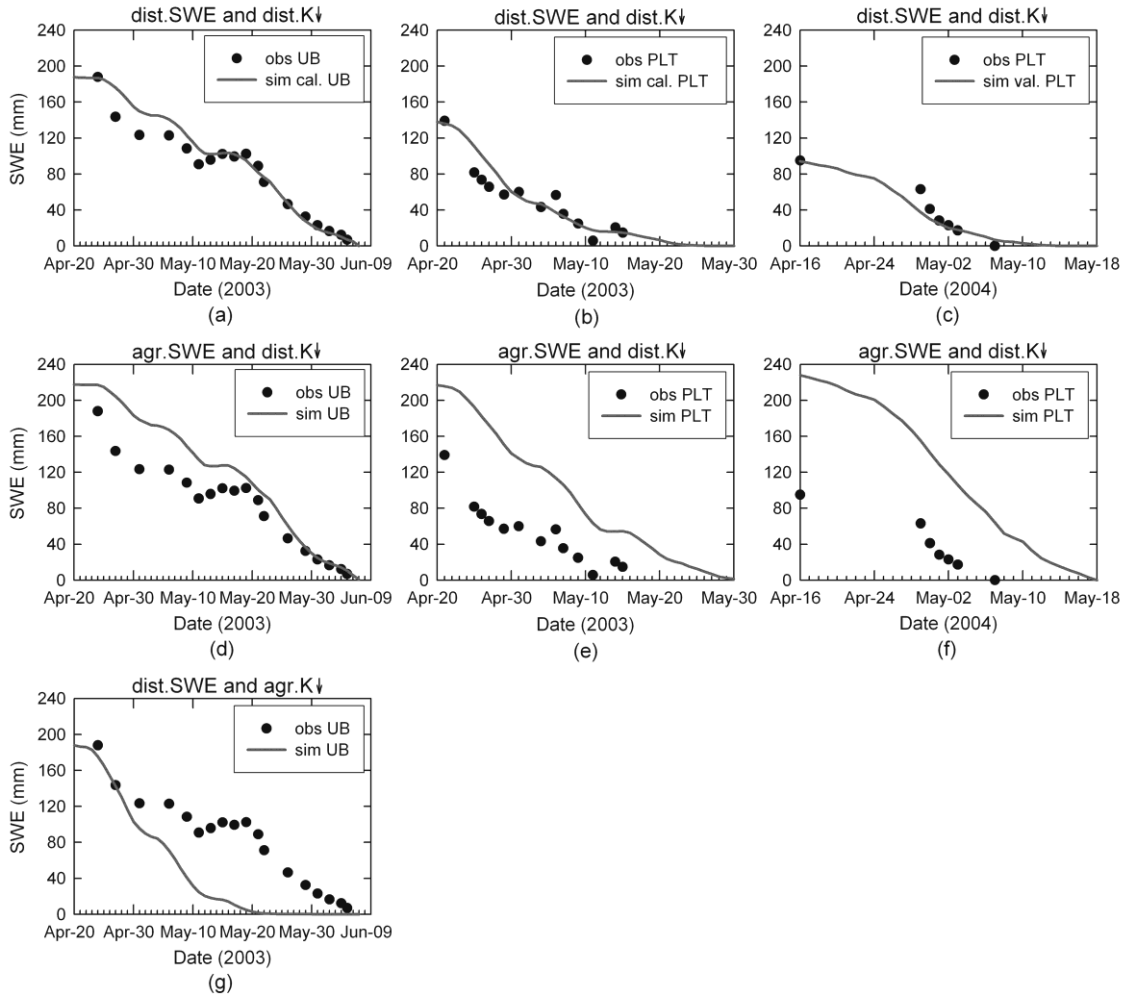

Figure 5.6: Observed and simulated areal SWE values for the UB and PLT area using CLASS. Top: Simulations using distributed initial conditions (SWE) and forcing (K↓), a) UB: Upper basin 2003, b) PLT: Plateau area 2003, and c) PLT: Plateau area 2004. Middle: Simulations using aggregated SWE and distributed K↓, d) UB: Upper basin 2003, f) PLT: Plateau area 2003, and g) PLT: Plateau area 2004, and Bottom: Simulations using distributed SWE and aggregated K↓. g) UB: Upper basin 2003.

b) Simulations using aggregated initial conditions and distributed forcing data

Distributed simulations of SWE using a basin-aggregated (i.e. homogeneous) initial snowcover but distributed forcing data are shown in Figures 5.6d-f, 5.7d-f, 5.8d-f, and 5.9d-f for the calibration and validation seasons respectively. These simulations represent the model performance in each landscape unit of the optimum parameter set calibrated in 2003, when no wind redistribution of the winter snow fall is considered.

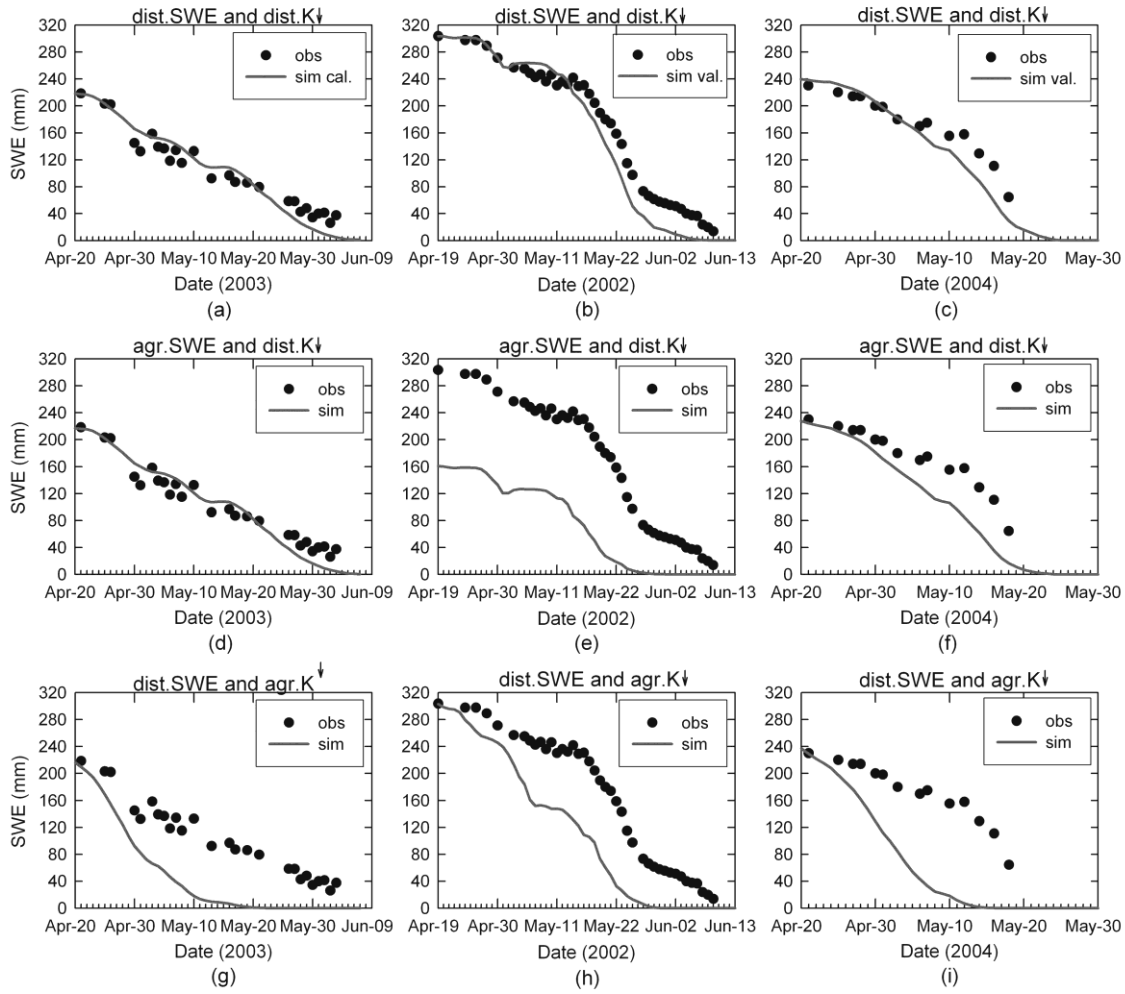

Figure 5.7: Observed and simulated areal SWE values for the North Facing slope (NF) slope in 2002, 2003 and 2004 using CLASS. Top: Simulations using distributed initial conditions (SWE) and forcing (K↓),Middle: Simulations using aggregated SWE and distributed K↓, and Bottom: Simulations using distributed SWE and aggregated K↓.

Obvious discrepancies with the observed values were seen mainly at early stages of the snowmelt season in those landscape units where the aggregated initial SWE value did not agree with the observed value (Figures 5.6e-f, and 5.7e). Therefore, negative *E* values indicating unacceptable model performance, were found at the PLT area and NF slope. For those landscape units where the initial differences were not substantial, differences between simulated and observed values, resulted in similar snowmelt rates along the snowmelt season, however model performance was degraded in almost all the cases.

c) Simulations using distributed initial conditions and aggregated forcing data

The effects of using homogeneous forcing data (incoming short wave) without considering slope and aspect effects but using distributed initial conditions on simulating distributed SWE values are shown in Figures 5.6 to 5.8 for the UB, NF and SF slopes respectively. Lower performance criteria compared with those runs using distributed forcing were found in all the landscapes studied. The simulations had markedly higher melt rates as compared to the observed values, which resulted in a significant shortening of the snow melt season. This is illustrated by negative *E* values in the UB in 2003 (Figure 5.6g) and by negative or very low NS values in NF slope (Figures 5.7g-i). On the other hand, these effects were less noticeable on the SF slope presumably due to the weakness in simulating snowmelt of the model parameterisation obtained using distributed forcing in 2003. Simulations showed more uniform melt rates than both the simulations using distributed forcing and the observations. As a result the duration of the snowmelt seasons were lengthened and model performances were degraded when greater snow accumulation was observed such in 2003 and 2004 (Figures 5.8g-i). In the 2002 snow melt season (Figure 5.8h), although high model performance was observed (NS= 0.87), the estimation of the duration of the snowmelt season was lengthened by approximately 6 days.

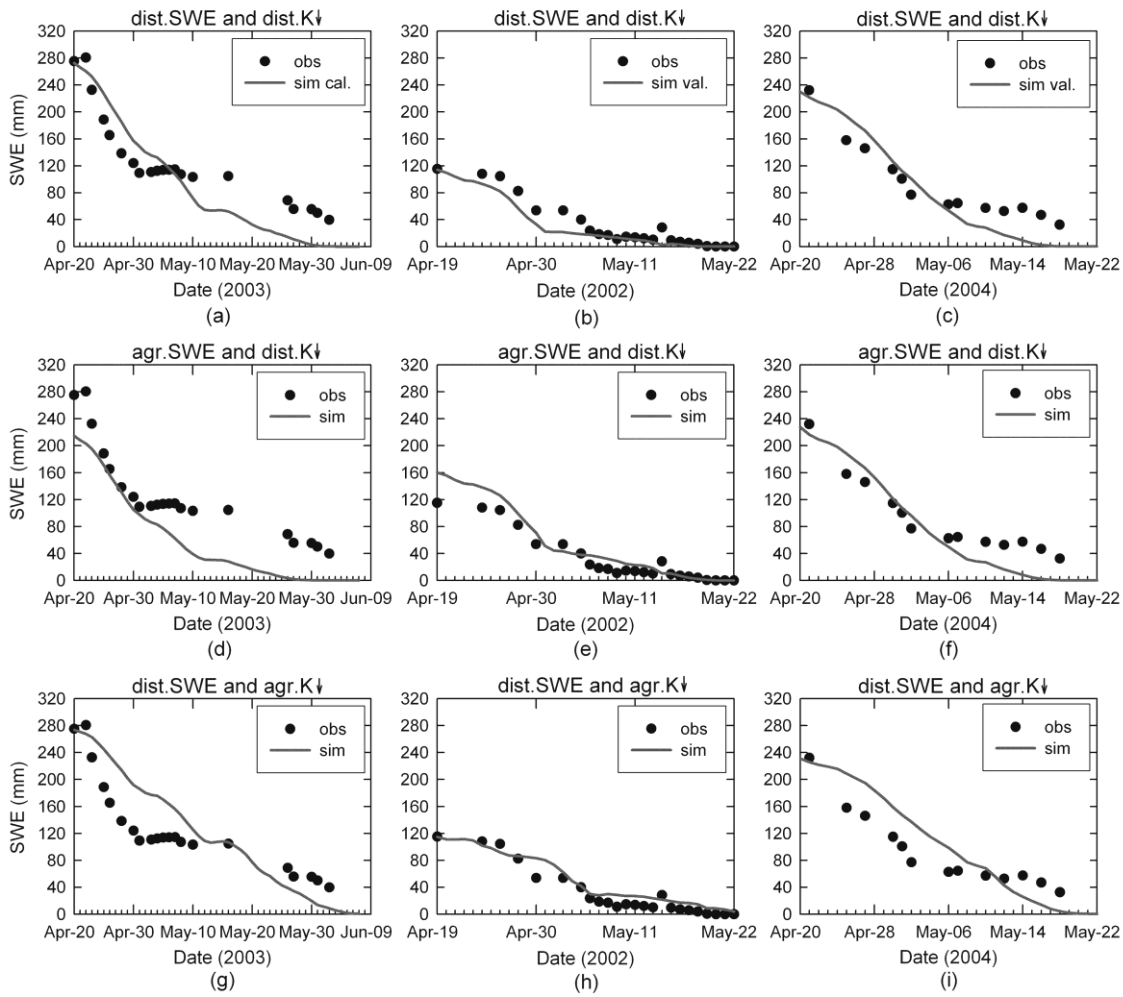

Figure 5.8: Observed and simulated areal SWE values for the South facing slope (SF) slope using CLASS. Top: Simulations using distributed initial conditions (SWE) and forcing (K↓), Middle: Simulations using aggregated SWE and distributed K↓, and Bottom: Simulations using distributed SWE and aggregated K↓.

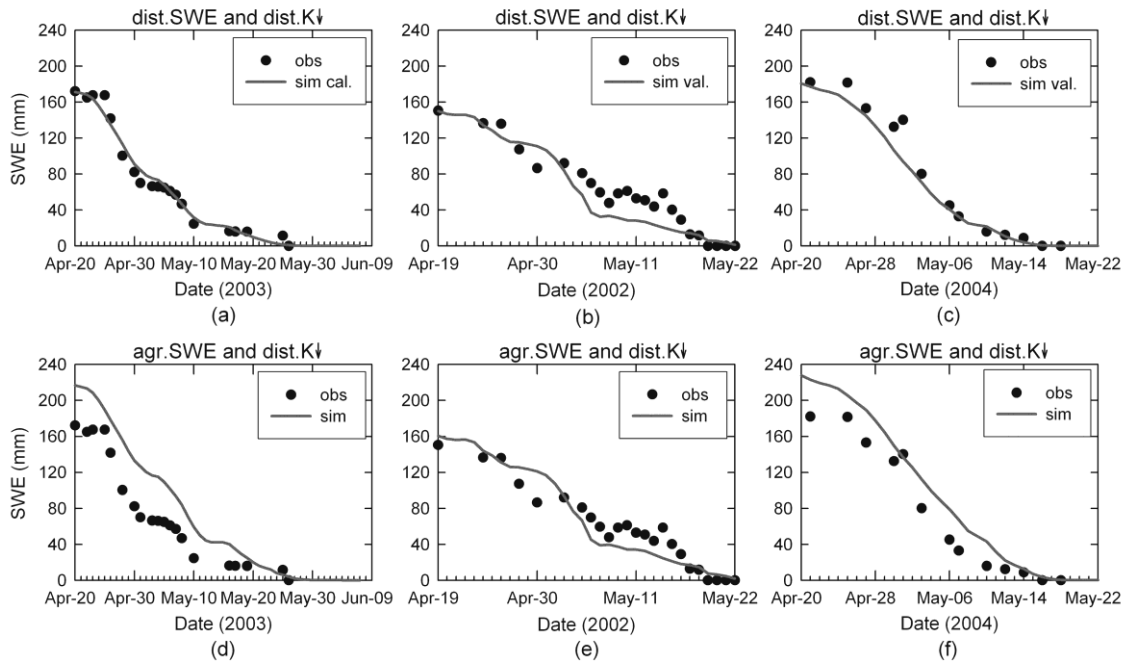

Figure 5.9: Observed and simulated areal SWE values for the Valley bottom (VB) in 2002, 2003, and 2004 using CLASS. Top: Simulations using distributed initial conditions (SWE) and forcing (K↓), and Bottom: Simulations using aggregated SWE and distributed K↓.

Table 5.5: Comparison of model performance in simulating snowcover ablation using CLASS in each landscape unit of GB. *IC*: Initial conditions (SWE), *F*: solar forcing (K↓), *E*: Nash- Sutcliffe coefficient.

Modelling strategy	Year	UB		PLT		NF		SF		VB	
		RMSE (mm)	E	RMSE (mm)	E	RMSE (mm)	E	RMSE (mm)	E	RMSE (mm)	E
Dist. I.C. and F.	2003	**13.3**	**0.93**	**16.7**	**0.76**	**19.6**	**0.87**	**36.2**	**0.70**	**8.8**	**0.98**
	2002					28.0	0.92	12.0	0.89	19.4	0.8
	2004			10.8	0.86	25.5	0.72	28.3	0.73	16.3	0.94
Agr. I.C.	2003	31.4	0.58	81.8	-4.87	19.5	0.87	44.9	0.54	41.6	0.46
	2002					112.3	-0.36	17.9	0.75	17.0	0.83
	2004			100.3	-10.69	44.2	0.16	27.7	0.74	27.0	0.84
Agr. F.	2003	**57.1**	**-0.38**			**65.9**	**-0.44**	**44.9**	**0.54**		
	2002					78.4	0.34	12.8	0.87		
	2004					101.3	-3.44	37.3	0.54		

d) Aggregated versus distributed modeling approaches

Figure 5.10 illustrates the comparison of the simulated basin-scale snowcover ablation using both aggregated and distributed modelling approaches. The aggregated

model used the basin-average of both SWE and incoming solar radiation, whereas in order to compare both modelling approaches, the distributed model used the re-aggregated distributed model outputs from each landscape unit. Comparisons were performed on those landscape units where snow survey data were available in all of the three years compared; hence observations were spatially-weighted averages. Similarly to Figure 5.4, only the NF and SF slopes, and VB were considered. The model parameterisation was set by using the spatially-weighted average of the optimum parameter sets obtained in 2003 in the three landscapes considered.

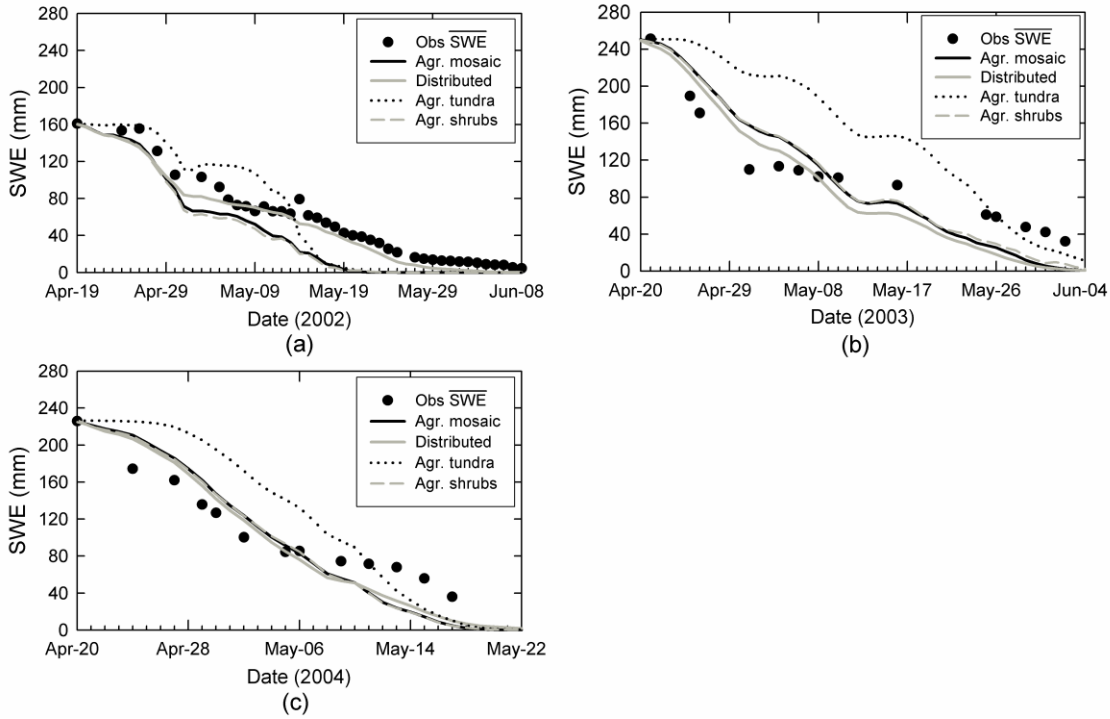

Figure 5.10: Comparison between spatially weighted basin-average simulations of snow-cover ablation using CLASS. Aggregated: avg. initial SWE and K□ over flat terrain. Distributed: re-aggregated simulations on NF, SF, and VB. Mosaic, tundra, and shrubs refer to the vegetation cover applied.

The comparison of the different modelling approaches among the considered years showed dissimilar model performances (Table 5.6). Differences between aggregated (using a mosaic representation of vegetation) and distributed modelling

approaches were minor in 2003 and 2004 (Figure 5.10b-c) due to small spatial variability compared to 2002 (Figure 5.10a). For the 2002 snow melt season, simulated SWE values of both the aggregated and the distributed models showed a close agreement with the observations at the early stages of the snowmelt season, however model results diverged in later melt. The distributed model adequately described the snow cover ablation with a *E* value of 0.96, whereas the aggregated model was unable to simulate the later half of the melt, showing a much more rapid depletion than the observed with a *E* decreasing to a value of 0.68. This difference in performance resulted in an increase of the RMSE from 9 mm to 24.5 mm of SWE. Conversely, for the 2003 and 2004 snowmelt periods, simulated SWE values of both the aggregated and the distributed models exhibited a very similar description of the evolution of the snow cover depletion. Analysis of the model performances showed NS values for the aggregated and distributed model of 0.70 and 0.72 for 2003 and 0.74 and 0.80 for 2004 respectively. Similar performance in terms of the RMSE was also observed. Further, the assumption of a continuous vegetation cover over the model grid in the aggregated approach, proved to have negative effects on simulations. Sensitivity analysis showed larger differences respect to the observed values that resulted in lower melt rates when alpine tundra was assumed as vegetation cover. Simulations based on a continuous shrub cover were close to those using the distributed approach as a result of the shrub dominance in the considered landscapes (i.e. NF, SF, and VB).

Table 5.6: Comparison of model performance in simulating snowcover ablation using CLASS between the basin-aggregated (AGR) with a mosaic vegetation cover and distributed (DIST) modelling approach. E: Nash- Sutcliffe coefficient.

Year	AGR		DIST	
	RMSE (mm)	**E**	**RMSE (mm)**	**E**
2003	**32.2**	**0.70**	**28.8**	**0.72**
2002	24.5	0.68	9.0	0.96
2004	26.7	0.74	23.1	0.80

One of the possible reasons that may explain the dissimilar results from the comparisons between the aggregated and the distributed approaches could be related to the differences in the ratio of the initial SWE on the NF and SF slopes amongst the analysed snowmelt seasons. The 2002 snowmelt season showed a very high spatial variability of the initial SWE with 303 and 120 mm of SWE in the NF and SF slopes respectively resulting in a difference of the 60 %. Conversely in 2003 the SF slope showed higher initial SWE values (280mm) than those seen in the NF slope (230 mm) resulting in a difference of 18 % whereas similar initial SWE values were observed in 2004. As a result larger differences between the aggregated and distributed approaches were seen when the differences in the initial SWE increased. Another reason could be the spatial covariance between initial SWE and melt energy. The coincidence of low SWE and high melt energy on the SF slope in 2002 raised the spatial variability of the snow cover depletion (SCD), whereas the coincidence of high SWE and high melt rate (2003 and 2004) reduced the variability of the SCD. Additionally, the high sub-grid variability of SWE due to the presence of an unusual drift in the SF slope (McCartney, 2006) not properly considered in the spatial discretisation of the model may explain why unsatisfactory simulations were observed on the SF slope for 2003 and 2004. Therefore, and given the areal dominance of the SF, no significant differences were observed between the aggregated and the distributed modeling approaches.

5.5 Conclusions

The effects of different aggregation methodologies on modelling snowcover ablation and basin runoff for a small basin in a high latitude, mountainous environment were evaluated. From the comparison of the two model aggregation approaches using a small-scale hydrological model (CRHM), the distributed approach best described the observed magnitudes of both snowcover ablation and basin runoff. Conversely, the aggregated approach could not properly represent the evolution of the differential

snowmelt rates during the course of the snowmelt period. Late stages of melt modelled by the aggregated approach showed substantially faster snowmelt rates than did the observations. Basin runoff predictions showed a dissimilar performance between the aggregated and the distributed models. While timing differences in the rising and falling limbs of the hydrograph were seen, runoff volumes were still adequately represented using the aggregated approach for a continuous, single snowmelt event, as observed in 2002. However, for a more complex snowmelt season with discontinuous snowmelt events, such as in 2003, the aggregated model was unable to predict timing and runoff volume because topographic effects in incoming shortwave radiation are not effectively represented. On the other hand, the distributed approach was able to describe the different runoff response observed in both of the studied years.

Calibration was obviously simpler in the aggregated model; however, the greater degrees of freedom in the distributed model allowed for a better description of basin runoff. The fact that minimal calibration was performed to model snowcover ablation suggested that the EBSM is a simple yet reliable physically-based snowmelt model. This also agrees with the findings of Walter et al (2005), in which better snowmelt simulations, compared with temperature-index models, were obtained using physically-based models with minimal data requirements. The presence of a continuous baseflow, the relatively low percentage of the initial SWE that becomes snowmelt runoff, and the role of the organic soil layer in generating fast runoff response at early stages of the snowmelt season, suggest the necessity of improving the conceptual soil moisture balance approach. The new formulation should link groundwater flow with streamflow, improve basin storage options, and adequately account for interflow or subsurface runoff. Further investigations involving the testing of the infiltration into frozen soil equation on slopes, and the evaluation of canopy effects enhancing snowmelt rates and abrupt albedo changes will contribute to the proper definition of model complexity at small to medium scales in northern mountain environments.

Similarly, the inclusion of spatially-distributed information in a LSS clearly improved simulations of snowcover ablation. The modeling strategy has been formulated applying a combined approach. First, the landscape heterogeneity is explicitly represented in the model (i.e., basin division) based on the previous understanding of the main controls over the hydrological processes in this environment. On this basis, a detailed description was used to generate the physically based forcing data and process representations. This was also achieved in the context of a calibration problem, where the effective parameters values were automatically optimized to best represent the complexity of the system.

Results showed that CLASS, using the pre-processing of the incoming short wave radiation by CRHM and considering spatially distributed SWE initial condition to represent wind redistribution effects, was able to successfully describe the snowcover ablation in the landscape units studied. Model simulations performed in the different landscapes using distributed information accurately described the observed snowmelt rates and timing of the melt. This highlights the importance of including spatially distributed information such as snow redistribution and topography in order to reduce input uncertainty. Conversely, the conceptualisation of the model grid as a single flat unit was not generally able to properly describe the observed snow ablation. Simulations using such an aggregated approach when the spatial variability of the SWE increased or when the spatial covariance between SWE and energy inputs was negative (i.e. opposite spatial association between melt energy and accumulated snow in a given landscape), showed a degradation of model performance, compared to the distributed model. This was illustrated in 2002 whit the greatest discrepancies between the two approaches resulting in a reduction of the *E* coefficient from 0.96 to 0.68. However, in those years when less spatial variability of the SWE was observed as a result of more homogeneous distribution of snow and a positive covariance between accumulation and melt energy, there were not significant differences between the aggregated and

distributed modeling approaches. On the contrary, the distributed approach adequately described the snowcover ablation in all the cases.

The effect of aggregating the initial conditions by using a basin-average initial snowcover (no snow redistribution by wind) degraded the LSS performance. In most cases examined, the differences with the observed initial SWE in each landscape unit were drastic, resulting in unsuitable model predictions. The effects were more noticeable in those landscapes units with high wind exposure (PLT) and sheltered sites (NF slope) respect to the predominant winds that developed large snow drifts. These results emphasise the importance for hydrological model predictions of incorporating snowcover heterogeneity caused by wind redistribution. Aggregation of forcing data (i.e., radiation not corrected for slope and aspect effects) had also unfavourable effects on model predictions. Thus, the assumption of uniform topography within the model grid significantly shortened or lengthened the duration of the melt in the NF and SF slopes respectively. This resulted in inappropriate model predictions reflected by negative E values and unreasonably larger RMSE values. However, it should be stressed that despite the effects due to either initial conditions or forcing data, combined effects as a result of the positive covariance between accumulation and melt are smaller and some times unimportant, resulting in similar model performances between aggregated and distributed approaches.

In summary, the consideration of snowcover heterogeneity due to wind redistribution and the effects of small scale topography on melt energetics enhanced predictions of snow ablation. This is also consistent with the findings in Déry et al. 2004, Davison et al. 2006, and Pohl et al. (2006) in arctic environments, where distributed approaches led to enhanced model simulations of LSS and hydrological models. Therefore, the incorporation of explicit representation of the landscape heterogeneity in LSSs can improve the estimate of snow covered area, melt rate, and land surface-atmospheric interaction at both small and larger scales.

CHAPTER 6

INCLUSION OF LANDSCAPE HETEROGENEITY IN DISTRIBUTED HYDROLOGICAL SIMULATIONS

6.1 Introduction

This chapter describes the distributed simulations of snowcover ablation and snowmelt runoff using the MESH modelling system in WC basin. The modelling approach is based on the results and evidence presented in Chapter 5. Therefore, landscape heterogeneity is explicitly included in the model spatial representation, in order to take into account its effects on the initial SWE and solar forcing.

6.2 Background

Snowmelt is typically the principal source for soil moisture, groundwater recharge, and streamfow in mountainous regions of the western Canada, US, and other similar regions of the world (Marks et al., 1999). The inherent complexity of these environments requires that information on the timing, magnitude, and contributing area be known for a successful water resource management. Conceptual snowmelt models, typically based on the temperature-index approach, are still applied for operational forecasting because they require less input data than physically based snowmelt models (Hock, 2003). Examples of temperature-index based models include the HBV-model (Bergström, 1976), the SRM-model (Martinec and Rango, 1986) and the UBC-model

(Quick and Pipes, 1977). Even though the implementation of this parsimonious approach is often accomplished using spatially distributed representations of the landscape (e.g. TOPMODEL, Ambroise et al., 1996; SWAT, Fontaine et al., 2002), it is unlikely that temperature-index models using conceptual parameters can meaningfully capture the spatial heterogeneity of snowmelt processes. Further, temperature-index models require substantial information to calibrate the 'melt factor' which challenges the main assumption for their applicability. Hock (2003) proposed the use of robust temperature-index models (i.e. spatially distributed and temporal variable degree-day factors), however Pietroniro et al. (1997) found that only marginal improvements were seen in the performance of temperature-index based models when combined temperature-radiation indices were added to melt estimations. On the other hand, since the work of Anderson (1976), physically based models have been able to accurately simulate the energy and mass balance of a snowpack. However, one of the main limitations is that while those snowmelt models retain an accurate representation of the physics of the energy balance and a detail snowpack structure, they have been often limited to point applications or simulations over small experimental sites.

Snowcovers show a significant spatial and temporal variability over both accumulation and ablation periods that are controlled by spatially and temporally variable atmospheric forcing conditions and their interactions with local topography and vegetation (e.g. Elder et al., 1991; Liston and Sturm, 2002; Liston et al., 2002; Essery and Pomeroy, 2004a). Modelling approaches developed to represent the spatial and temporal variability of accumulation and ablation processes include the incorporation of elevation effects and variation of solar radiation with topography. Elevation bands are often the only criterion for spatial discretisation in temperature-index models. For

example, Quick and Pipes (1972) incorporated elevation bands in the UBC model where melt rates for each model unit only vary as a function of elevation resulting from an air temperature lapse rate. Effects of elevation on air temperature and hence on the partioning between snowfall and rainfall (Dodson and Marks, 1997) have been incorporated into snow models (e.g. MicroMet; Liston and Elder, 2006a). Algorithms describing the variation of the solar radiation at the surface as a function of topography, latitude, season, time of day, cloud cover, and turbidity of the clear air (e.g. Garnier and Ohmura, 1970; Dozier, 1980) were effectible incorporated with the availability of gridded elevation data sets (e.g. Dozier and Frew, 1990; Blöschl et al., 1991; Marks et al., 1999). Similarly, improvements in the model performance were seen in the conceptual HBV-ETH-runoff model when the elevation bands were further divided into three aspect classes (Braun et al., 1994).

Elder et al. (1995) analysed the effect of the grid size on estimating SWE in grid-based snow models. Results from a nonlinear regression model showed that for high accumulation levels a large increase in the grid size resulted in a small increase in the predicted SWE as a result of linear snow-free areas being averaged into larger snow covered grids. However grid size becomes critical late in the melt season when small snow covered areas are averaged out into larger snow-free cells resulting in a significant underestimation of the predicted SWE. Blöschl (1999) showed that for non-linearly aggregating processes (e.g. enhancement of melt due to advection processes) there will be a scale effect on the mean grid values, which is also related to the validity of effective parameter values. Blöschl (1999) concluded that in general for practical applications, an optimum element size may not exist and that the model element scale may be dictated by data availability and the required resolution of the predictions. Examples of point scale snow models distributed over a grid representation of a basin include the UEB model (Tarboton et al., 1995, Tarboton et al., 2001), the ISNOBAL model (Marks et al., 1999), and the SnowModel (Liston and Elder, 2006b). Blöschl et al. (1991) after

comparing a grid-based distributed model with a snow band model and a parameteric model in a small alpine catchment concluded that for reliable distributed snowmelt modelling the major problem was the accurate estimation of spatial variation of snow water equivalent. Further, Luce et al. (1999) suggested that the approach of applying a 'point' model at many points on a fine grid is often impractical to use, so a subgrid parameterisation is necessary to enable modelling with larger model elements.

Examples of modelling applications in WC basin (Lacroix et al., 2002) include the use of the Simple LUmped Reservoir Parametric model (SLURP; Kite 1975 and 1978). The model conceptually simulates the behaviour of a drainage area by solving a vertical water balance of four reservoirs (canopy, snow-pack, fast and slow soil storage) for each model element and then routing the resulting runoff between the model units. SLURP is a daily time step model that divides a watershed into a number of sub-basins known as Aggregated Simulation Areas (ASAs), typically defined using landcover types and elevation data with the requirement that each ASA must contribute runoff to a definable stream channel. Model performance was analysed on inter annual basis focussing on the enhancement of basin discharges by optimising the number of ASAs. Similarly, Armstrong and Martz (2008) analysed the sensitivity of hydrological response using SLURP to coarsened land cover information. Comparisons with a calibrated model using detailed base cover map showed that reducing the level of detail of land cover information generally has a limited effect on hydrological response at the basin outlet. These results indicate that either SLURP is capable of minimizing the effect of land cover generalisation on the hydrology of Wolf Creek, because the model is unable to handle detailed land cover information, or that the parameterisation is not physically based and hence not related to land cover information. Further, calibration adjustments can absorb differences due to land cover. The WATCLASS model was also applied on WC basin (Bastien, 2004) using a 1km by 1km grid size. Overall, the inter-annual streamflow basin simulations were satisfactory in terms of the timing of the mayor

spring events; however spring estimation errors were the largest seasonal streamflow inaccuracies. Based on the past modelling experiences and on the difficulty in predicting snowmelt runoff in complex subarctic environments, the objective of this chapter was to apply a landscape based modelling approach to snowmelt simulations using a physically based land surface hydrological model. This modelling approach uses a landscape based model parameterisation and incorporates basin-wide information on the dominant hydrological processes that control snowmelt in those environments such as the initial spatial redistribution of SWE and topographic effects on incoming solar forcing.

6.3 Modelling setup

The model used in this study was the stand-alone 1.0b version of MESH. This model couples a land surface model (CLASS) with hydrological routing schemes (Pietroniro et al., 2007). For more details see Section 4.3.3. The simulation period included the 2002 and 2003 snowmelt seasons. In order to evaluate the performance of the distributed landscape based model, these model results were compared to simulations using an aggregated modelling approach assuming basin- average initial SWE and incoming solar radiation not corrected for slope and aspect effects.

6.3.1 Spatial discretisation

As it was described in Chapter 4, the spatial discretisation used to aggregate runoff calculations in the MESH model for WC basin was defined with a regular grid of 3 km by 3 km (see Figure 4.8). As a result, a model domain of 10 columns by 7 rows was defined. The spatial resolution was chosen in order to perform an upscaling exercise from GB to WC basin; therefore a grid size that approximates the area of GB was selected.

The Group Response Units (GRUs) were defined for each model grid according to topographic (i.e. slope and exposure) and vegetation characteristics (i.e. alpine, shrubs, and forest). Slopes with angles lower than 20 degrees were assumed equivalent to horizontal terrain while the exposures explicitly considered were those relevant to both snow accumulation and ablation processes. Therefore, NF and SF slopes were distinguished due to their distinct energy and snow accumulation regimes, whereas the EF slope was also distinguished due to its susceptibility to snow drift formation as a result of its lee location with respect to the dominant west to east wind flow (McCartney, 2006). As a result, twelve GRUs were defined using landscape based properties as well as the one addition GRU that incorporated water bodies (Table 6.1 and Figure 4.9).

Table 6.1: Group response units (GRUs) defined for landscape representation of WC basin. NF, SF, EF, and WF: north, south, east, and west facing slopes.

	slope-aspect	landcover type
GRU 1	NF	forest
GRU 2	SF	forest
GRU 3	EF	forest
GRU 4	WF + flat	forest
GRU 5	NF	shrubs
GRU 6	SF	shrubs
GRU 7	EF	shrubs
GRU 8	WF + flat	shrubs
GRU 9	NF	alpine
GRU 10	SF	alpine
GRU 11	EF	alpine
GRU 12	WF + flat	alpine
GRU 13		water

6.3.2 Observations and initial conditions

Distributed values of solar forcing corrected for topography were generated with CRHM according to the methodology described in Chapter 4. In order to include the

topographic effects on the incoming short-wave radiation in the MESH model, the code that reads the forcing-data was modified. MESH reads the forcing data with one entry per square grid or computational unit per one time step. The modification included the independent allocation of the solar forcing for each GRU; therefore forcing data was read with one entry per GRU per time step instead (Figure 6.1). The advantages of this methodology are that it allows for a more realistic representation of the differential solar forcing than when a single forcing per computational grid is used and it does not involve additional computational time compared to the former approach, since in this case, the same forcing was later assigned to the different GRUs where snow energetics calculations were performed.

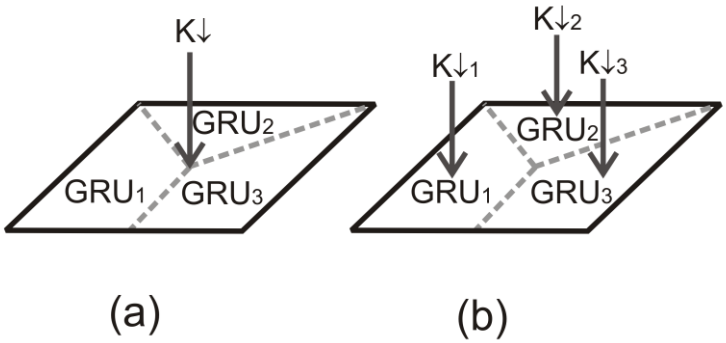

Figure 6.1: Schematic representation of the forcing-data reading scheme of MESH. Solid line square: model grid, dashed lines: GRU delimitation. a) One forcing per computational grid, b) modified forcing configuration with independent solar forcing for each GRU within the computational grid. GRU: group response unit, K↓: incoming short-wave radiation.

Four meteorological stations were used to generate the distributed forcing data for the MESH model. The stations are located in the three major environments (forest, shrubs, alpine), covering not only the different landscape types but also the basin elevation ranges (see Figure 3.1). Two stations, PLT and BB, are located in the shrub area representing slightly different conditions since PLT station was situated (uninstalled in 2004) in a windswept area whereas BB station is located in a more sheltered site with taller shrubs. All the stations were monitored by Yukon

Environment, with the exception of the PLT station installed and operated by University of Saskatchewan. Parameters monitored using half-hour observations included: incoming (K↓) and outgoing (K↑) short-wave radiation, incoming long-wave radiation (L↓), air temperature (T_a), relative humidity (RH), wind speed (U), precipitation (P), barometric pressure (P_{atm}), snow depth (S_d), soil temperature (T_s), and soil moisture (S_m). Table 6.2 describes the location and observations of the meteorological stations used in this study.

Table 6.2: Meteorological stations of Wolf Creek basin.

Station ID	UTM location		Elevation (m.a.s.l.)	Meteorological and state variables measured
	Northing (km)	Easting (km)		
Forest (F)[1]	6718	503	750	K↓, K↑, T_a, RH, U, P, S_d,T_s, S_m
Alpine (ALP)[2]	6715	492	1616	K↓, K↑, T_a, RH, U, P_{atm}, P, S_d,T_s, S_m
Buck brush (BB)[2]	6710	489	1250	K↓, K↑, T_a, RH, U, P, S_d,T_s, S_m, snow pillow
Plateau (PLT)[2]	6712	490	1460	K↓, K↑, L↓,T_a, RH, U, P, S_d,T_s, S_m

Elevation from ground surface for meteorological sensors: (1) 10 m (above canopy), (2) 2 m.

Distributed values of each forcing variable for the model domain were obtained by linear interpolation of the four stations values. The interpolation method was selected due to both its simplicity and similar values respect to the kriging and inverse-weight distance interpolation methods as a result of the relatively simple model domain (10 cols. by 7 rows). The interpolation was applied using MATLAB software. This approach was used for $K\downarrow$, T_a, and RH. Although monthly variable lapse rates were suggested for northern environments (Kunkel 1989; Liston and Elder, 2006a), a constant environmental lapse-rate correction (-7.65°C/km) was performed in each model grid to compensate for elevation effects on T_a values (Dodson and Marks, 1997). The basin environmental lapse rate was calculated from air temperature observations using a radiosonde attached to weather balloon. Observations were conducted during the melt

period in WC basin (Essery, personal communication) as the average between the observed day (15:00) and night (3:00) lapse rates respectively. In order to account for influences of elevation and temperature on surface pressure, the distribution of P_{atm} values over the model domain was conducted by calculating for each grid element the P_{atm} values using equation 6.1. Thus, no interpolation of the station pressure was required.

$$P_{atm} = P_0 e^{-mgh/RT_a} \quad 6.1$$

where P_0 is the air pressure at the sea level (1013.25 hPa), m is the molar mass of the air (0.028964 kg mol^{-1}), h is the elevation above sea level [km], g is gravitational acceleration at the earth's surface (9.81 m sec^{-2}), R is the Ideal Gas Law constant, (8.314 $kg\,m^2\,sec^{-2}\,K^{-1}\,mol^{-1}$), T_a is the gridded air temperature [K].

Atmospheric long wave radiation is calculated from the Stefan-Boltzmann equation $L\downarrow = \varepsilon\sigma T^4$, where ε is the air emissivity, σ is the Stefan-Boltzmann constant (5.67E-8 W m^{-2} K^{-4}) and T is the temperature of the radiating body [K]. Estimates of the ε values are uncertain. A general approach is based on parametric relationships between standard meteorological measurements and cloud-cover (e.g. Sicart et al., 2006). However, cloud-cover information is rarely available and remains subject to substantial errors (Granger and Gray, 1990). Alternatively, if observations of $L\downarrow$ are available and assuming that ε is conservative; the ε can be obtained from the Stefan-Boltzmann equation. However, the usual assumption of the air temperature as an estimate of the clouds temperature could lead to highly uncertain estimates of ε and hence $L\downarrow$ values. Therefore, values of $L\downarrow$ measured at the PLT station were uniformly distributed over the model domain. Distributed T_a, RH, and P_{atm} values were used to calculate the gridded values of specific humidity (q). Due to uncertainties in the P values recorded using unheated tipping bucket devices (i.e. rain gauge funnel often becomes clogged by snow and ice at the beginning of the melt season) at the F, PLT, and ALP stations, P values

measured at the BB station using an automatic precipitation gauge were corrected by wind-induced undercatch (Pomeroy and Li, 2000) and uniformly distributed over the model domain since no consistent relationship between snowfall and elevation was observed in the basin (Pomeroy et al., 1999). This automatic precipitation gauge consists of a storage bin filled with antifreeze used to convert snow to liquid water. As snow melts, the change of the level in the antifreeze reservoir is recorded and converted to millimetres of precipitation. Although it is unshielded rain gauge subject to wind-induced undercatch, it has the advantage over the tipping buckets rain gauges, that it does not underestimate intense rain and it can measure other forms of precipitation, including rain, hail and snow. Pomeroy et al. (1999) found that the seasonal and areally-weighted basin snowfall exceeded that measured at the Whitehorse airport by 33% to 47% of the airport measurement. Comparisons for the melt season between recorded *P* values at BB station and the Whitehorse airport station showed larger differences than the relationships found by Pomeroy et al. (1999). The *P* values recorded at the BB station for the 2002 and 2003 snowmelt seasons were 30.8 and 11.9 mm whereas the *P* values for the Whitehorse Airport station were 12 and 2.3 mm respectively.

Snowcover conditions prior to the onset of melt in WC are primarily related to the vegetation cover (i.e. boreal forest, shrubs and alpine tundra), exposure, and the occurrence of blowing snow events. Pomeroy et al. (1999) found remarkable consistent differences in SWE between landscapes. Snow accumulation regimes showed that shrubs areas registered the deepest snowcovers whereas shallow and eroded snowcovers were seen at the forest and alpine sites respectively. In the forest site, intercepted snow is mostly retained in the canopy from where it sublimates resulting in shallow snow covers. In the shrub area, the principal role of the vegetation in the development of the snow cover is the modification of the aerodynamic roughness to the atmosphere and on the flow of blowing snow due to the variable shrub height and density. Snow is blown from short shrubs and exposed areas to sheltered and tall shrub sites resulting in very

heterogeneous snowcovers. At the alpine site, the lack of a conspicuous vegetation cover and its exposed location due to the elevation, leads to eroded snow covers as a result of its source role in the snow transport process. Initial snow cover conditions for the study periods were determined from snow surveys at the F, BB, ALP, and GB (Appendix A) sites. Observed values were consistent with the described snow accumulation patterns with deeper snow covers at the shrub sites. To account for snowcover redistribution, field observations describing the typical presence of snow-drifts on the NF and EF slopes (Pomeroy et al. 2003 and 2004; McCartney, 2006) were considered. As a result, SWE values corresponding to snow-drift conditions were assigned to the GRUs with NF and EF slopes in the shrub landscape area. In the forest landscape the same initial snowcover was applied to all GRUs reflecting interception rather than wind redistribution of SWE. The alpine environment was initialised with values from the ALP station and UB snow survey in GB.

Soils types can be related to the three principle ecosystems, boreal forest, sub-alpine taiga (shrub-tundra) and alpine tundra of WC basin (Francis, 1997; Janowicz et al., 2002 and 2003). Forest soils are coarse consisting of loamy sand and sandy loam to a depth of about 40 cm with a thin organic layer. The parent material consists of moderately stony morainal deposits mixed with alluvial and lacustrine material. Shrub tundra soils are medium to coarse textured consisting of silty loam in the upper horizons (0 to 18 cm) with sandy loam in the lower horizons. The organic layer is usually less than 10 cm thick with the exception of the NF slopes where it is usually well defined with depths of about 18-25 cm (Carey and Woo, 2001b). Alpine tundra soils are primarily silty loam with a very thin (< 2 cm) or nonexistent organic layer. Presence of boulders of up to 1 m is frequent and scattered about the landscape. The soil column is represented in MESH by three soil layers with depths of 0.10 m, 0.25 m, and 3.75 m respectively (Table 6.3). Based on the soil description for the WC basin, GRUs for the same landcover type (i.e. boreal forest, shrub-tundra, and alpine tundra) shared the same

soil parameterisation with the exception of the NF slopes on the shrub tundra area with a thicker organic layer of 25 cm. Since soils are fully frozen at the time of snowmelt, initial soil moisture content was based on fall observations using Time-Domain Reflectometry (TDR) sensors at the A, BB and F sites. The depth of measurements of soil moisture varied with location. Soil moisture at the F and BB sites is measured at 5 cm, 15 cm, 30 cm and 80 cm whereas at the A site is measured at 5 cm and 15 cm. As for pre-melt conditions, no ponded water was considered and minimal liquid water content (0.04) was assumed for the entire soil column. Since similar soil moisture contents were measured in the fall prior to the studied years, the same initial soil moisture values were used in 2002 and 2003 respectively. Initial ice water content for the soil layers expressed as a percentage of the pore volume is detailed in Table 6.3. However, these values are indicative since soil moisture contents can potentially be affected by sporadic melt or infiltration events during winter. Hydraulic soil properties are incorporated into the MESH model using the Clapp and Hornberger (1978) parameterisation of soil water properties with fitting parameters from Cosby et al. (1984). Initial soil temperatures were obtained from observations at the same sites using buried thermocouples with the same reading depths. Temperatures of the canopy were set to match the air temperature, following Sicart et al. (2004).

Table 6.3: Soil parameters for MESH expressed as percentage for each soil layer and land-cover type of Wolf Creek basin. Soil types according to Janowicz et al. (2002 and 2003), porosity values (θ_p) in MESH are determined by Cosby et at. (1984) for mineral soils whereas for organic soils (Org) values are assigned following Letts et al. (2000). θ_i: initial water (ice) content, Fp and Sp are fibric and sapric peat respectively.

Landcover Type	Layer 1					Layer 2					Layer 3			
	Sand	Clay	Org	θp	θi	sand	clay	Org	θp	θi	Sand	Clay	θp	θi
Forest	--	--	F_P	93	7	75	10	--	39	10	20	10	46	15
Shrub-tundra	--	--	F_P	93	25	20	10	--	46	22	55	10	42	18
Shrub-tundra (NF)	--	--	F_P	93	25	--	--	S_p	83	22	55	10	42	18
Alpine	20	10	--	46	25	20	10	--	46	25	20	10	46	25

Distributed simulations of MESH were validated where data were available. Thus, snowcover ablation was evaluated in GB using snow survey data (Appendix A), at BB station using snow-pillow data, and at the F site for 2003 using snow survey data from a snow grid of 21 by 21 points. The snow-pillow measures the hydrostatic pressure created by overlying snow. It consists of an antifreeze fluid-fill bag with a diameter of approximately 3 m connected by a pipe to an adjacent instrument house. The weight of the snow pushes an equal weight of the antifreeze solution. Level changes in the standpipe are recorded by a float connected to a shaft encoder and stored in a data collection platform (DCP).

Streamflow model performance was analysed in four points within the WC basin (see Figure 3.1) where stage records are available. Streamflow data is measured by Yukon Environment using standard stage-discharge relationships. The gauge stations are located in dissimilar sites and subject to different regimes during the melt season (Table 6.4). The Upper Wolf Creek (UWC) and Granger Creek (GC) gauge stations both measure the discharge from the alpine tundra environments. In both stations a base flow component observed before melt indicates an active winter groundwater contribution to the streamflow. Discharge from the Wolf Creek at Coal Lake outlet (CL) station is naturally regulated by the Coal Lake water level. Jasek and Ford (1997) observed an unusual lake outburst as a result of an ice dam that delayed the lake's outflow for 9 days after the onset of melt in 1996. Lower than normal temperatures froze the lake outlet to the bed restricting stream discharge. High temperatures in the spring breached the ice dam causing a significant flow wave to move downstream. Although, such ice dams have been observed in the past and are plausible due to shallow cross section at the Coal Lake outlet, this phenomenon was not observed during the study periods. Overall, observed streamflow proved to be highly variable during the study periods resulting in markedly dissimilar hydrographs presumably due to differences in snow redistribution. A possible error that could potentially lead to a late

beginning of the streamflow response and a subsequent sharp rising limb of the observed hydrograph is the difficulty to access to the stream gauges in order to perform the maintenance work before the onset of melt and snow dam effects in the stream channel (Woo and Souriol, 1980). Additionally the assumption of no flow under ice contributes to the observational uncertainty.

Table 6.4: Streamflow gauges of Wolf Creek basin (from Bastian, 2004).

Station ID	UTM location		Drainage Area (km)	Regime
	Northing (km)	Easting (km)		
Granger Creek (GC)	6712	503	6	Natural
Upper Wolf Creek (UWC)	6706	484	15	Natural
Wolf Creek at Coal Lake outlet (CL)	6708	491	71	Regulated
Wolf Creek at Alaska Highway (WCAH)	6719	503	195	Natural

6.3.3 Model calibration

Automatic calibration of the MESH model was performed using the DDS global optimisation algorithm. The calibration problem was solved using a single objective function by maximising the E coefficient between simulated and observed streamflow values at the WC basin outlet (WCAH). The 2002 snowmelt season was used as calibration year while the 2003 snowmelt season was selected as the validation period. Since the modelling of the entire WC basin is an up-scaling exercise of the results found in GB (Chapter 5), calibration was restricted to the hydrological parameters that describe flow routing at the landscape or GRU scale (i.e. overland, subsurface flow) and streamflow, while the values of the parameters that describe snowmelt were set according to the optimum values found for CLASS in GB (see Table 5.3). Forest parameters not included in the simulations of GB were set applying default values used in GEM simulations (Appendix B). To reduce the degree of freedom in the calibration process due to the large number of parameters, calibration was constrained by assigning

the same parameter value to all GRUs within each main vegetation cover. For example, NF slope, SF slope, EF slope, and WF slope and flat landscape units in the shrub area shared the same parameterisation. Similar approaches were applied in the alpine and forest area. Table 6.5 illustrates the parameters values found using the DDS algorithm.

Table 6.5: Optimised flow routing parameter values for MESH in Wolf Creek basin. Forest, Shrub, and Alpine GRUs include the NF, SF, EF, and WF-flat landscape units. Parentheses indicate parameter bounds.

Parameter	GRU			River network
	Forest	Shubs	Alpine	
DRN - Drainage index	0.500 (0 - 1)	0.615 (0 - 1)	0.817 (0 - 1)	
D_d - Drainage density [m^{-1}]	2.765 (1-5)	2.324 (1-5)	3.350 (1-5)	
XSLP - Average slope of GRU [$m \cdot m^{-1}$]	0.015 (0.01 - 0.05)	0.047 (0.01 - 0.05)	0.005 (0.01 - 0.05)	
GRKF - Coef. of Ksat change in the first metre of soil.	0.22 (0.2 - 1)	0.40 (0.2 - 1)	0.92 (0.2 - 1)	
MANN - Manning's n for overland flow	0.034 (0.025 - 0.1)	0.040 (0.025 - 0.1)	0.046 (0.025 - 0.1)	
WFCI - Surface Ksat [$m \cdot s^{-1}$]	5.9E-6 (1E-9 -1E-5)	4.1E-6 (1E-9 -1E-5)	9.9E-6 (1E-9 -1E-5)	
wf_r2 - River rougnnes				0.792 (0.1 - 0.95)
ZPLIMS - Lower limit ponding water [m]				0.078 (0.02 - 0.15)
ZPLIMG - Upper limit ponding water [m]				0.176 (0.15 - 0.19)

6.4 Model results

In order to include in the evaluation of the model performance the contrasting runoff responses observed at the different gauge stations for the studied snowmelt seasons, the same graphical scale for both years in each gauge station was used to illustrate the comparison between observed and simulated streamflow values. Figure 6.2 shows the streamflow simulations at the WCAH station, at the outlet of the basin, for

the 2002 and 2003 snowmelt seasons using distributed and aggregated approaches respectively. Overall a reasonable representation of the observed hydrograph was seen when the distributed approach (i.e. using distributed initial conditions and solar forcing) was applied in both the calibration and the validation periods (Table 6.6). Simulated values satisfactorily described the different dynamics of the of the observed streamflow that resulted in a steady and late hydrological response in 2002 with a gradual rise and recession of the hydrograph limbs compared to the early, sharp and ephemeral peak observed in 2003. The model efficiency resulted in *E* coefficients of 0.88 and 0.68 for 2002 and 2003 respectively. Although underestimation of the hydrograph peak degraded the model performance in the validation period in 2003, an appropriate representation of both the timing of the peak and the recession was seen.

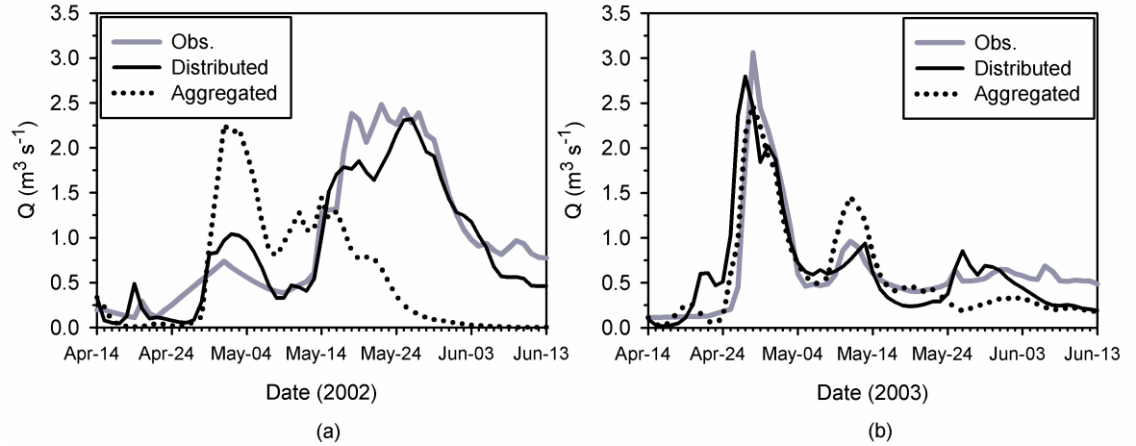

Figure 6.2: Comparison between observed and simulated hydrographs at the WCAH gauge station. a) 2002 calibration, b) 2003 validation.

Conversely, when the aggregated approach was applied by assuming a basin-wide average initial snowcover and uniform (i.e. over horizontal terrain) incoming solar radiation, the model performance was drastically degraded in 2002 with a less noticeable effect in 2003 compared to the distributed approach. To avoid the possible influence of calibration in the comparison between distributed and aggregated approaches, simulations using the aggregated approach were also calibrated in 2002

using the DDS algorithm. The inappropriate prediction of the observed hydrograph that resulted in a negative *E* coefficient, highlighted the importance of considering the spatial distribution of initial conditions and solar forcing in model performance.

Table 6.6: Streamflow model performance (E, Nash-Sutcliffe coefficient) obtained at the WCAH gauge station in Wolf Creek basin. DIST. and AGR: Distributed and aggregated modelling approaches. In bold calibration year.

year	Modelling approach	
	DIST	**AGR**
2002	**0.88**	**-1.06**
2003	0.68	0.67

Reasons that might explain the different model performance from using both distributed and aggregated approaches can be found by analysing the basin streamflow response. Typically, the streamflow response of the WC basin is controlled by sequential melt timing between the different ecosystems and by the shrub tundra zone due to its larger extent, central location, and deeper snowpacks compared to the forest and alpine areas. Melt starts around the middle of April in the forest area, followed by the shrub tundra zone with an onset of melt around Apr 20 whereas melt in the alpine area starts around the end of April. Furthermore, streamflow dynamics can by affected by warm air advection over the melting snowcover, enhancing melt and accelerating streamflow response. Combination of these processes can lead to synchronised or unsynchronised melt events between the different landscapes resulting in different basin streamflow responses. For the 2002 snowmelt season, the onset of melt was rather late and consequently driven by increases in both air temperature and incident solar radiation. These atmospheric factors, combined with large snowdrifts observed on NF slopes resulted in a late and single peak streamflow response. Therefore, the aggregated model using a basin average initial SWE and incoming solar radiation not corrected by topography, simulated earlier melts than occurred. On the other hand, the 2003 snowmelt season showed an onset of melt as a consequence of above freezing air

temperatures earlier in the season that stopped as the temperatures fell below the freezing point in May 2. This phenomenon generated a sharp and early streamflow response (Figure 6.3). Later in the season, the increasing air temperatures and solar radiation combined with lower amounts of initial snow on the NF slopes and comparatively larger snowcovers on the SF slopes, resulted in a steady streamflow response. Consequently, simulations using the aggregated approach at the basin outlet did not differ from those using the distributed approach and both replicated the observed peak hydrograph, although the model performance degraded as the season progressed. Moreover, simulated streamflow values in 2003 showed an early melt event in concordance with an air temperature increase around Apr 20 that was not recorded in the observed hydrograph presumably due to due the delay of streamflow as a result of snow dam effects. This phenomenon was described by Woo and Souriol (1980) in the Canadian Arctic where small damburst floods following the breaking of snow dams increased the stream discharge by up to five times in a few hours.

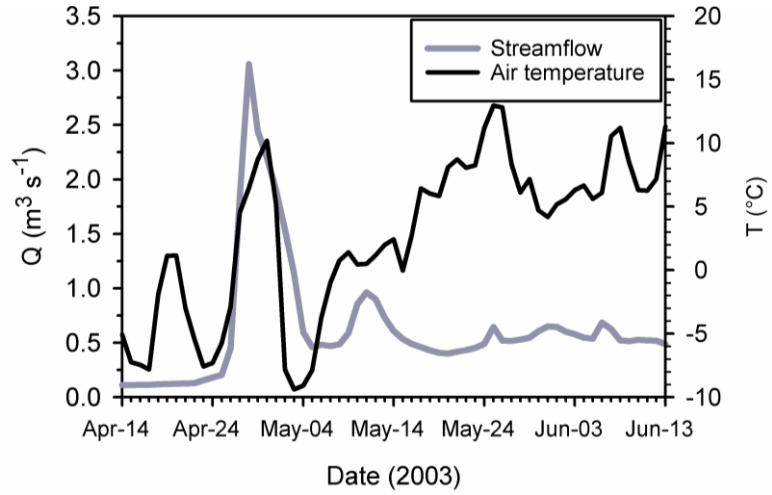

Figure 6.3: Illustration on a daily basis of the incidence of air temperatures in the dynamics of the streamflow response observed at WCAH gauge station in the 2003 snowmelt season.

The natural reservoir effects on streamflow of the Coal Lake were incorporated in the MESH model by including, in the corresponding model grid, the lake outlet flow

values measured at the CL gauge station. The main contribution of the reservoir is the maintenance of a base flow at the basin outlet. This situation was observed in 2003 where the flows at the CL outlet did not influence the peak hydrograph at the basin outlet, however a larger contribution of the reservoir releases to the dynamic of the basin response was observed in the 2002 snowmelt season, where both hydrographs showed the same shape and timing. Inclusion of the CL reservoir in the model simulations proved to have a small effect on downstream simulations since an overall a good agreement between observed and simulated values at the CL gauge station in both years was observed, although larger differences were seen in 2003 (Figure 6.4). Results indicated a reasonable representation of the snowmelt runoff upstream of Coal Lake.

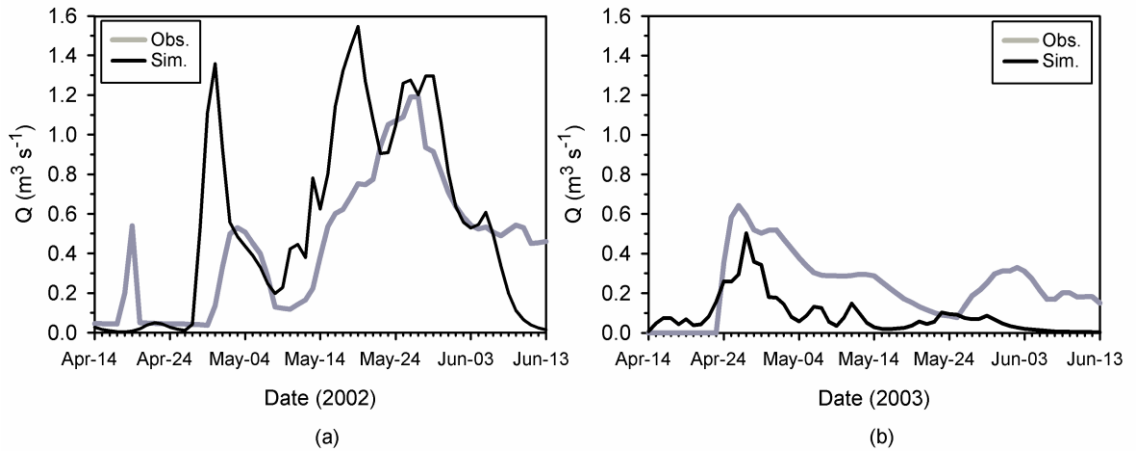

Figure 6.4: Comparison between observed and simulated hydrographs at the CL gauge station located at the Coal Lake outlet. a) 2002, b) 2003.

Distributed streamflow simulations are displayed in Figures 6.5 and 6.6 in GC and UWC gauge stations for 2002 and 2003 respectively. For the 2002 snowmelt season simulated values at the GC station (Figure 6.5a) showed an appropriate timing of the peak, however a underestimation of the observed hydrograph peak value was seen. For the 2003 snowmelt season (Figure 6.5b), simulated streamflow values showed a lack of agreement with the observed hydrograph resulting in earlier runoff volumes and

lower peak estimations. Simulated values resulted in an underestimation of the observed spring runoff volume.

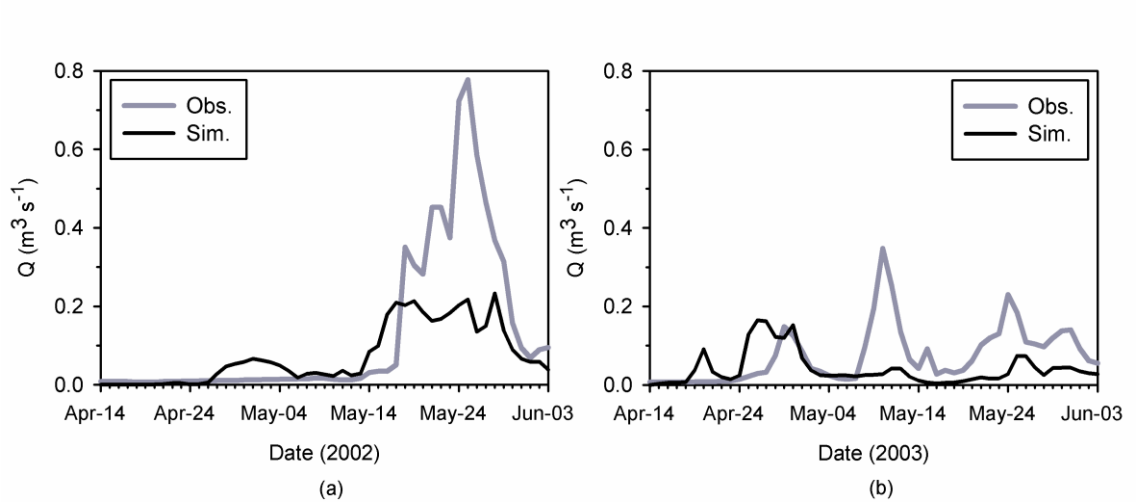

Figure 6.5: Comparison between observed and simulated hydrographs at the GC gauge station. a) 2002, b) 2003.

Comparison between observed and simulated values at the UWC gauge station in 2002 snowmelt season (Figure 6.6a) showed early runoff volumes that were not recorded in the observed hydrograph. Despite the differences between the observed and the simulated hydrograph shapes, spring runoff volumes were reasonably close. Similarly, and despite the differences in runoff volumes compared to the 2002 snowmelt season, an earlier snowmelt runoff response was simulated in 2003 (Figure 6.6b). Overall, differences between distributed simulated and observed streamflow values illustrate that the model with the given spatial resolution is not able to accurately replicate the complexity of small-scale snowmelt runoff processes. However, reasonable simulated runoff volumes and less important differences in replicating the runoff dynamics were seen in 2002 when the snowmelt runoff response was characterised by a single peak event. Conversely, larger differences in describing both the observed dynamics and runoff volumes were seen in 2003 as a result of the complex runoff response that resulted in lower flows and multi-peak hydrographs. Furthermore, the inherent observation errors due to low flow volumes and the inaccessibility of the

gauge stations early in the melt season could contribute to observational uncertainty early in the snowmelt seasons.

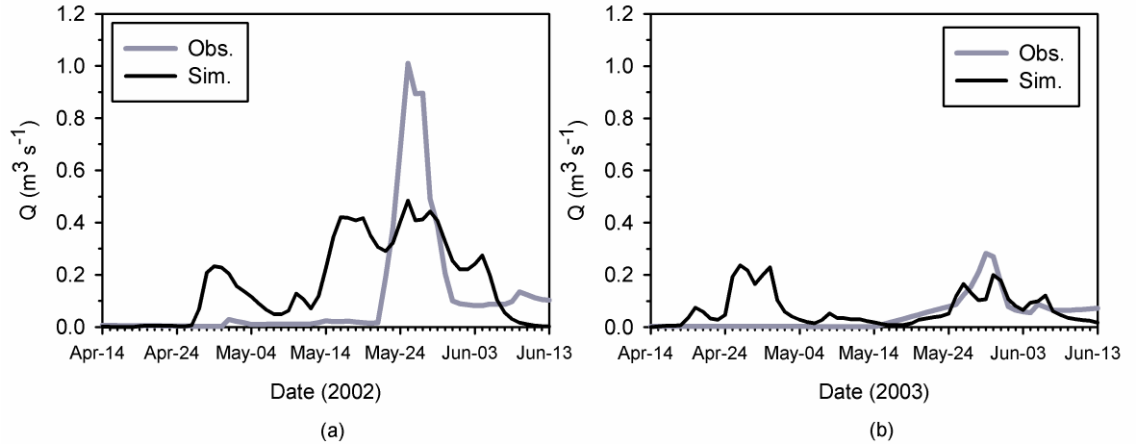

Figure 6.6: Comparison between observed and simulated hydrographs at the UWC gauge station. a) 2002, b) 2003.

Distributed simulated values of snowcover depletion were extracted in those places where distributed observations were available. Thus, in Figure 6.7 are compared the simulated snowcover depletion values with the snow-pillow observations in the BB station for 2002 and 2003 and with the snow survey values measured in the F station in 2003. Evaluation of the model performance against snowpillow data were conducted by comparing the simulations against the 5-day average of the observational data. Overall, reasonable simulations of the snowcover depletion were found for both years (Figure 6.7 a and b) considering that the snowpillow data represents the melting of a snowpack with no vegetation effects.

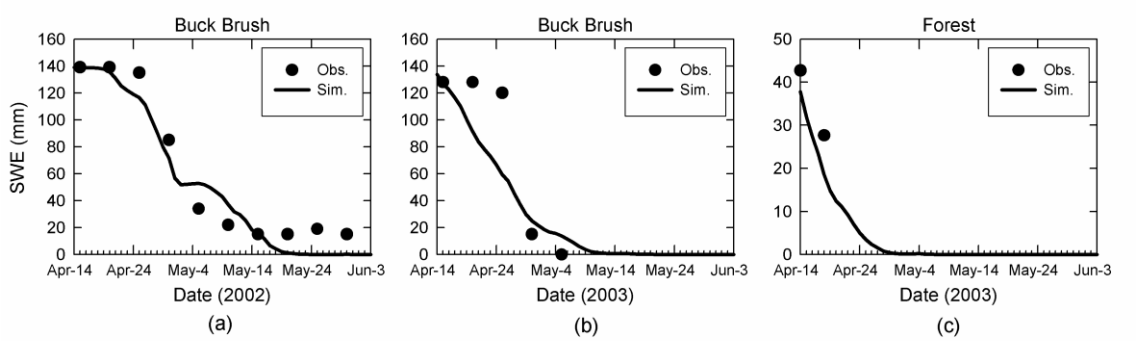

Figure 6.7: Comparison between distributed observations and simulations of snowcover depletion. a) and b) Snow pillow data in Buck Brush (BB) station, and c) Snow survey grid data in forest (F) station.

Differences were more evident in 2003 where the model results were not totally able to describe the observed fast depletion of the snowpack. In the forest area (Figure 6.7c), despite the lack of enough data along the entire snowmelt season, an adequate description of the early stages of melt was seen.

6.5 Conclusions

A physically based modelling approach that is founded on the combination of an inductive reasoning approach for basin segmentation and a deductive reasoning approach for process descriptions, has been applied to simulate snowcover ablation and snowmelt runoff in a complex subarctic environment. The inductive approach is based on a basin-wide understanding of the main factors that drive the snowmelt processes in northern mountainous areas. Therefore, landscape based model units defined according to slope and aspect, end of winter snow redistribution, along with the main landcover types were used for representing the landscape heterogeneity. In each unit, physically based process descriptions were applied using a deductive approach.

Simulations using distributed initial conditions and incoming solar forcing showed an appropriate representation of the basin hydrographs. Simulated streamflow values were able to properly describe the different timing and magnitude of the basin responses observed in both of the study years. Additionally, the distributed approach

showed a satisfactory description of the snowcover ablation in the shrub tundra and forest environments. On the contrary, when the aggregated approach was applied dissimilar model results were seen. The aggregated model was unable to simulate the dynamics of the basin streamflow in 2002 when the runoff response was largely governed by solar radiation and the negative association between snow accumulation and melt energy observed in the shrub tundra area. Conversely, less important differences between the distributed and aggregated approaches were seen when temperature was a key factor on the onset of melt in 2003. These results agree with the findings of Pomeroy et al. (2004 and 2005b). They observed that when synchronicity of melt between the different ecosystems was present; no spatial association between melt rate and initial SWE was observed. Melt synchronicity was reduced with greater incoming shortwave radiation, so the more that clear skies prevailed, the greater the duration of melt over the basin. Consequently, the distributed modelling approach including distributed information of initial SWE and incoming solar radiation was able to properly describe the sequential melt timing under clear skies, whereas the aggregated approach drastically failed. On the other hand, under conditions with greater cloudy skies, both modelling approaches had a very similar performance as a result of a less important effect of the initial conditions and solar forcing on the onset of melt.

Validation of the streamflow simulations using the distributed modelling approach at the sub-basin scale (i.e. GC and UWC) exhibited less satisfactory results. Streamflow simulations consistently showed an earlier streamflow response than the observed hydrograph. It is evident that the spatial model resolution is too large and hence it is not able to properly account for small scale processes such as snow dams in the stream channel or ponding surface water that delayed streamflow response. Furthermore, the observed low flow values and its related observational uncertainty make it very difficult to properly simulate snowmelt runoff, because almost no routing

processes were included in the model since only one or a small number of grid cells are considered at this scale.

Model parameterisation was defined according to observations when possible and using a step-wise calibration procedure, where the majority of the parameters controlling snowmelt were calibrated at the landscape scale based on the evidence collected from research investigations in the area. With this landscape based parameterisation, satisfactory distributed simulations of streamflow and snowcover depletion were obtained and later validated by calibrating the remaining parameters such as those controlling the flow routing. Therefore, this study showed the importance of including slope and aspect, snow redistribution, and vegetation types in the definition the spatial model units, for reliable snowmelt simulations. This landscape-based approach founded on a basin-wide process understanding is suitable for remote region predictions due to their inherent ungauged nature.

CHAPTER 7

REGIONALISATION OF LAND SURFACE HYDROLOGICAL MODEL PARAMETERS IN SUBARCTIC AND ARCTIC ENVIRONMENTS

7.1 Introduction

This chapter describes the transference of landcover based parameters of a distributed and physically based LSH model between two basins in northern cold regions. This approach is intended for use in distributed models where typical basin-wide regionalisation relationships are conceptually unsuitable due to scale issues. The analysis focuses on the application of a detailed physically based process descriptions developed in cold region environments within modelling units which are delimited based on a basin-wide understanding of the responses of the main hydrological processes. Results were published in Dornes et al. (2008c).

7.2 Background

One of the main challenges for the hydrological modelling community is to produce accurate and reliable predictions in ungauged or poorly gauged basins. This issue had led to the IAHS initiative on Prediction in Ungauged Basins (PUB) (Sivapalan et al., 2003a) which mainly focuses in the need of improved processes understanding as a framework to developed enhanced knowledge and modelling strategies. Current debate is also centred on the difficulty of incorporating landscape heterogeneity and

finding distributed information that can fulfill the requirements of distributed physically based models. These issues have forced the hydrologist to some degree to conceptualise the physics of distributed models and seek effective parameter values typically at the catchment scale. As a result, hydrological models are usually calibrated against observed streamflow data (Klemeš, 1986). The importance of parameter calibration in regionalisation methods was stressed by Blöschl (2005) by showing that calibrated parameters were able to represent regional differences in the hydrological conditions and suggesting that is possible to derive regional relationships between calibrated parameters and basin attributes.

Alternative methods for parameter estimation such as regionalisation techniques or the transference of information from other basins or sources are needed where the lack of streamflow data does not allow for calibration of hydrological models. Regionalisation methods usually imply the transference of model parameters from a basin that is expected to behave similarly to the basin of interest. The similarity measure can be based on spatial proximity, basin attributes, or similarity indices Blöschl (2005). Typically, regionalisation techniques involve the definition of relationships based on regression methods between calibrated model parameters and basin attributes (Abdulla and Lettenmair, 1997). The difficulty is that the relationships are likely to be weak due to parameter equifinality since many parameter sets might produce similar simulations. For example, Kuczera and Mroczkowski (1998) suggested that the problem of parameter identifiability in conceptual catchment models due to the existence of multiple optima and high correlation amongst model parameters, makes the regionalisation of model parameters in ungauged basins virtually impossible.

Hydrological regionalisation studies have so far shown limited success and in general depend on the degree of similarity between the basins and on the type of the data used in the regional analysis (Littlewood, 2003). Fernandez et al. (2000) addressed this issue by performing a regional calibration approach where parameters were identified by both minimising model biases and maximising goodness of fit of relationships between parameters and basin characteristics. Regional calibration techniques were also performed by Hundecha and Bárdossy (2004) using a semi distributed conceptual model in 95 sub-basins of the Rhine basin where the coefficients of the relationships between basin attributes and parameters were calibrated rather than the model parameters, however a limitation of these methods could be the large number of coefficients to be calibrated. Alternatively, Parajka et al. (2007) proposed an iterative regional calibration method as a solution to the dimensionality of the calibration problem where local information such as streamflow data was combined with regional information such as an a priori distribution of the model parameters from gauged basins in the area in one objective function. Götzinger and Bárdossy (2007) showed that regionalisation methods using conditions imposed on the parameters by basin characteristics in distributed conceptual models were the ones that performed best due to the reduction of parameter space. Merz and Blöschl (2004) after comparing several regionalisation methods in 308 Austrian basins found that methods based on spatial proximity performed better than regression methods based on basin attributes. Similarly Parajka et al. (2005) showed that both a kriging approach (i.e. based on spatial proximity) and a similarity approach had similar performance. Goswami et al. (2007) demonstrated that the regionalisation of rainfall-runoff model parameters which were calibrated against regional pooling of streamflow data of twelve basins in France was the one that performed best amongst three methods involving calibration, concluding that the assessment of regional homogeneity and analysis of data are very important for regionalisation approaches using calibration methods.

Arctic environments due to their remote location, inaccessibility, and importance of the winter processes (e.g. snow accumulation and redistribution) in the hydrological cycle, are generally poorly-gauged or ungauged (Pomeroy et al., 2005a). Thus, improved regionalisation approaches in these environments are even more important for accurate predictions of snowcover ablation and snowmelt runoff.

7.3 Methodology

7.3.1 Regionalisation strategy

The regionalisation strategy used to transfer parameters from GB to TVC (see Figures 3.1 and 3.4) was based on the understanding of the main factors that control snow cover ablation and runoff. The transference of the parameters was derived from a landcover (i.e. vegetation cover) similarity criterion, therefore parameters from the PLT and NF slope landscape units of GB were transferred to TVC basin in order to represent the most similar and dominant landscape units (i.e. open tundra and shrub tundra). The parameterisation of the forest area in TVC was not included in the regionalisation due to both its low coverage (2 %) and the lack of a forested area in GB. Forest parameter values were set according to Davison et al (2006). There are common features in both basins, open tundra areas act as source of blowing snow whereas shrubs behave as sink or snow trap areas resulting in the formation of characteristic snow drifts in the direction of the prevailing winds that play a significant role in the timing (i.e. lengthering) of the snowmelt runoff. Both basins also show a similar snowmelt pattern, with higher snowmelt rates on the SF slopes than on the NF slopes due to the increased incident solar radiation. Observations of streamflow runoff show that peak flows are due to snowmelt, with the timing of the peak controlled by the timing of the snowmelt in the shrub tundra vegetation zone, while the duration of the peak is associated with the duration of the snowmelt on the NF slopes and high elevation zones.

The modelling framework used to transfer the physically based model parameters from GB to TVC Basin consisted of three steps (Figure 7.1); the first two were described in Chapter 5:

1. Run CRHM in GB in order to correct the observed incoming short wave radiation (K_{obs}) due to slope and aspect effects. This was accomplished in the GLOBAL and the SLOPE modules using theoretical formulations based on those proposed by Garnier and Ohmura (1970) and a cloudiness index calculated from the relation between the K_{obs} and the estimated theoretical radiation on the horizontal surface (K_{theo});
2. Run CLASS in a point model in each landscape unit of GB to simulate snow cover ablation using the corrected incoming short wave radiation (K_{cor}) calculated with CRHM along with the rest of the meteorological observations; and
3. Run MESH in TVC basin using the vegetation parameters determined in point 2 to simulate both depletion of the snow covered area and snowmelt runoff.

The selection of this regionalisation strategy was based on the data availability and the understanding of the underlying hydrological processes in the basin. Snowmelt parameters were calibrated in GB where distributed observations of snow cover ablation were available and tested in TVC basin using remotely sensed data of snow cover depletion. The regionalisation involved the transference of all the CLASS (landcover-based) parameters, except the snow cover depletion curve (SDC) parameter. The decision to exclude the SDC parameter from regionalisation was based on the differences between the theoretical considerations of the evolution of the SCA during melt (Pomeroy et al., 1998a; Pomeroy et al., 2004; Essery and Pomeroy, 2004b) and the topographic differences (i.e. exposure) between GB and TVC that influence snow redistribution. The snowpack ablation in the model is conceptualised by assuming a

continuous snow cover until a given snow depth (D_{100}) is reached. A straight line is then used to simulate the changing in SCA with time (Donald et al., 1995) and thus relate snow depth to SCA. Although the D_{100} is a landcover-based parameter it involves both vegetation cover and surface roughness characteristics, therefore it is strongly affected by snow redistribution by wind and topography influences such as slope, aspect, and micro-relief that affect both snow accumulation and energetics. Daily observations of snow cover depletion (i.e. snow depth and density) measured over a snow transect every 5 m in GB indicate instability in the D_{100} value. For example, a complete snowcover was observed until a snow depth of 44 cm was reached at the PLT in 2003, whereas the NF showed D_{100} values of 69, 55, 69 cm for the 2002-04 snowmelt seasons. In the shrub tundra area of TVC, on the other hand a lower value (29 cm) was measured in 1996 presumably due to a larger survey scale (10 m). Sensitivity analysis of the D_{100} parameter showed an effect only in the early stages of melt, resulting in a delay or acceleration of the beginning of melt for lower and higher D_{100} values respectively. Similarly, the variability of D_{100} affected the estimation of the early streamflow peak. These results agreed with the findings of Pohl et al. 2005. As a result of these uncertainties and mainly due to the difficulty to derive a value from observations, the SDC parameter was not transferred and calibrated in TVC instead.

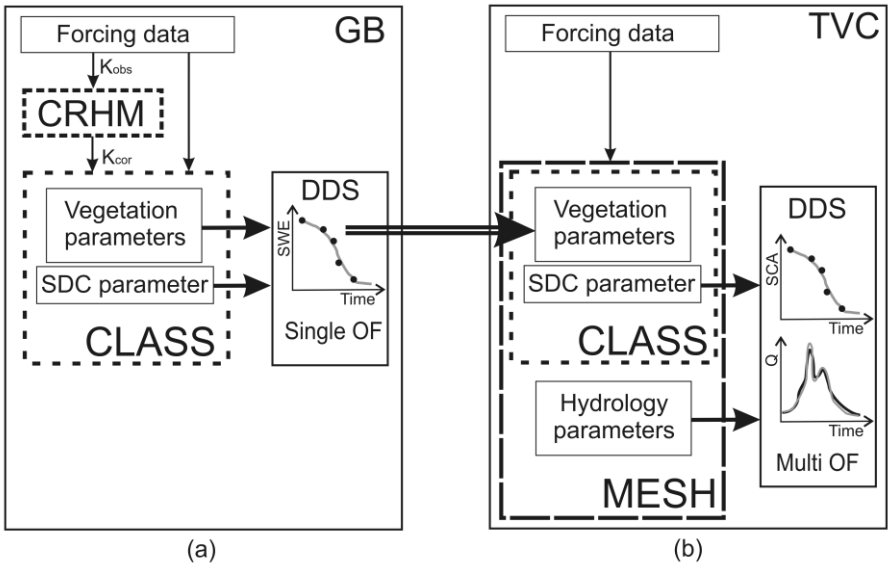

Figure 7.1: Outline of the coupled modelling and regionalisation (double line arrow) frameworks. a) Granger Basin (GB), b) Trail Valley Creek Basin (TVC). CRHM: Cold Regions Hydrological Model, CLASS: Canadian Land Surface Scheme, MESH: Modélisation Environmentale - Surface and Hydrology, DDS: Dynamically Dimensioned Search optimization algorithm, Kobs and Kcor: observed and corrected incoming short wave radiation (W·m-2), SCD: snow cover depletion, and OF: objective function.

7.3.2 Model calibration

Calibration was performed using the DDS global optimization algorithm. A two step-wise calibration procedure was applied: (1) the CLASS (i.e. vegetation and D_{100}) parameters that control snow cover ablation (Table 5.3) in GB were estimated using a single objective function, the root mean square error (RMSE) with respect to the observations of snow water equivalent (SWE) (see Chapter 5), and (2) MESH was calibrated in TVC on the D_{100} and hydrological parameters (Table 7.1) that conceptualise tile flow (i.e. overland and interflow) and streamflow, whereas the vegetation parameters that govern snowmelt were set according to the values obtained in GB.

Simulations of snowcover ablation in GB were calibrated in 2003 and validated in 2002 and 2004 in those landscapes where observations were available, whereas in

TVC simulations of both SCA and basin streamflow were calibrated and validated in 1996 and 1999 respectively (see Figure 7.1).

Table 7.1: Optimised parameter values using a multi-objective approach in Trail Valley Creek. GRU: Group Response Unit (model tile). Parentheses indicate parameter bounds.

Parameter	GRU		River network
	Open tundra	Shrub tundra	
D_{100} - lower snow depth limit for 100% SCA [m]	0.121 (0.05- 0.4)	0.111 (0.05- 0.4)	
D_d - Drainage density [m^{-1}]	4.725 (1-5)	3.177 (1-5)	
XSLP - Average slope of GRU [$m \cdot m^{-1}$]	0.094 (0.01 - 0.1)	0.061 (0.01 - 0.1)	
GRKF - Coef. of Ksat change in the first metre of soil.	0.879 (0.01 - 1)	0.946 (0.01 - 1)	
MANN - Manning's n for overland flow	0.073 (0.025 - 0.1)	0.063 (0.025 - 0.1)	
WFCI - Surface Ksat [$m \cdot s^{-1}$]	8.9E-6 (1E-9 -1E-5)	4.3E-6 (1E-9 -1E-5)	
wf_r2 - River rougnnes			0.168 (0.1 - 0.95)
ZPLIMS - Lower limit ponding water [m]			0.052 (0.02 - 0.15)
ZPLIMG - Upper limit ponding water [m]			0.176 (0.15 - 0.19)

Calibration of the MESH model in TVC was formulated using a multi-objective function (E_{agr}), which aggregates the Nash Sutcliffe efficiency coefficient, (E; Nash and Sutcliffe, 1970) of the simulations SCA and basin streamflow:

$$E_{agr} = w_1 \cdot \left[1 - \frac{\sum_{i=1}^{n} (S_{SCA} - O_{SCA})^2}{\sum_{i=1}^{n} (O_{SCA} - \overline{O}_{SCA})^2} \right] + w_2 \cdot \left[1 - \frac{\sum_{i=1}^{n} (S_Q - O_Q)^2}{\sum_{i=1}^{n} (O_Q - \overline{O}_Q)^2} \right] \quad (7.1)$$

where S_{SCA} and O_{SCA} are the simulated and observed basin average snow covered area, S_Q and O_Q are the simulated and observed basin streamflow, n is the number of samples evaluated, and w_1 and w_2 are the weights used to reflect the relative priorities of each

variable given to certain objectives. In this case they were set to 0.20 and 0.80 respectively.

Effective parameter sets (i.e. hydrology and D_{100}) in TVC, were identified after performing 500 simulations using DDS (Table 7.1).

7.4 Results and discussion

Independent simulations of CLASS in a point mode in each landscape unit of GB showed reasonable descriptions of the snow cover ablation with *E* values that ranged from 0.70 to 0.98 for both the calibration and validation periods (see Table 5.5). Figure 7.2 displays the comparisons between calibrated and validated SWE simulations of CLASS using the calibrated and the default parameter sets in the landscape units of GB (i.e. NF and PLT) used to regionalise the parameter sets. The default parameters are the standard values, set according to literature for the open tundra and shrub tundra, used in the numerical weather predictions of the GEM model. Figures 7.2*a* and *b* show the simulations corresponding to calibration period (2003) while the validations were conducted in 2002 and 2004 where additional snow survey data were available (Figures 7.2*c-e)*. Overall, a good agreement between simulated values using calibrated and default parameters was observed in the NF, however in the PLT area when the default parameters were used; underestimation of the observed melt drastically degraded the model performance (Table 7.2).

This discrepancy was not unexpected, since the parameterisation of the operational GEM model assumes uniform land-cover for each GRU (i.e. landscape unit) and the same SDC is used in both cases. In this parameterisation dissimilar melt rates such as in the PLT were poorly described. On the other hand, more homogenous melt on the NF due to the coincidence of high SWE and lower incoming solar radiation were adequately described. In contrast, SWE simulations using calibrated parameters with parameters ranges defined according to local observations such as density and height of

the vegetation were able to better describe the observed values with *E* values of 0.87 and 0.76 for the NF and PLT landscape units respectively, whereas reasonable model performances for the validation period with *E* values between 0.92 and 0.72 corroborated the representativeness of the effective parameter sets used to simulate snow cover ablation in the NF and PLT of GB.

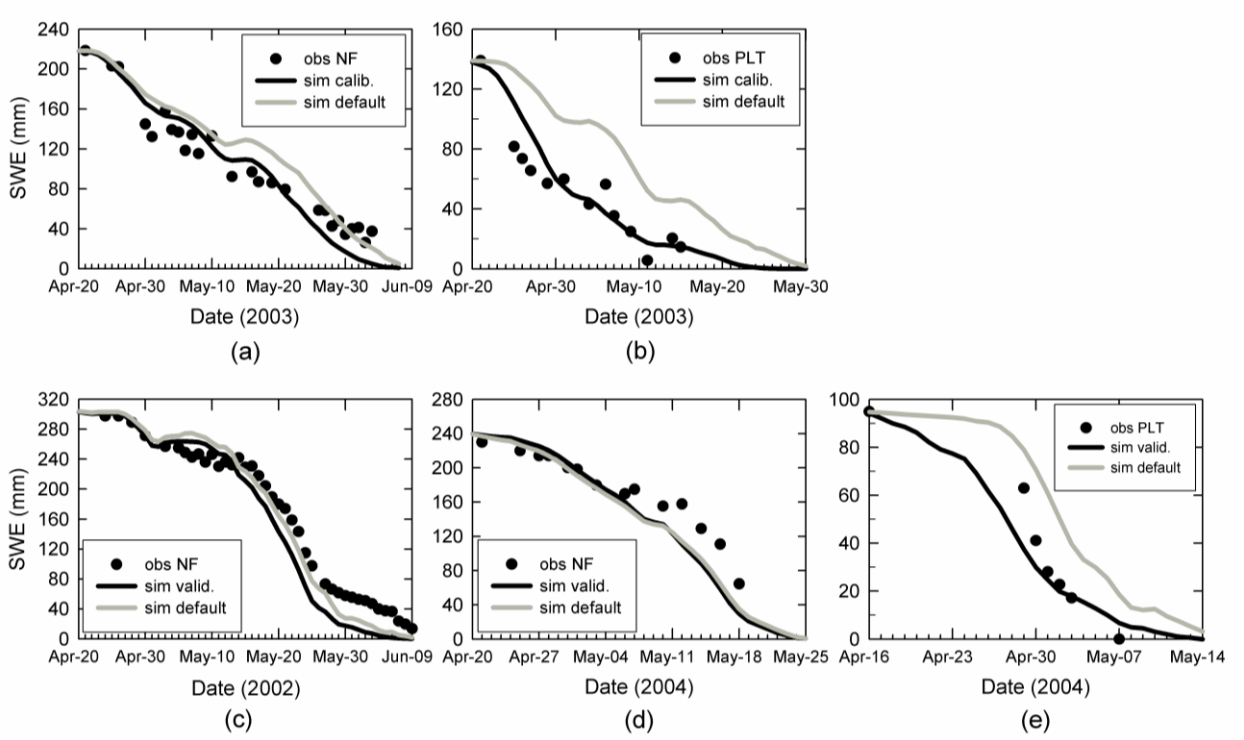

Figure 7.2: Observed and simulated areal snow water equivalent (SWE) values using calibrated and default parameters in the North facing slope (NF) and Plateau area (PLT) of Granger Basin. (a) 2003 NF calibration, (b) 2003 PLT calibration, (c) 2002 NF validation, (d) 2004 NF validation, and (e) 2004 PLT validation.

Table 7.2: Comparison of model performances (*E*; Nash Sutcliffe coefficient) in the PLT and NF landscape units of GB, and in TVC. *Calib.*: simulations obtained calibrating all the parameters, *Regional.*: simulations using regionalised vegetation parameters, *Default*: simulations using default vegetation parameters. SWE: snow water equivalent, *SCA*: basin average snow covered area, and *Q*: streamflow. *Cal.* and *val.* correspond to calibration and validation periods respectively.

Simulated variable	GB				TVC		
	NF		PLT		Calib.	Regional.	Default
	Calib.	Default	Calib.	Default			
SWE cal. 2003	0.87	0.85	0.80	-0.76			
SWE val. 2002	0.92	0.95					
SWE val. 2004	0.72	0.72	0.86	0.37			
SCA cal. 1996					0.98	0.96	0.65
SCA val. 1999					0.28	0.63	0.32
Q cal. 1996					0.94	0.83	0.52
Q val. 1999					0.81	0.67	0.47

Regional transference of the snowmelt (i.e. vegetation) parameters from GB to TVC basin was evaluated in Figures 7.3 and 7.4 and Table 7.2 where remotely sensed SCA and observed streamflow were compared to MESH simulations using both the regionalised and the default vegetation parameters. In both cases, a multi-objective calibration was performed on the SDC and hydrological parameters. In order to evaluate the incidence of the vegetation parameters on the results, simulations using the regionalised parameters were compared with those obtained through the calibration of all the model parameters (i.e. vegetation, SDC, and hydrology parameters). Results showed the model ability to capture the variability of both the snow cover depletion and basin runoff using a multi-objective calibration approach. Simulations of snowcover ablation for the calibration period in 1996 (Figure 7.3*a*) with the regionalised parameters gave a very accurate description of the SCA with an *E* value of 0.96 whereas the simulated ablation with the default vegetation parameters underestimated the snow free area during most of the melt season, degrading the model performance to 0.65. Similarly, for the validation period in 1999 (Figure 7.3*b*) the snow ablation using the regionalised parameters was reasonably well described. However, due to the model

overestimation of the SCA early in melt season, the model efficiency decreased to a *E* value of 0.63. Validated results with the default parameters showed similar snow-cover decay with larger differences early in the melt season that reduced the model performance. These early melt discrepancies indicate that the assumption of a uniform end-of-winter snowcover without considering redistribution of the snow by wind can lead to considerable errors in the predicted SCA, resulting in inaccurate surface energy fluxes for open arctic environments. This agrees with the findings of Déry et al. (2004) and Pohl and Marsh (2006) where it was suggested that both snowcover and snowmelt energy heterogeneity be incorporated to properly simulate snowcover depletion and energy fluxes. The fully calibrated simulation showed a slightly better description of the snowcover ablation in 1996 than the simulation using the regionalised parameters, whereas a less accurate simulation was seen for the validation period in 1999.

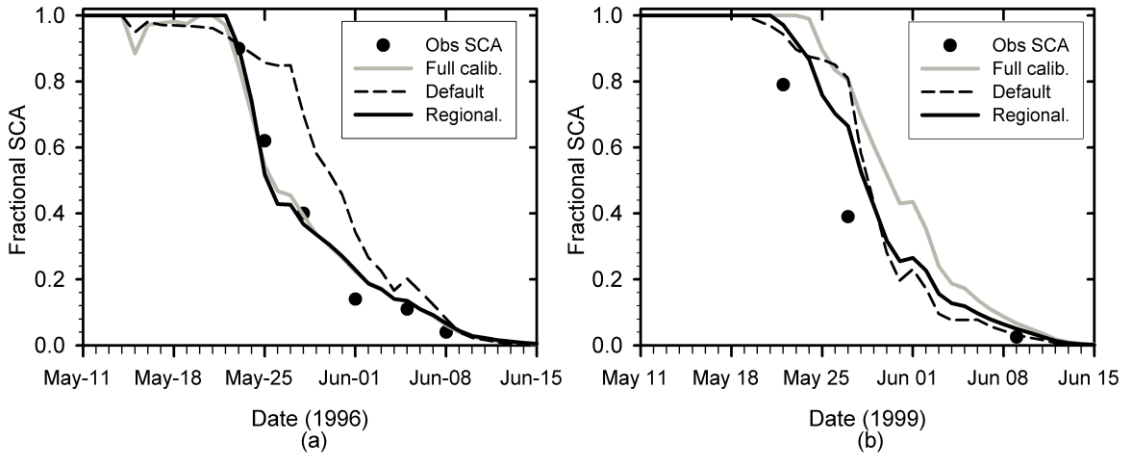

Figure 7.3: Observed and simulated basin average snow covered area (SCA) in TVC using regionalised parameters from GB and default parameters. a) 1996 calibration period, and b) 1999 validation period.

Figure 7.4*a* displays the observed and simulated basin streamflow in TVC for the calibration period in 1996. Overall, simulations using the regionalised parameters showed an accurate description of the observed hydrograph with a *E* value of 0.83.

Despite some small differences early in melt season, the timing of the rising and falling limbs, time-to-peak, and the magnitude of the peak were accurately described. However a faster recession limb than in the observed hydrograph was seen in the simulated streamflow. In contrast, when default vegetation parameters were used the simulations did not capture the dynamics of the observed streamflow which dropped the model efficiency to a *E* value of 0.52. Validated results in 1999 (Figure 7.4*b*) using the regionally transferred parameter set showed a reasonable overall description of the observed hydrograph in terms of the timing, reflecting a satisfactory snowmelt parameterisation, however a significant overestimation of the peak dropped the model performance to a *E* value of 0.67. Results using the default parameters showed an even poorer description with a *E* value of 0.47. The fully calibrated simulations on the other hand, showed a better performance than those using the regionalised parameters for the calibration period in 1996. This resulted in a more accurate description of the dynamic of the streamflow (*E*= 0.94) for the entire period, particularly in the model ability to replicate the second peak and recession curve of the observed hydrograph. Validation of this parameterisation in 1999 (Figure 7.4*b*) exhibited a good description of the timing however a less accurate description of the peak was observed.

Comparatively the improvement of the results using the fully calibrated parameter set was less noticeable in the simulations of SCA than on the simulations of snowmelt runoff. The improvement of the simulations when all the parameters were included in the calibration scheme showed the importance of the vegetation parameters in modelling performance in shrub tundra environments. It also indicates that the satisfactory results obtained using the regionalised parameters are not just due to calibration of the remaining parameters (i.e. SDC and hydrology parameters). Further the lack of difference in the estimation of the snowcover ablation in early stages of melt and the enhancement of the streamflow results over the entire simulation period showed that the influence of the SDC parameter is small, and hence not more important than the

vegetation parameters, given that its sensitivity is constrained to the early stages of melt (Pohl et al., 2005).

As expected, the use of a default parameterisation for the vegetation and its atmospheric transport fluxes had a poorer performance than the regional parameterisation defined using observations such as the initial snow pack and vegetation (e.g. height, density) measurements. This parameterisation is necessary in order to simulate important effects of the albedo and the timing of the shrubs exposure (Pomeroy et al., 2006). The default parameterisation constrained the remaining parameter space (i.e. SDC and hydrology parameters) and thus did not permit the DDS algorithm to find a parameter set that closely matched the observed streamflow, leading to poorer descriptions of both SCA and streamflow. The solutions were greatly enhanced by use of the regional values despite the 1350 km distance and topographic differences between the basins

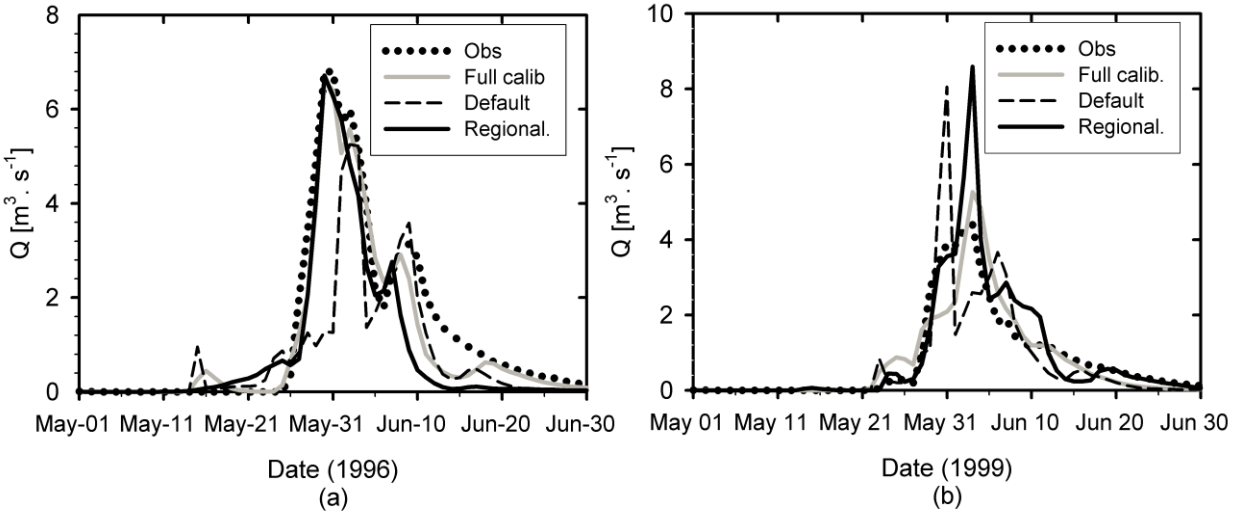

Figure 7.4: Observed and simulated streamflow in TVC using regionalised parameters from GB and default parameters. a) 1996 calibration period, and b) 1999 validation period.

7.5 Conclusions

A regionalisation approach for transferring parameters of a physically based LSH model in subarctic and arctic environments has been presented. This approach was based on a landscape similarity criterion and focused on two aspects. First, model parameters are landcover-based rather than basin-based, and second a step-wise calibration procedure was used to estimate the effective parameters. The landcover-based parameters offer an interesting alternative for PUB due to the difficulties in finding basin-based criteria for transferring parameters. Further, the separate calibration of parameters that govern snowmelt from those controlling streamflow provides a useful framework that reduces computational time (i.e. run CLASS in a point mode) and focuses in the main hydrological processes one at a time.

Results also showed that when effective landscape-based parameters are defined considering the effects of the initial conditions (e.g. redistribution of the snowcover by wind) and forcing data (e.g. topographic effects on the incoming solar radiation) such as those in GB, better simulations of both snowcover depletion and snowmelt runoff than the descriptions obtained using a default parameterisation are seen.

In summary, the identification of landscape units according to a basin-wide process understanding led to the definition of reliable effective landscape-based parameters for predicting both snowcover depletion and snowmelt runoff. In contrast, calibration is used only to deal with uncertainties in the data, lack of distributed information, or when parameters such as the SDC could not be derived from observations. Therefore for distributed and physically based models, landscape-based parameters appear to be a more feasible framework for transferring information between catchments than regionalisation schemes using regression methods based on basin characteristics. This is likely due to the large number of parameters involved.

CHAPTER 8

CONCLUDING SUMMARY

This thesis focussed on the development of a modelling strategy for snowcover ablation and snowmelt runoff in complex subarctic environments. Reliable statements about modelling hydrological processes require an understanding of scale, in order to deal with the natural variability in catchment characteristics. Over the years there have been attempts to make more rigorous tools and more realistic representations of hydrological processes, through incorporation of spatial and physical descriptions. However, the resulting more sophisticated models continue to suffer from similar restrictive assumptions, especially in regard to the representation of the landscape heterogeneity and its associated parameter uncertainty. Furthermore, the inherent ungauged nature of northern basins due to their remote location, inaccessibility, and dominance of the winter processes in hydrological cycle, becomes a non trivial problem for the generation of accurate model predictions. Although it could be argued that the application of distributed and physically based models in those environments is restricted due to the lack of data, the use of models where process descriptions are physically-based offers a strong tool for extrapolation beyond the region of observation.

This study illustrates the implementation of a new modelling philosophy for reducing predictive uncertainty in snowmelt modelling in cold regions environments with limited data while retaining integrity in the process representations. This modelling methodology is based on the combination of a basin-wide understanding of

the main factors controlling snowcover depletion and snowmelt runoff with a physically based process description. The following case studies supported this new approach.

1. A small, scale physically-based hydrological model was successfully applied with minimal calibration to a small subarctic mountain basin. Based on previous research studies and observations, the spatial representation of landscape heterogeneity was accomplished by incorporating landscape units as the spatial model elements. The identification and definition of these landscape units was based on the role of slope, aspect, exposure, and vegetation types in governing snow redistribution by wind and hence in modifying the initial snowcover conditions and snowcover energetics. Results show that the distributed model approach, which incorporates topographic and vegetation effects on initial snowcover and incident solar radiation, was able to properly simulate snowcover ablation and snowmelt runoff whereas the aggregated modelling approach that did not incorporate these factors was unable to represent the differential snowmelt rates and complex snowmelt runoff dynamics.

2. Land surface scheme (LSS) simulations satisfactorily describe snowcover ablation when independent applications were conducted on the previously defined landscape units. Comparisons at the basin scale between distributed simulations that considered the redistribution of snow and corrected solar forcing and aggregated simulations that did not, showed that the aggregated model based on the assumption of uniform initial conditions and solar forcing was not able to account for a proper description of snowmelt dynamics. A sensitivity analysis showed the importance of including redistribution of snow by wind for the definition of the initial snowcover conditions and corrected incoming solar

radiation by topography to successful simulations of snowcover deletion. These explicit considerations enhanced LSS simulations of snowcover depletion, such that they appropriately described the differential snowmelt rates observed on the different landscapes. LSS simulations without considering these topographic and vegetation effects on both snow redistribution and snow energetic drastically failed to predict the evolution of snowcover during the melt season.

3. Application of a land surface hydrological (LSH) model to a larger basin using the same spatial considerations (i.e. distributed initial snow water equivalent, corrected incoming solar radiation, and a spatial model representation based on landscape units), with previously defined landscape based parameters controlling snowmelt, showed satisfactory results in simulating snowcover ablation and basin snowmelt runoff with minimal calibration. Conversely, the assumption of uniform initial conditions and incoming solar radiation, degraded model performance substantially.

4. Verification of this landscape based parameterisation was conducted by a regionalisation exercise where the parameters controlling snowmelt of a physically based LSH model were transferred about 1000 km to an Arctic basin. Satisfactory model results illustrated that the identification of landscape units according to process understanding led to the definition of reliable effective landscape based parameters for predicting both snowcover depletion and snowmelt runoff. The results also showed that when effective landscape based parameters are defined based on initial conditions (e.g. redistribution of the snowcover by wind) and forcing data (e.g. topographic effects on the incoming solar radiation), then improved simulations of both snowcover depletion and snowmelt runoff can be obtained, compared to those obtained using default parameterisations.

Based on the previous evidence it can be concluded that the proposed modelling approach is a suitable strategy for reliable predictions of snowcover depletion and snowmelt runoff in cold regions and complex environments. The strength of this physically based modelling approach is founded on the combination of the two main modelling philosophies. An inductive (i.e. top-down or downward) modelling approach based on a basin-wide understanding of the main factors that drive the snowmelt processes in northern mountainous areas was used for representing the landscape heterogeneity (i.e. choose the aggregation level), hence the spatial model representation was based on landscape units. On the other hand, the deductive (i.e. bottom-up or upward) modelling approach was used for detailed process descriptions that incorporated physically based algorithms with a priori parameter sets describing snowmelt. The philosophical basis of the modelling approach is the desire to describe the processes in as physically-realistic a manner as possible, given the availability of data and parameters to run the model.

The implementation of this modelling strategy was based on research studies in cold regions environments. In subarctic alpine tundra environments, studies have shown that the natural variability of snowcover during melting is complex and multi-scale but there are apparent 'scale breaks' in the variability of forcing variables and parameters that lead to apparent 'process scales' with reduced variability within these scales. Spatial heterogeneity of the snowcover conditions prior to melt is therefore highly influenced by topography and vegetation characteristics. These heterogeneous end-of-winter conditions and vegetation characteristics led to different spatial associations between melt energy and SWE at different scales. In summary, the consideration of snowcover heterogeneity due to wind redistribution and the effects of small-scale topography on melt energetics enhanced predictions of snow ablation. Therefore, the definition of landscape units according to slope and aspect, and the main landcover types offers a reliable option for basin segmentation in physically based land surface

hydrological models. Moreover, the combination of deductive and inductive modelling approaches appears to offer advantages to either top-down or bottom-up approaches alone for reducing data requirements, model structural complexity, and parameter uncertainties and for regionalising snowmelt runoff models at small to medium scales in sub-arctic mountainous environments

Comparisons between this distributed landscape based approach to observations always showed appropriate model performance, whereas aggregated approaches assuming uniform or basin average initial snowcover conditions and incident solar radiation were not always able to accurately describe the dynamics of melt and runoff. These differences were most evident in those years when there was a high spatial variability of the snowcover and melt energy. Conversely, less noticeable differences between the distributed and aggregated approaches were seen when the spatial variability was low mainly as a result of different snow redistribution patterns. Similarly, when melt was enhanced by advection from warm air, particularly in early stages of melt, smaller differences in model performance between the modelling approaches were observed as a result of the synchronised melt and runoff response among the different landscapes such as alpine, shrub tundra and boreal forest.

Furthermore, the definition of landscape based parameters was accomplished by an automatic and multi-objective calibration procedure where model performances were evaluated according to their ability in describing both snowcover ablation and snowmelt runoff. This multi-objective approach contributes to the definition of more stable landscape based effective parameters since different physical processes (e.g. melt and runoff generation) and their spatial associations with vegetation and snow accumulation are implicitly included in the calibration process. However, to reduce the degree of freedom in the calibration process, calibration was restricted as much as possible within physically reasonable limits. For example, only conceptual modules and parameters that could not be derived from observations, or flow routing parameters were automatically

calibrated whereas landscape based parameters describing snowcover ablation were set according to the values previously determined from field observations for those landscapes. This landscape based parameterisation showed successful results not only in a up-scaling exercise from Granger Basin to Wolf Creek Basin but also in a regionalisation evaluation that involved the transference of landscape based parameters describing snowmelt from Wolf Creek Basin to Trail Valley Creek Basin in the Arctic.

In summary, this modelling approach provides a new methodology for regionalisation of physically based and distributed land surface hydrological models, where landscape based model parameterisations and basin segmentation according to landscape units offers a suitable modelling strategy for subarctic and complex environments. This study also illustrates that the definition of the number of model units should be in concordance with the association between initial snow water equivalent and melt energy. In others words, there should be a spatial coherence between basin segmentation and snow process heterogeneity in cold regions hydrological models. This has a significant importance for accurate predictions in northern and mountain basins typically characterised as ungauged or poorly gauge basins and for land surface-atmospheric interactions at both small and larger scales. Further, this modelling approach agrees with the analysis about the 'art of hydrology' recently published by Savenije (2009). The analysis focussed on the need to improve hydrological models, indicating that the process of modelling should be inductive (top-down) by learning from the data while at the same time connection should be established with the underlain physical theory, that is deductive (bottom-up) approach.

Limitations to this approach were:

i) Coarse scale of modelling compared to small sub-basins with stream gauges in WC prevented small scale validation of the model.

ii) SDC in CLASS/MESH was non-physical and could not be related to field observations.

iii) Calibration of shrub and vegetation parameters may have masked effects of shrub emergence, small-scale advection and micrometeorological differences between tiles that need further examination for their need to be included in the model.

Further improvements to the method within a tile might include specifying differing reference atmospheric conditions for each tile and that this could not be tested in this thesis.

Recommendations for future work are needed in the method to calculate initial SWE (e.g. coupling a blowing snow model) and in the method to calculate radiation to tiles (needs to be coupled in MESH).

REFERENCES

Abbott, M. B., Bathurst, J. C., Cunge, J. A., O'Connel, P. E., and J. Rasmussen. 1986. An introduction to the European Hydrological System - Systeme Hydrologique Européen "SHE", 1: History and philosophy of a physically-based distributed modelling system. *J. Hydrol.*, **87**, 45-59.

Abdulla, F. A. and D. P. Lettenmaier. 1997. Development of regional parameter estimation equations for a macroscale hydrologic model. *J. Hydrol.*, **197**, 230-257.

Ambroise, B., Freer, J., and K. J Beven. 1996. Application of a generalised TOPMODEL to the small Ringelbach catchment, Vosges, France. *Water Resour. Res.*, **32**, 2147-2159.

Anderson, E. A. 1973. *National Weather Service River Forecast System-Snow accumulation and ablation model*. NOAA Tech. Memo. NWS Hydro-17, U.S. National Weather Service. (Available from NOAA/NWS, Office of Hydrology, 1325 East-West Highway, Silver Springs, MD 20910).

Anderson, E. A. 1976. *A point energy and mass balance model of snow cover*. US Department of Commerce, National Oceanic and Atmospheric Administration, National Weather Service. NOAA Technical Report NWS 19, pp: 150.

Arnold, J. G., Srinivasan, R., Muttiah, R.S., and J. R. Williams. 1998. Large area hydrologic modeling and assessment. Part 1: model development. *J. American Water Resour. Asso.*, **34**, 73-89.

Armstrong, R. N. and L. Martz. 2008. Effects of reduced land cover detail on hydrological model response. *Hydrol. Process.*, **22**, 2395-2409.

Atkinson, S. E., Sivapalan, M., Wood, R. A, and N. R Vinley. 2003. Dominant physical controls on hourly flow predictions and the role of spatial variability: Mahurangi catchment, New Zealand. *Adv. Water Resour.*, **26**, 219-235.

Bastien, J. N. 2004. *Testing the WATCLASS 3.0 distributed hydrologic model on two Canadian watersheds: data preparation, model calibration and performance assessment*. MSc Thesis University of Waterloo, Waterloo, ON.pp:180.

Becker, A. and P. Brown. 1999. Disaggregation, aggregation and spatial scaling in hydrological modelling. *J. Hydrol*., **217**, 239-252.

Bergström, S., 1976. *Development and application of a conceptual runoff model for Scandinavian catchments*. (Department of Water Resources Engineering, Lund Institute of Technology/University of Lund, Bulletin Series A, No. 52, 134 pp.).

Bergström, S. and L. P. Graham. 1998. On the scale problem in hydrological modelling. *J. Hydrol.*, **211**, 253-265.

Beven K. J. and M. Kirkby.1979. A physically based variable contributing area model of basin hydrology. *Hydrol. Sci. Bull.*, **24**, 43-69.

Beven, K. J. and A. Binley. 1992. The future of distributed models. Model calibration and uncertainty prediction. *Hydrol. Process.*, **6**, 279-298.

Beven, K. J., Lamb, R., Quinn, P., Romanowicz, R., and J. Freer. 1995. TOPMODEL. In: *Computer Models of Watershed Hydrology*. Singh, V.T. (Ed.), Water Resources Publications, pp: 627-688.

Beven, K. J. 2001a. *Rainfall-runoff modelling. The primer*. John Wiley & Sons, Chichester, UK, pp: 372.

Beven, K. J. 2001b. How far can we go in distributed hydrological modelling? *Hydrol. Earth Syst. Sci.*, **5**, 1-12.

Beven, K. J. 2002. Towards an alternative blueprint for a physically based digitally simulated hydrologic response modelling system. *Hydrol. Process.*, **16**, 189-206.

Beven, K. J. 2006. Rainfall-Runoff Modelling: Introduction. In: *Encyclopedia of Hydrological Sciences*. Anderson, M.G. (Ed). John Wiley, Chichester, U.K., 1857-1868.

Bartelt, P. B. and M Lehning. 2002. A physical SNOWPACK model for avalanche warning. Part I. Numerical Model. *Cold Regions Sci. Tech.*, **35**, 123-145.

Bewley, D. 2006. *Shrub-tundra effects on snowmelt energetics and the atmospheric interaction with snow*. PhD Thesis. Institute of Geography and Earth Sciences, University of Wales, Aberystwyth, UK, pp: 196.

Bewley, D., Pomeroy J. W., and R. L. H. Essery. 2007. Solar radiation transfer through a sub-arctic shrub canopy. *Arct. Alp. Res.*, **39**, 365-374.

Blöschl, G., Gutknecht, D., and R. Kirnbauer. 1991. Distributed snowmelt simulations in a alpine catchment 2. Parameter study and model predictions. *Water Resour. Res.*, **27**, 3181-3188.

Blöschl, G. and M. Sivapalan. 1995. Scale issues in hydrological modelling - a review. *Hydrol. Process.*, **9**, 251-290.

Blöschl, G., Grayson, R. B., and M. Sivapalan. 1995. On the representative elementary area (REA) concept and its utility for distributed-runoff modelling. *Hydrol. Process.*, **9**, 313-330.

Blöschl, G. 1999. Scaling issues in snow hydrology. *Hydrol. Process.*, **13**, 2149-2175.

Blöschl, G., 2005. Rainfall-runoff modeling of ungauged catchments. In: *Encyclopedia of Hydrological Sciences*. Anderson, M.G. (Ed). John Wiley, Chichester, U.K., 2061-2080.

Boyle, D. P., Gupta, H. V., and S. Sorooshian. 2000. Toward improved calibration of hydrologic models: Combining the strengths of manual and automatic methods. *Water Resour. Res*., **36**, 3663-3674.

Braun, L. N., Aellen, M., Funk, M., Hock, R., Rohrer, M.B., Steinegger, U., Kappenberger, G., and H. Müller-Lemans. 1994. Measurement and simulation of high alpine water balance components in the Linth-Limmern head watershed (Northeastern Switzerland). Z. Gletscherkd. *Glazialgeol*.,*30*, 161-185.

Brubaker, K., Rango, A., and W. Kustas. 1996. Incorporating radiation inputs into the snowmelt runoff model. *Hydrol. Process.*,**10**, 1329-1343.

Carey, S. K. and M. K. Woo. 1999. Hydrology of two slopes in subarctic Yukon, Canada. *Hydrol. Process*., **13**, 2549-2562.

Carey, S. K and M. K. Woo. 2000. The role of soil pipes as a slope runoff mechanism, subarctic Yukon, Canada. *J. Hydrol.*, **223**, 206–222.

Carey, S. K and M. K. Woo. 2001a. Slope runoff processes and flow generation in a subarctic, subalpine environment. *J. Hydrol.*, **253**, 110–129.

Carey, S. K. and M. K. Woo. 2001b. Spatial variability of hillslope water balance, wolf creek basin, subartic region. *Hydrol. Process.*, **15**, 3113-3132.

Carey, S. K. and W. L. Quinton. 2005. Evaluating runoff generation during summer using hydrometric, stable isotope and hydrochemical methods in a discontinuous permafrost alpine catchment. *Hydrol. Process.*, **19**, 95-114.

Chow, V. T., Maidment, D. R., and L. W. Mays. 1998. *Applied Hydrology*. McGraw-Hill, New York, US, pp: 585

Clapp, R. B. and G. M. Hornberger. 1978. Empirical equations for some soil hydraulic properties. *Water Resour. Res.*, **14**, 601-604.

Cosby, B. J., Hornberger, G. M., Clapp, R. B., and T. R. Ginn. 1984. A statistical exploration of the relationships of soil moisture characteristics to the physical properties of soils. *Water Resour. Res.*, **20**, 682-690.

Crawford N. H. and R. K. Linsley. 1966. *Digital simulation in hydrology: Stanford Watershed Model IV*. Stanford Univ., Dept. Civ. Eng. Tech. Rep. 39. pp

Davison, B., Pohl, S., Dornes, P., Marsh, P., Pietroniro, A., MacKay, M., 2006. Characterizing snowmelt variability in a land surface hydrologic model. *Atmos. Ocean*, **44**, 271-287.

De Boer, D. 2001. Linking GCMs and surface hydrology: the challenge of spatial scale. *Can. Geogr.*,**45**, 79-84.

Déry, S. J., Crow, W. T., Stieglitz, M., and E. F. Wood. 2004. Modeling snow-cover heterogeneity over complex arctic terrain for regional and global climate models. *J. Hydromet.*, **5**, 33-48.

Déry, S. J., Salomonson, V. V., Stieglitz, M., Hall, D. K., and I. Appel. 2005. An approach to using snow areal depletion curves inferred from MODIS and its application to land surface modelling in Alaska. *Hydrol. Process*.,**19**, 2755-2774.

Dodson, R. and D. Marks. 1997. Daily air temperature interpolation at high spatial resolution over a large mountainous region. *Climate Res.*, **8**, 1-20.

Donald, J. R., Soulis, E. D., Kouwen, N., and A. Pietroniro, 1995. Snowcover depletion curves and satellite snowcover estimates for snowmelt runoff modelling. *Water Resour. Res.*, **31**, 995-1009.

Dornes, P. F., Pomeroy, J. W., Pietroniro, A., Carey, S. K., and W. L. Quinton. 2006. The use of inductive and deductive reasoning to model snowmelt runoff from northern mountain catchments. In: *Proc. iEMSs Third Biennial Meeting "Summit on Environmental Modelling and Software"*. Voinov, A., Jakeman, A. J., and A. E. Rizzoli (Eds). International Environmental Modelling and Software Society, 9-13 July, Burlington, VT, USA. CD Rom. http ://www.iemss.org/iemss2006/sessions/all.html.

Dornes, P. F., Pomeroy, J. W., Pietroniro, A., Carey, S. K., and W .L. Quinton. 2008a. Influence of landscape aggregation in modeling snow-cover ablation and snowmelt runoff in subarctic mountainous environment. *Hydrol. Sci. J.*, **53**, 725-740.

Dornes, P. F., Pomeroy, J. W., Pietroniro, A., and D. L. Verseghy. 2008b. Influence of landscape aggregation in modeling snow-cover ablation and snowmelt runoff in subarctic mountainous environment. *J. Hydrometeor.*, **9**, 789-803.

Dornes, P. F., Tolson, B., Davison, B., Pietroniro, A., Pomeroy, J. W., and P. Marsh. 2008c. Regionalisation of Land Surface Hydrological Model Parameters in Subarctic and Arctic Environments. *J. Phys. Chem. Earth*, **33**, 1081-1089.

Dozier, J. 1980. A clear-sky spectral solar radiation model for snow-covered mountainous terrain. *Water Resour. Res.*, **16**, 709-718.

Dozier, J. and J. Frew. 1990. Rapid calculation of terrain parameters for radiation modeling from digital elevation data. *IEEE Transactions in Geoscience and Remote Sensing*, **28**, 963-69.

Duan, Q., Sorooshian, S, and V. K. Gupta. 1992. Effective and efficient global optimization for conceptual rainfall-runoff models. *Water Resour. Res.*, **28**, 1015-1031.

Duan, Q., Sorooshian, S, and V. K. Gupta. 1994. Optimal use of the SCE-UA global optimization method for calibrating watershed models. *J. Hydrol*., **158**, 265-284.

Elder, K., Dozier, J., and J. Michaelsen. 1991. Snow accumulation and distribution in an alpine watershed. *Water Resour. Res.*, **27**, 1541-1552.

Elder, K., Michaelsen, J., and J. Dozier. 1995. Small basin Modeling of Snow Water Equivalence Using Binary Regression Tree Methods. In: *Biogeochemistry of Seasonally Snow-Covered Catchments*. Tonnessen K.A., Williams M.W., Tranter M. (Eds); Proc. Boulder Symposium, 3-14 July, IAHS Publ. no. 228, pp. 129-139.

Essery, R., Li, L., and J. Pomeroy. 1999. A distributed model of blowing snow over complex terrain. *Hydrol. Process.*, **13**, 2423-2438.

Essery, R. and J. Pomeroy. 2004a. Vegetation and topographic control of wind-blown snow distributions in distributed and aggregated simulations for an arctic tundra basin. *J Hydromet.*, **5**, 735-744.

Essery, R. and J. Pomeroy. 2004b. Implications of spatial distributions of snow mass and melt rate for snow-cover depletion: theoretical considerations. *A. Glaciol*., **38**, 261-265.

Essery, R. and P. Etchevers. 2004. Parameter sensitivity in simulations of snowmelt. *J. Geophys*. *Res*., **109**, D20111, doi:10.1029/2004JD005036.

Essery, R. L. H., Granger, R. J., and J. W. Pomeroy. 2006. Boundary-layer growth and advection of heat over snow and soil patches: modelling and parameterization. *Hydrol. Process.*, **20**, 953-967.

Etchevers, P., Martin, E., Brown, R., Fierz, C., Lejeune, Y., and 18 others. 2004. Validation of the surface energy budget simulated by several snow models (SnowMIP project). *Ann. Glaciol.*, **38**, 150-158.

Fang, X. and J. W. Pomeroy. 2007. Snowmelt runoff sensitivity analysis to drought on the Canadian Prairies. *Hydrol. Process.*, **21**, 2594-2609.

Faria, D. A., Pomeroy, J. W., and R. L. H. Essery. 2000. Effect of covariance between ablation and snow water equivalent on depletion of snow-covered area in a forest. *Hydrol. Process.*, **14**, 2683-2695.

Ferguson, R. I. 1999. Snowmelt runoff models. *Prog. Phys. Geog*., **23**, 205-227.

Fernandez, W., Vogel, R. M., and A. Sankarasubramanian. 2000. Regional calibration of a watershed model. *Hydrol. Sci. J.*, **45**, 689-707.

Flügel, W. A. 1995. Delineating hydrological response units by geographical information system analyses for regional hydrological modeling using PRMS/MMS in the drainage basin of the river Bröl, germany. *Hydrol. Process.*, **9**, 423-436.

Foster, J., Liston, G., Koster, R., Essery, R., Beher, H., Dumenil, L., Verseguy, D., Thompson, S., Pollard, D. and J. 1996. Snow cover and snow mass intercomparisons of general circulation models and remotely sensed datasets. *J. Climate*, **9**, 409-426.

Fontaine, T. A. Cruickshank, T.S., Arnold, J.G., and R.H. Hotchkiss. 2002. Development of a snowfall-snowmelt routine for mountainous terrain for the soil water assessment tool (SWAT). *J. Hydrol.*, **262**, 209-223.

Francis, S. R. 1997. Data integration and ecological stratification of Wolf Creek watershed, south-central Yukon. Applied Ecosystem Management Ltd. Whitehorse, Yukon Territory.

Frazer, G. W., Canham, C. D. and Lertzman, K. P. 1999. Gap Light Analyzer GLA, Version 2.0: Imaging Software to Extract Canopy Structure and Gap Light Transmission Indices from True-color Fisheye Photographs, Users Manual and Program Documentation. Burnaby, BC, Simon Fraser University, and Millbrook, NY: Institute of Ecosystem Studies. 1-40 pp.

Freeze R. A. and R. L Harlan. 1969. Blueprint for a physically-based digitally simulated, hydrologic response model. *J. Hydrol.*, **9**, 237–258.

Garen, D. C. and D. Marks. 2005. Spatially distributed energy balance snowmelt modelling in a mountainous river basin: estimation of meteorological inputs and verification of model outputs. *J. Hydrol.*, **315**, 126-153.

Garnier, B. J. and A. Ohmura. 1970. The evaluation of surface variations in solar radiation income. *Solar Energy*, **13**, 21-34.

Giesbrecht, M. A. and M. K. Woo. 2000. Simulation of snowmelt in a sub-arctic spruce woodland: 2. Open woodland model. *Water Resour. Res.*, **36**, 2287-2295.

Goodison, B. E. 1978. Accuracy of Canadian snow gauge measurements. *J. Appl. Meteorol.*, **27**, 1542-1548.

Goodison, B. E., Louie P. Y. T., and D. Yang. 1998. WMO solid precipitation measurement intercomparison final report. WMO Instruments and Observing Methods Report No. 67, WMO/TD No. 872.

Goswami, M., O'Connor, K. M., and K. P. Bhattari. 2007. Development of regionalisation procedures using a multi-approach for flow simulation in an ungauged catchment. *J. Hydrol.*, **333**, 517-531.

Götzinger, J. and A. Bárdossy. 2007. Comparison of four regionalization methods for a distributed hydrological model. *J. Hydrol*., **333**, 374-384.

Granger, R. J., Gray, D. M., and G. E. Dyck. 1984. Snowmelt infiltration to frozen prairie soils. *Can. J. Earth Sci.*, **21**, 669–677.

Granger, R. J. and D. M. Gray. 1989. Evaporation from natural non-saturated surfaces. J. *Hydrol.*, **111**, 21-29.

Granger, R. J. and D. M. Gray. 1990. A net radiation model for calculating daily snowmelt in open environments. *Nordic Hydrol.*, **21**: 217–234.

Gray, D. M. and D. H. Male. 1981. *Handbook of snow: Principles, processes, management and use*. Pergamon Press, Toronto, Canada, pp: 776.

Gray, D. M. and G. P. Landine. 1987. Albedo model for shallow prairie snowcovers. *Can. J. Earth Sci*., **24**, 1760-1768.

Gray, D. M. and P. G. Landine. 1988. An energy-budget snowmelt model for the Canadian Prairies. *Can. J. Earth Sci.*, **25**, 1292-1303.

Gray, D. M., Toth, B., Pomeroy, J. W., Zhao, L., and R. J. Granger. 2001. Estimating areal snowmelt infiltration into frozen soils. *Hydrol. Process.*,**15**, 3095-3111.

Grayson R. and G. Blöschl. 2001. Spatial modelling of catchment dynamics. In: *Spatial Patterns in Catchment Hydrology*. Observations and modelling. Grayson R. and G. Blöschl (Eds). Cambridge University Press, UK, pp: 51-81.

Gupta, H. V., Sorooshian, S., and P.O. Yapo. 1998. Toward improved calibration of hydrologic models: multiple and noncommensurable measures of information. *Water Resour. Res*, **34**, 751-763.

Gupta, H. V., Sorooshian, S., Hogue, T. S. and D. P. Boyle. 2003. Advances in the automatic calibration of watershed models. In: *Calibration of Watershed Models*. Water Science and Application Series 6. Duan Q., Gupta H. V., Sorooshian S., Rousseau A. N., and R. Turcotte (Eds.). American Geophysical Union. Washington, US, pp. 9–28.

Gupta, V. K., Rodríguez-Iturbe, I., and E. F. Wood (Eds.). 1986. Scale problems in hydrology. D. Reidel, Dordrecht, pp: 246.

Hedstrom, N. R. and J. W. Pomeroy. 1998. Measurements and modelling of snow interception in the boreal forest. *Hydrol. Process.*, **12**, 1611-1625.

Heginbottom, J. A., Dubreuil, M. A., and P. T. Harker. 1995. Canada-Permafrost (1:7 500 000 scale). In: *The National Atlas of Canada.* 5th Edn. Ottawa: National Resources Canada, sheet MCR 4177.

Henderson-Sellers, A., Pitman, A. J., Love, P. K., Irannejad P., and T. H. Chen, 1995. The Project for Intercomparison of Land Surface Schemes (PILPS): Phases 2 and 3. *Bull. Amer. Meteor. Soc.*, **73**, 489-503.

Hock, R. 2003. Temperature index melt modelling in mountain areas. *J. Hydrol.*, **282**, 104-115.

Hundecha, Y. and A. Bárdossy. 2004. Modeling of the effect of land uses changes on runoff generation of a river basin through parameter regionalisation of a watershed model. *J. Hydrol.*, **292**, 281-295.

Jasek, M. and G. Ford. 1997. Coal Lake outlet freeze-up, containment of winter inflows and estimates of related outburst flood on Wolf Creek, Yukon territory. In: *Proc. 54th Annual Meeting Eastern Snow Conference Join Meeting 65th Western Snow Conference*. Banff, AB. May 4-8.

Janowicz, J. R., 1986. *A methodology for estimating design peak flows for Yukon Territory*. Proc. Cold Regions Hydrology Symposium. Kane, D.L. (Ed). American Water Resour. Association, pp: 313-320.

Janowicz, J. R., Gray, D. M., and J. W. Pomeroy. 2002. Characterisation of snowmelt infiltration scaling parameters within a mountainous subarctic watershed. In: *Proceedings 59th Eastern Snow Conference*. Stowe, USA, pp: 67-81.

Janowicz, J. R., Gray, D. M., and J. W. Pomeroy. 2003. Spatial variability of fall soil moisture and spring snow water equivalent within a mountainous sub-arctic watershed. In: *Proceedings 60th Eastern Snow Conference*. Sherbrooke, QB, Canada, pp: 127-139.

Johnson, G. L. and C. Handson. 1995. Topographic and atmospheric influences on precipitation variability over mountainous watershed. *J. Appl. Meteor.*, **34**, 68-87.

Jordan, R. 1991. *A one-dimensional temperature model for a snowcover: Technical documentation for SNTHERM.89*. Special Rep. 91-96. U.S. Army Corps of Engineers Cold Region Research and Engineering Laboratory, Hanover, NH, pp: 49.

Kane D. L., Hinzman L. D., Benson C. S., and G. E. Liston. 1991. Snow hydrology of a headwater arctic basin. 1. Physical measurements and process studies. *Water Resour. Res.*, **27**, 1099-1109.

Kavetski, D., Frank, S. W., and G. Kuczera. 2003. Confronting input data uncertainty in environmental modelling. In: *Calibration of Watershed Models*. Water Science and Application Series 6. Duan Q., Gupta H. V., Sorooshian S., Rousseau A. N., and R. Turcotte (Eds.). American Geophysical Union. Washington, US, pp. 49–68.

Kavvas, M. L, Chen, Z. Q., Tan, L., Soon, S. T., Terakawa, A., Yosohitani, J., and K. Fukami. 1998. A regional-scale land surface parameterization based on areally-averaged hydrological conservation equations. *Hydrol. Sci. J.*, **43**, 611-631.

Kavvas, M. L. 1999. On the coarse-graining of hydrological processes with increasing scales. *J. Hydrol.,* **217**, 191-202.

Kite, G. W. 1975. Performance of two deterministic hydrological models. *ASH-AISH Publication,* **115**, 136-142.

Kite, G. W., 1978. Development of a hydrologic model for a Canadian watershed. *Can. J. Civil Eng.*, **5**, 126-34.

Kite, G. W. and N. Kouwen. 1992. Watershed modelling using land classifications. *Water Resour. Res.*, **28**, 3193-3200.

Klemeš, V., 1983. Conceptualization and scale in hydrology. *J. Hydrol*., **65**, 1-23.

Klemeš, V., 1986. Operational testing of hydrological simulation models. *Hydrol. Sci. J*, **31**, 13-24.

Kouwen, N. 1988. WATFLOOD: A microcomputer-based flow forecasting system based on real-time weather data. *Can. Water. Resour. J.*, **13**, 62-77.

Kouwen, N., Soulis, E. D., Pietroniro, A., Donald, J., and R. A. Harrington. 1993. Grouped response units for distributed hydrological modeling. *J. Water Resour. Plann. Manage.*, **119**, 289-305.

Kuczera, G. and M. Mroczkowiski. 1998. Assesment of hydrological parameter uncertainty and the worth of multiresponse data. *Water Resour. Res.*, **34**, 1481-1489.

Kunkel, K. E. 1989. Simple procedures for extrapolation of humidity variables in the mountainous western United States. *J. Climate*, **2**, 656-669.

Kustas W. P, Rango, A., and R. Uijlenhoet. 1994. A simple energy budget algorithm for the snowmelt runoff model. *Water Resour. Res.*, **30**, 1515-1527.

Kuchment, L. S. and A. N. Gelfan. 1996. The determination of the snowmelt rate and the meltwater outflow from a snowpack for modelling river runoff generation. *J. Hydrol*., **179**, 23-26.

Kuchment, L. S., Deminov, V. N., Naden, P. S., Cooper, D. M., and P. Broadhirst. 1996. Rainfall-runoff modelling of the Ouse basin, North Yorkshire: an application of a physically based distributed model. *J. Hydrol.*, **181**, 323-342.

Kuz'min, P. P. 1960. Formirovanie Snezhnogo Pokrova i Metody Opredeleniya Snegozapasov. Gidrometeoizdat: Leningrad. (Published 1963 as *Snow Cover and Snow Reserves*. [English Translation by Israel Program for Scientific Translation, Jerusalem]. National Science Foundation: Washington, DC).

Lacroix, M. P., Martz, L. W., Kite, G. K., and J. Garbrecht. 2002. Using digital terrain analysis modeling techniques for the parameterization of a hydrological model. *Environ. Model. Softw.*, **17**, 127-136.

Letts, M. G., Roulet, N. T., Comer, N. T., Skarupa, M. R., and D. L.Verseghy. 2000. Parametrization of peatland hydraulic properties for the Canadian Land Surface Scheme. *Atmos. Ocean*, **38**, 141-160.

Lewkowicz, A. G. and M. Ednie. 2004. Probability Mapping of Mountain Permafrost Using the BTS Method, Wolf Creek, Yukon Territory, Canada. *Permafrost Periglacial Process.*, **15**, 67-80.

Liston, G. E., 1995: Local advection of momentum, heat, and moisture during the melt of patchy snow covers. *J. Appl. Meteor.*, **34**, 1705-1715.

Liston, G. E., 1999. Interrelationships among snow distribution, snowmelt, and snow cover depletion: Implications for atmospheric, hydrologic, and ecologic modeling. *J. App. Meteor.*, **38**, 1474-1487.

Liston, G. E. and M. Sturm. 2002. Winter precipitation patterns in arctic Alaska determined from a blowing-snow model and snow-depth observations. *J. Hydrometeor.*, **3**, 646-659.

Liston, G. E., McFadden, J. P., Sturm, M., and R. A. Pielke. 2002. Modelled changes in arctic tundra snow, energy and moisture fluxes due to increased shrubs. *Global Change Biology*, **8**, 17-32.

Liston, G. E. and K. Elder. 2006a A Meteorological Distribution System for High-Resolution Terrestrial Modeling (MicroMet). *J. Hydrometeor.*, **7**, 217-234.

Liston, G. E. and K. Elder. 2006b. Distributed Snow-Evolution Modeling System (SnowModel). *J. Hydrometeor.*, **7**, 1259-1276.

Littlewood, I. G. 2003. Improved unit hydrograph identification for seven Welsh rivers: implications for estimating continuous streamflow at ungauged basins. *Hydrol. Sci. J.*, **48**, 743-762.

Luce, C. H., Tarboton, D. G., and K. R. Cooley. 1999. Subgrid parameterisation of snow distribution for and energy and mass balance snow cover model. *Hydrol. Process.*, **13**, 1921-1933.

Luce, C. H. and D. G. Tarboton. 2004. The application of depletion curves for parameterization of subgrid variability of snow. *Hydrol. Process.*, **18**, 1409-1422.

Lundberg, A. and S. Halldin. 2001. Snow interception evaporation—rates, processes and measurement techniques. In: *Land-surface/Atmosphere Exchange in High-latitudes Landscapes*. Grassl, H., Halldin, S., Gryning, S. E., and C. R. Lloyd CR (Eds). Theoretical and Applied Climatology 70, pp: 117-133.

Lundberg, A., Nakai, Y., Thunehed, H. and S. Hallin. 2004. Snow accumulation in forest from ground and remote-sensing data. *Hydrol. Process.*, **18**, 1941-1955

Madsen, H., 2000. Automatic Calibration of a conceptual rainfall-runoff model using multiple objectives. *J. Hydrol.*, **235**, 276-288.

Madsen, H., 2003. Parameter estimation in distributed hydrological catchment modelling using automatic calibration with multiple objectives. *Adv. Water Resour.*, **26**, 205-216.

Male, D. H. 1980. The seasonal snowcover. In: *Dynamics of Snow and Ice Masses*. Colbeck, S. H. (Ed.). Academic Press. pp: 305-395.

Male, D. H. and R. J. Granger. 1981. Snow surface energy exchange. *Wat. Resour. Res.*, **17**, 609-627.

Marks, D., Kimball, J., Tingey, D., and T. Link. 1998 The sensitivity of snowmelt process to climate conditions and forest covers during rain on snow: a study of the 1996 Pacific Northwest flood. *Hydrol. Proces.*, **12**, 1569-1587.

Marks, D., Domingo, J., Susong, D., Link, T., and D. Garen. 1999. A spatially distributed energy balance snowmelt model for application in mountain basins. *Hydrol. Proces.*, **13**, 1935-1959.

Marks, D., T. Link, A. Winstral, and D. Garen. 2001. Simulating snowmelt processes during rain-on-snow over a semi-arid mountain basin. *A. Glaciol.*, **32**,195-202.

Marks, D., A. Winstral, and M. Seyfried. 2002. Investigation of terrain and forest shelter effects on patterns of snow deposition, snowmelt and runoff over a semi-arid mountain catchment using simulated snow redistribution fields. *Hydrol. Process.*,**16**, 3605-3626.

Marsh P. and M. K. Woo. 1984a. Wetting front advance and freezing of meltwater within a snow cover 1. Observations in the Canadian Arctic. *Water Resour. Res.*, **20**, 1853-1864.

Marsh, P. and M. K. Woo. 1984b. Wetting front advance and freezing of meltwater within a snow cover. 2. A simulation model. *Water Resour. Res.*, **20**, 1865-1874.

Marsh, P. and J. W. Pomeroy. 1996. Meltwater fluxes at an arctic forest–tundra site. *Hydrol. Process.*, **10**, 1383-1400.

Marsh, P., Pomeroy, J. W., and N. Neumann. 1997. Sensible heat flux and local advection over a heterogeneous landscape at an Arctic tundra site during snowmelt. *A. Glaciol*., **25**, 132-136.

Martinec, J. 1985. Snowmelt runoff models for operational forecasts. *Nord. Hydrol.*, **16**, 129-136.

Martinec, J. and A. Rango. 1986. Parameter values for snowmelt runoff modelling. *J. Hydrol.*, **84**, 197–219

McCartney, S. E. 2006. *Spatial variability of snowmelt water balances in a subarctic catchment*. MSc Thesis, University of Saskatchewan, Saskatoon, Saskatchewan, Canada.

McCartney, S. E., Carey, S. K., and J. W. Pomeroy. 2006. Intra-basin variability of snowmelt water balance calculations in a subarctic catchment. *Hydrol. Process.*, **20**, 1001-1016.

McNamara, J. P., Kane, D. L., and L. D. Hinzman. 1998. An analysis of streamflow hydrology in the Kuparuk River basin, arctic Alaska: a nested watershed approach. *J. Hydrol*., **206**, 39-57.

Merz, R. and G. Blöschl, 2004. Regionalisation of catchment model parameters. *J. Hydrol.*, **287**, 95-123.

Neumann, N. and P. Marsh. 1998. Local advection of sensible heat in the snowmelt landscape of arctic tundra. *Hydrol. Process.*, **12**, 1547-1560.

Morris, E. M. 1989. Turbulent transfer over snow and ice. *J. Hydrol.*, **105**, 205-24.

Mougout, C. M. and C. A. S. Smith. 1994. *Soil Survey of the Whitehorse Area*. Vol 1, Takhini Valley. Research Branch, Agriculture and Agri – Food Canada. Whitehorse, (unpublished manuscript) 56pp

Nash, J. E. and J. V. Sutcliffe. 1970. River flow forecasting through conceptual models. Part I: A discussion of principles. *J. Hydrol.*, **10**, 280-290.

Parajka, J., Blöschl, G., and R. Merz. 2007. Regional calibration of catchment models: potential for ungauged catchments. *Water Resour. Res.*, **43**, 6406, doi: 10.1029/2006WR005271.

Pietroniro, A., Prowse, T, Hamlin, L., Kouwen, N., and E.D. Soulis. 1996. Application of a grouped response unit hydrological model to a northern wetland region. *Hydrol. Process.*, **10**, 1245-1261.

Pietroniro, A., Hamlin, L., Prowse, T., Soulis, E., and N. Kouwen. 1997. Application of a radiation-temperature index snowmelt model to the lower Liard River valley. Proc. 2nd Sci. workshop for Mackenzie GEWEX Study (MAGS). March 23-26, Saskatoon, pp: 89-90.

Pietroniro, A. and E.D. Soulis. 2003. A hydrology modeling framework for the Mackenzie GEWEX programme. *Hydrol. Process.*, **17**, 673-676.

Pietroniro, A., Fortin, V., Kouwen, N., Neal, C., Turcotte, R., Davison, B., Verseghy, D., Soulis, E., Caldwell, R., Evora, N., and P. Pellerin. 2007. Development of the MESH modelling system for hydrological ensemble forecasting of the Laurentian Great Lakes at the regional scale. *Hydrol. Earth Syst. Sci.*, **11**, 1279-1294.

Pohl, S., Marsh, P., and A. Pietroniro. 2005a. Spatial-temporal variability in solar radiation during spring snowmelt. *Nord. Hydrol.*, **37**, 1-19.

Pohl, S., Davison, B., Marsh, P., and A. Pietroniro. 2005b. Modelling spatially distributed snowmelt and meltwater runoff in a small arctic catchment with a hydrology – land surface scheme (WATCLASS). *Atmos. Ocean*, **43**, 193-211.

Pohl, S. and P. Marsh. 2006. Modelling the spatial-temporal variability of spring snowmelt in an arctic catchment. *Hydrol. Process.*, **20**, 1773-1792.

Pohl, S., Marsh, P., and G. Liston. 2006. Spatial-temporal variability in turbulent fluxes during spring snowmelt. *Arct. Antarct. Alp. Res.*, **38**, 116-146.

Pomeroy, J. W., Gray, D. M., and P. G. Landline. 1993. The Prairie Blowing Snow Model: Characteristics, validation, operation. *J. Hydrol.*, **144**, 165–192.

Pomeroy J. W. and D. M. Gray. 1995. *Snowcover accumulation, relocation and management*. National Hydrology Research Institute, Science Report No. 7, Saskatoon, Environment Canada, pp: 144.

Pomeroy, J. W. and B. E. Goodison. 1997. Winter and snow. In: *The surface climates of Canada*. Bailey, W.G., Oke, T.R., and W.R. Rouse. McGill-Queen's University Press, Montreal.

Pomeroy, J. W., Marsh, P., and D. M. Gray. 1997. Application of a distributed blowing snow model to the arctic. *Hydrol. Process.*, **11**, 1451-1464.

Pomeroy J. W., Parviainen, J., Hedstrom, N., and D. M. Gray. 1998a. Coupled modelling of forest snow interception and sublimation. *Hydrol. Process.*, **12**, 2317-2337.

Pomeroy J. W., Gray, D. M., Shook, K. R., Toth, B., Essery, R. L. H., Pietroniro, A., and H. Hedstrom. 1998b. An evaluation of snow accumulation and ablation processes for land surface modelling. *Hydrol. Process.*, **13**, 2339-2367.

Pomeroy, J. W., Hedstrom, N., and J. Parviainen. 1999. The snow mass balance of Wolf Creek, Yukon: effects of snow sublimation and redistribution. In: *Wolf Creek Research Basin: Hydrology, Ecology, Environment*. Pomeroy, J. W. and R. J. Granger (Eds). Environment Canada, Saskatoon, pp: 15-30.

Pomeroy, J. W. and L. Li. 2000. Prairie and Arctic areal snow cover mass balance using a blowing snow model. *J. Geophys. Res.*, **105**, 26619-26634.

Pomeroy, J. W., Gray, D. M., Hedstrom, N. R., and J. R. Janowicz. 2002. Prediction of seasonal snow accumulation in cold climate forests. *Hydrol. Process.*, **16**, 3543-3558.

Pomeroy, J. W., Toth, B., Granger, R. J., Hedstrom, N. R., and R. L. H. Essery. 2003: Variation in surface energetics during snowmelt in a subarctic mountain catchment. *J. Hydrometeor.*, **4**, 702–719.

Pomeroy, J., Essery, R., and B. Toth. 2004. Implications of spatial distributions of snow mass and melt rate for snow-cover depletion: observations in a subarctic mountain catchment. *A. Glaciol.*, **38**, 195-201.

Pomeroy, J. W., Granger, R. J., Hedstrom, N. R., Gray, D. M., Elliot, J., Pietroniro, A., and J. R. Janowicz. 2005a. The process hydrology approach to improving prediction of ungauged basins in Canada. In: *Predictions in Ungauged Basins: Approaches for Canada's Cold Regions*. Spence, C., Pomeroy, J.W, and A. Pietroniro (Eds). Canadian Water Resources Association, Yellowknife, Canada, pp: 67-99.

Pomeroy, J., Ellis, C., Essery, R., Hedstrom, N., Granger, R., and R. Janowicz. 2005b. Factors affecting the synchronicity and covariance of snowmelt in a high latitude mountain catchment. Workshop 6: Transferring hydrological data across spatial and temporal scales. VIIth IAHS Scientific Assembly. Foz do Iguaçu, Brazil. 3-9 April.

Pomeroy, J. W., Bewley, D. S., Essery, R. L. H., Hedstrom, N. R., Link, T., Granger, R. J., Sicart, J. E., Ellis, C. R., and J. R. Janowicz. 2006. Shrub tundra snowmelt. *Hydrol. Process.*, **20**, 923-942.

Pomeroy, J. W., Gray, D. M., Brown, T., Hedstrom, N. R., Quinton, W. L., Granger, R. J., and S. K. Carey. 2007. The cold regions hydrological model: a platform for basing process representation and model structure on physical evidence. *Hydrol. Process.*, **21**, 2650-2667.

Quick, M.C. and A. Pipes. 1972. Daily and seasonal forecasting with a water budget model. In: *Role of Snow and Ice in Hydrology*. Proc. UNESCO/WMO/IAHS Symposium, Banff, September 1972), pp. 1017-1034: IAHS Publ. no. 106.

Quick, M.C. and A. Pipes. 1977. UBC watershed model. *Hydrol. Sci. Bull.*, **221**, 153–161.

Quinton, W. L. and P. Marsh. 1998. The influence of mineral earth hummocks on subsurface drainage in the continuous permafrost zone. *Permafrost and Periglacial Process.*, **9**, 213–228.

Quinton, W. L. and P. Marsh. 1999. A conceptual framework for runoff generation in a permafrost environment. *Hydrol. Process.*, **13**, 2563–2581.

Quinton, W. L., Gray, D. M., and P. Marsh. 2000. Subsurface drainage from hummock-covered hillslopes in the arctic tundra. *J. Hydrol.*, **237**, 113–125.

Quinton, W. L., Shirazi, T., Carey, S. K., and J. W. Pomeroy. 2005. Soil water storage and active-layer development in a sub-alpine tundra hillslope, southern Yukon Territory, Canada. *Permafrost and Periglacial Process.*, **16**, 369-382.

Refsgaard, J. C. 1996. Terminology, modelling protocol and classification of hydrological model codes. In: *Distributed Hydrological Modelling*. Abbott, M.B., and Refsgaard, J.C. (Eds.). Kluwer Academic Publishers, Dordrecht, pp. 17-39.

Refsgaard, J. C. and B. Storm. 1996. Construction, calibration and validation of hydrological models. In: *Distributed Hydrological Modelling*. Abbott, M. B. and Refsgaard, J.C. (Eds.). Kluwer Academic Press, Dordrecht, pp. 41-54.

Refsgaard, J. C. 1997. Parameterisation, calibration and validation of distributed hydrological models. *J. Hydrol.*, **198**, 69-97.

Reggiani, P, Sivapalan, M., and S. M. Hassanizadeh 2000. Conservation equations governing hillslope responses. *Water Resour. Res.*, **38,** 1845-1863.

Reggiani, P. and J. Schellekens. 2003. Modelling of hydrological responses: the representative elementary watershed approach as an alternative blueprint for watershed modelling. *Hydrol. Process.*, **17**, 3785-3789.

Satterlund, D. R. 1979. An improved equation for estimating longwave radiation from the atmosphere. *Water Resour. Res.*, **15**, 1643-1650.

Savenije, H. H. G. 2009. The art of hydrology. *Hydrol. Earth. Syst. Sci*., **13**, 157-161.

Seguin, M. K., Stein, J., Nilo, O., Jalbert, C., and Y. Ding. 1999. Hydrogeophysical investigation of the Wolf Creek Watershed, Yukon Territory, Canada. In: *Wolf*

Creek Research Basin: Hydrology, Ecology, Environment. Pomeroy, J.W and R.J. Granger (Eds). National Water Research Institute: Saskatoon, 33-43.

Sicart, J. E, Pomeroy, J. W., Essery, R. L. H., Hardy, J., Link, T., and D. Marks. 2004. A sensitivity study of daytime net radiation during snowmelt to forest canopy and atmospheric conditions. *J. Hydrometeor.*, **5**, 774-784.

Sicart, J. E., Pomeroy, J. W., Essery, R. L. H., and D. Dewley. 2006. Incoming longwave radiation to melting snow: observations, sensitivity and estimation in northern environments. *Hydrol. Process.*, **20**, 3697-3708.

Sivapalan, M., Takeuchi, K., Franks, S. W., Gupta, V. K., Karambiri, H., Lakshmi, V., Liang, X., McDonnell, J. J., Mendiondo, E. M., O'Connell, P. E., Oki, T., Pomeroy, J. W., Schertzer, D., Uhlenbrook, S., and E. Zehe. 2003a. IAHS Decade on Predictions in Ungauged Basins (PUB), 2003-2012: Shaping an exciting future for the hydrological sciences. *Hydrol. Sci. J.*, **48**, 857-880.

Sivapalan, M., Blöschl, G., Zhang, L., and R. Vertessy. 2003b. Downward approach to hydrological prediction. *Hydrol. Process.*, **17**, 2101-2111.

Shook, K. R. 1995. *Simulation of the ablation of prairies snowcovers*. Ph. D. Thesis, University of Saskatchewan, pp: 189.

Shook, K. and D. M. Gray. 1997. The role of advection in melting shallow snowcovers. *Hydrol. Process.*, **11**, 1725-1736.

Singh, V.P (Ed). 1995. Computer models of watershed hydrology. Water Resources Publications. Littleton, pp: 1144.

Slater G., Schlosser C. A., Desborough C. E., Pitman A. J., Henderson- Sellers, A., and 31 others. 2001. The Representation of Snow in Land-surface Schemes; results from PILPS 2(d). *J. Hydrometeor.*, **2**, 7-25.

Sorooshian, S. and V. K. Gupta. 1995. Model calibration. In: *Computer Models of Watershed Hydrology*. Singh, V.P. (Ed). Colorado. Water Resources Publications, pp: 23-68.

Soulis, E. D., Snelgrove, K. R., Kouwen, N., and F. R. Seglenieks. 2000. Towards closing the vertical water balance in Canadian atmospheric models: coupling of the land surface scheme CLASS with the distributed hydrological model WATFLOOD. *Atmos. Ocean*, **38**, 251-269.

Soulis, E. D., Kouwen, N., Pietroniro, A., Seglenieks, F. R., Snelgrove, K. R., Pellerin, P., Shaw, D. W., and L.W. Martz. 2005. A framework for hydrological modelling in MAGS. In: *Predicton in Ungauged Basins: Approaches for Canada's Cold Regions*. Spence, C., Pomeroy, J.W, and A. Pietroniro (Eds). Canadian Water Resources Association (CWRA), Ottawa, Canada, 120-138

Steppuhn, H. and G. E Dyck. 1974. Estimating true basin snowcover. In: *Proc. Interdisciplinary Symp. on Advanced Concepts and Techniques in the Study of Snow and Ice Resources*. Monterey, CA. National Academy of Science, Washington, DC, pp. 314–328.

Sturm, M., McFadden, J. P., Liston, G. E., Chapin, F. S., Racine, C. H., and J. Holmgren. 2001. Snow–shrub interactions in arctic tundra: a hypothesis with climatic implications. *J. Climate*, **14**, 336-344.

Tarboton, D. G., T. G. Chowdhury, and T. H. Jackson. 1995. A spatially distributed energy balance snowmelt model. In: *Biogeochemistry of Seasonally Snow-Covered Catchments*. Tonnessen, K.A., Williams, M.W., and M. Tranter (Eds). IAHS Publ. No. 228, 141-155.

Tarboton, D. G. and C. H. Luce. 1997. Utah Energy Balance Snow Accumulation and Melt Model (UEB). *Computer Model Technical Description and Users Guide*. Utah Water Research Laboratory, Logan, Utah.

Tarboton, D., Blöschl. G., Cooley, K., Kirnbauer, R. and C. Luce. 2001. Spatial snow cover processes at Kühtai and Reynolds Creek. In: *Spatial Patterns in Catchment Hydrology*. Observations and modelling. Grayson R. and G. Blöschl (Eds). Cambridge University Press, UK, pp: 158-186.

Tolson, B.A. and C. A. Shoemaker. 2007. The Dynamically Dimensioned Search (DDS) Algorithm for computationally efficient watershed model calibration. *Water Resour. Res.*, **43**, 1413.

Verseghy, D. L. 1991. CLASS -A Canadian land surface scheme for GCMs. I. Soil model. *Int. J. Climatol.*, **11**, 111–133.

Verseghy, D. L., McFarlane, N. A., and M. Lazare. 1993. CLASS -A Canadian land surface scheme for GCMs. II. Vegetation model and coupled runs. Int. *J. Climatol*., **13**, 347–370.

Verseghy, D. L. 2000. The Canadian Land Surface Scheme (CLASS): Its History and Future. *Atoms.-Ocean*, **38**, 1-13.

Young, P. C. and A. J. Jarvis. 2002. Data-based mechanistic modelling and state dependent parameter models. CRES Report No. TR/177, Department of Environmental Science, Lancaster University, UK.

Young, P. 2003. Top-down and data-based mechanistic modelling of rainfall-flow dynamics at the catchment scale. *Hydrol. Process.*, **17**, 2195-2217.

Walter, M. T., Brooks, E. S., McCool, D. K., King, L. G., Molnau, M., and J. Boll. 2005. Process-based snowmelt modelling: does it require more input data than temperature-index modelling? *J. Hydrol.*, **300**, 65-75.

Woo, M. K. and P. Marsh. 1978. Analysis of error in the determination of snow storage for small high arctic basins. *J. Hydromet.*, **17**, 1537-1541.

Woo, M. K. and J. Sauriol. 1980. Channel development in snow-filled valleys, resolute, N.W.T., Canada. *Geogr. Ann.*, **62A**, 37-56.

Woo, M. K. 1983. Hydrology of a drainage basin in the Canadian high arctic. *Ann. Assoc. Am. Geogr.*, **73**, 577-596.

Woo, M. K., Stone, J. M. R., Rouse, W. R., and R. E. Stewart. 2005. Overview of the Mackenzie GEWEX study. In: *Final report of the Mackenzie GEWEX study (MAGS)*. Proc. of the Final (11th) Annual Scientific Meeting. Di Censo P. (Ed.). 22-25 Ottawa, ON.

Wood, E. F., Sivaplan, M., Beven, K., and L. Band. 1988. Effects of spatial variability and scale with implications to hydrologic modeling. *J. Hydrol.*, **102**, 29-47.

Woods, R., Sivapalan, M., and M. Dunccan. 1995. Investigating the Representative Elementary Area concept: An approach based on field data. *Hydrol. Process.*, **9**, 291-312.

Yapo, P. O., Gupta, H. V., and S. Sorooshian. 1998. Multi-objective global optimization for hydrological models. *J. Hydrol.*, **204**, 83-97.

Zhao, L. and D. M. Gray. 1999. Estimating snowmelt infiltration into frozen soils. *Hydrol. Process.*, **13**, 1827-1842.

Zehe, E., Lee, H., and M. Sivapalan. 2006. Dynamical process upscaling for deriving catchment scale state variables and constitutive relations for meso-scale process models. *Hydrol. Earth Syst. Sci.*, **10**, 981-996.

APPENDIX A: SNOW SURVEY CORRECTIONS

This appendix includes the snow survey values of Granger Basin (McCartney, 2006) that were subject to a correction method due to highly variable values of snow density. Survey values represent the snow transect average (i.e. areal values). Measurements of snow density at GB were performed using the ESC-30 snow sampler (MSC, Meteorological Service of Canada, standard for shallow snowpacks) whereas deeper snowpacks were sampled using the Mount Rose snow tube.

Corrections were performed when highly variable values of snow density or SWE were found. The main reason for those corrections were the random measurement errors associated with the difficulty to sample compacted snow in snowdrifts, where often a different snow sampler was needed or when different methods for measuring snow density were used such as snow pits in the drift of the NF slope (McCartney, 2006). Additional sources of random errors were the difficulty to get a good snow core due to presence of shrub branches embedded in snowpack and ice crusts, and very fragile depth hoar.

Snow survey SF slope 2002: Highly variable snow density values were replaced by a linear fit. A minimum snow density value of 0.2 g m^{-3} was set at the beginning of the melt season to better suit end-of-winter conditions.

date	Snow depth (cm)	Obs. Snow density [g cm^3]	Corrected Snow density [g cm^3]	SWE [mm]
19-Apr-02	57.6	0.146	0.200	115.1
24-Apr-02	54.0	0.192	0.200	108.0
26-Apr-02	50.2	0.207	0.203	102.1
28-Apr-02	38.3	0.200	0.215	82.2
30-Apr-02	24.0	0.187	0.227	54.4
3-May-02	23.2	0.184	0.244	56.6
5-May-02	16.7	0.236	0.256	42.6
6-May-02	9.5	0.353	0.261	24.9
7-May-02	7.2	0.367	0.267	19.2
8-May-02	6.4	0.343	0.273	17.6
9-May-02	4.1	0.350	0.279	11.3
10-May-02	5.3	0.158	0.285	14.9
11-May-02	4.8	0.321	0.290	13.9
12-May-02	4.1	0.308	0.296	12.2
13-May-02	3.4	0.241	0.302	10.2
14-May-02	9.2	0.319	0.308	28.3
15-May-02	2.9	0.315	0.314	9.2
16-May-02	2.1	0.407	0.319	6.7
17-May-02	1.7	0.281	0.325	5.6
18-May-02	1.2	0.282	0.331	3.9
19-May-02	0.2	0.310	0.337	0.5

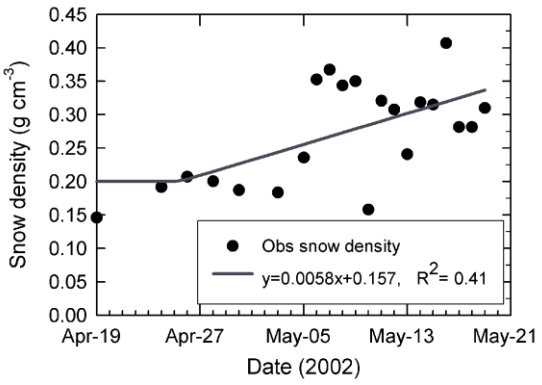

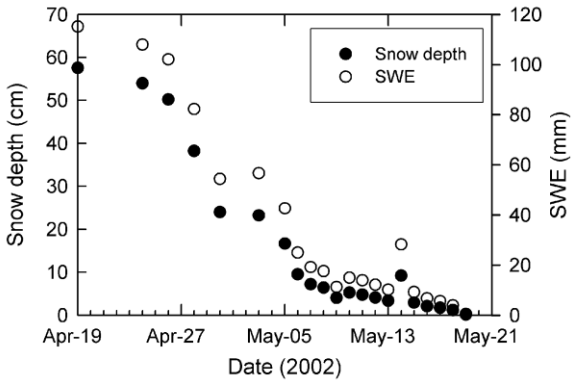

Snow survey NF slope 2002: Highly variable snow density values were replaced by a linear fit. Since a snow drift was observed, a minimum snow density value of 0.3 g m^{-3} corresponding to drifted snow was set at the beginning of the melt season.

date	Snow depth (cm)	Obs. Snow density [g cm^3]	Corrected Snow density [g cm^3]	SWE [mm]
19-Apr-02	101.2	0.203	0.300	303.6
24-Apr-02	104.3	0.171	0.300	312.8
26-Apr-02	106.3	0.203	0.300	318.9
28-Apr-02	96.4	0.269	0.300	289.1
30-Apr-02	90.4	0.238	0.300	271.1
3-May-02	85.6	0.245	0.300	256.7
5-May-02	85.0	0.325	0.300	254.9
6-May-02	82.9	0.317	0.300	248.6
7-May-02	80.9	0.316	0.300	242.6
8-May-02	82.2	0.320	0.300	246.7
9-May-02	78.6	0.287	0.300	235.9
10-May-02	82.0	0.305	0.306	251.4
11-May-02	75.9	0.411	0.313	229.4
12-May-02	76.0	0.339	0.319	235.2
13-May-02	73.1	0.241	0.326	231.4
14-May-02	74.4	0.319	0.332	241.1
15-May-02	68.9	0.315	0.338	228.3
16-May-02	67.9	0.407	0.345	229.9
17-May-02	62.8	0.281	0.351	217.2
18-May-02	57.6	0.282	0.358	203.6
19-May-02	52.4	0.310	0.364	188.8

date	Snow depth (cm)	Obs. Snow density [g cm^3]	Corrected Snow density [g cm^3]	SWE [mm]
20-May-02	48.8	0.340	0.370	179.4
21-May-02	46.2	0.320	0.377	173.3
22-May-02	41.4	0.380	0.383	158.1
23-May-02	36.6	0.381	0.390	142.7
24-May-02	28.8	0.428	0.396	114.4
25-May-02	24.0	0.449	0.402	97.2
27-May-02	17.7	0.343	0.415	73.0
28-May-02	15.8	0.431	0.422	66.0
29-May-02	14.4	0.468	0.428	61.3
30-May-02	13.2	0.418	0.434	57.4
31-May-02	12.5	0.403	0.441	55.3
1-Jun-02	11.7	0.394	0.447	52.4
2-Jun-02	11.2	0.441	0.454	50.9
3-Jun-02	10.1	0.392	0.460	46.9
4-Jun-02	8.5	0.395	0.466	39.9
5-Jun-02	7.8	0.570	0.473	37.3
6-Jun-02	7.5	0.576	0.479	36.4
7-Jun-02	4.8	0.525	0.486	23.7
8-Jun-02	3.9	0.539	0.492	19.6
9-Jun-02	2.7	0.526	0.498	13.6

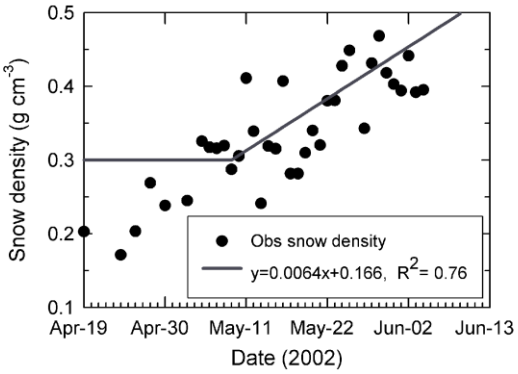

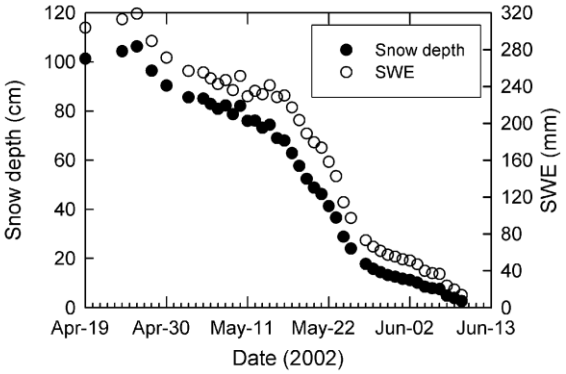

Snow survey VB 2002: Highly variable snow density values were replaced by a linear fit. A minimum snow density value of 0.185 g m^{-3} was set at the beginning of the melt season.

date	Snow depth (cm)	Obs. Snow density [g cm^3]	Corrected Snow density [g cm^3]	SWE [mm]
19-Apr-02	82.6	0.128	0.185	152.8
24-Apr-02	71.0	0.121	0.185	131.4
26-Apr-02	67.1	0.175	0.194	130.0
28-Apr-02	50.5	0.143	0.210	105.8
30-Apr-02	38.8	0.183	0.225	87.5
3-May-02	39.5	0.264	0.249	98.4
5-May-02	33.3	0.280	0.265	88.2
6-May-02	27.6	0.429	0.273	75.3
7-May-02	22.6	0.457	0.281	63.4
8-May-02	17.5	0.286	0.289	50.5
9-May-02	20.6	0.300	0.297	61.1
10-May-02	20.8	0.305	0.304	63.3
11-May-02	17.4	0.366	0.312	54.3
12-May-02	16.2	0.330	0.320	51.9
13-May-02	13.5	0.241	0.328	44.3
14-May-02	17.5	0.319	0.336	58.8
15-May-02	11.7	0.315	0.344	40.2
16-May-02	8.2	0.407	0.352	28.8
17-May-02	3.5	0.281	0.360	12.6
18-May-02	3.1	0.282	0.368	11.4

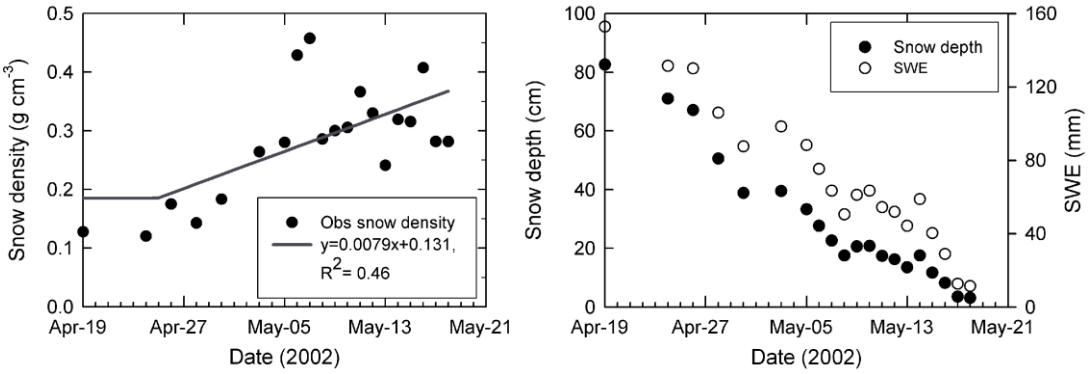

Snow survey UB 2003: SWE values for snow depth points without density measurements were obtained through a linear relationship between observed snow depth and SWE. Only lower points were included.

date	Snow depth (cm)	Observed SWE [mm]	Corrected SWE [mm]
24-Apr-03	51.3	187.8	187.8
27-Apr-03	35.0	143.5	143.5
1-May-03	25.2	123.3	123.3
6-May-03	27.1	122.8	122.8
9-May-03	21.2	108.2	108.2
11-May-03	17.5	90.7	90.7
13-May-03	20.9	95.6	95.6
15-May-03	20.7		104.7
17-May-03	20.1		101.8
19-May-03	19.8	102.3	102.3
21-May-03	15.6	88.8	88.8
22-May-03	14.3		73.5
26-May-03	9.2	46.4	46.4
29-May-03	6.3	32.4	32.4
31-May-03	4.1	22.9	22.9
2-Jun-03	3.1		18.8
4-Jun-03	2.3		14.7
5-Jun-03	1.2		9.4
7-Jun-03	0.6		6.4

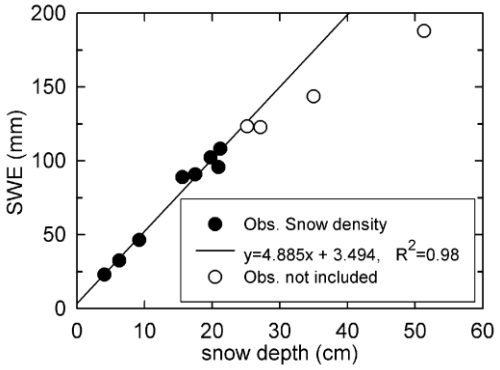

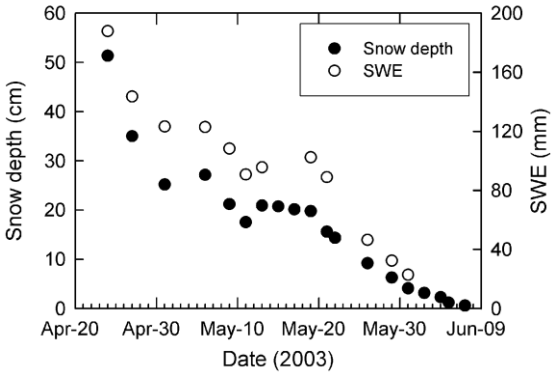

Snow survey SF slope 2003: Highly variable snow density values were replaced by a liner fit.

date	Snow depth [cm]	Obs. Snow density [g cm^3]	Corrected Snow density [g cm^3]	SWE [mm]
20-Apr-03	77.3	0.352	0.352	272.2
22-Apr-03	76.3	0.341	0.341	260.0
23-Apr-03	61.3	0.349	0.349	213.6
25-Apr-03	48.1	0.345	0.345	165.8
26-Apr-03	41.0	0.394	0.394	161.4
28-Apr-03	33.3	0.509	0.383	127.5
30-Apr-03	29.0	0.616	0.393	114.0
1-May-03	24.8	0.487	0.397	98.7
3-May-03	24.5	0.428	0.428	105.0
4-May-03	24.3	0.422	0.422	102.5
5-May-03	23.9		0.417	99.6
6-May-03	23.4		0.421	98.6
7-May-03	22.9		0.426	97.7
8-May-03	21.0		0.431	90.4
10-May-03	19.8	0.550	0.441	87.0
16-May-03	19.6		0.469	91.8
26-May-03	12.6		0.517	65.0
27-May-03	10.0	0.511	0.511	51.0
30-May-03	9.7		0.537	52.2
31-May-03	8.6	0.547	0.547	47.1
2-Jun-03	6.7		0.551	36.9

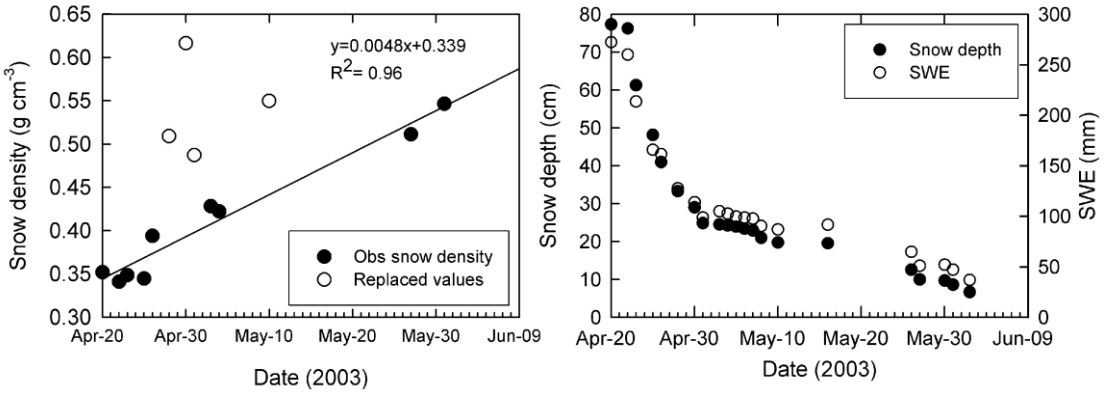

Snow survey NF slope 2003: SWE values for snow depth points without density measurements were obtained through a linear relationship between observed snow depth and SWE.

date	Snow depth (cm)	Observed SWE [mm]	Corrected SWE [mm]
21-Apr-03	72.8	218.4	218.4
25-Apr-03	64.6	203.1	203.1
26-Apr-03	55.5	202.1	202.1
30-Apr-03	48.1	144.8	144.8
1-May-03	43.2	132.3	132.3
3-May-03	44.0	158.3	158.3
4-May-03	42.3	139.2	139.2
5-May-03	41.8		138.5
6-May-03	41.5	118.4	118.4
7-May-03	40.9	0.1	135.8
8-May-03	35.3	115.2	115.2
10-May-03	27.8	132.8	132.8
13-May-03	25.7		91.8
16-May-03	27.4		96.7
17-May-03	23.8	0.3	86.4
19-May-03	23.4		85.3
22-May-03	21.0	0.3	78.4
25-May-03	13.5	0.4	56.5
26-May-03	13.4	0.5	56.2
28-May-03	9.7	42.7	45.7
29-May-03	9.7	0.3	45.5
30-May-03	7.9	34.3	34.3
31-May-03	6.7	0.4	37.0
1-Jun-03	7.1	41.2	38.2
2-Jun-03	6.1	26.1	26.1
3-Jun-03	5.9	0.3	33.4

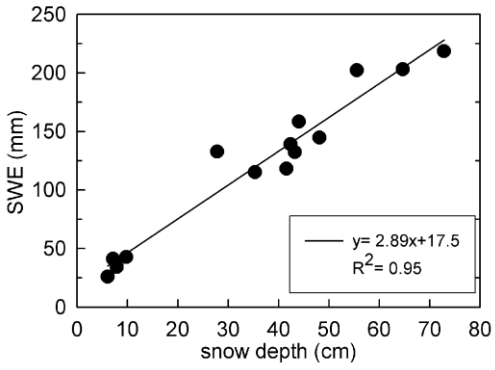

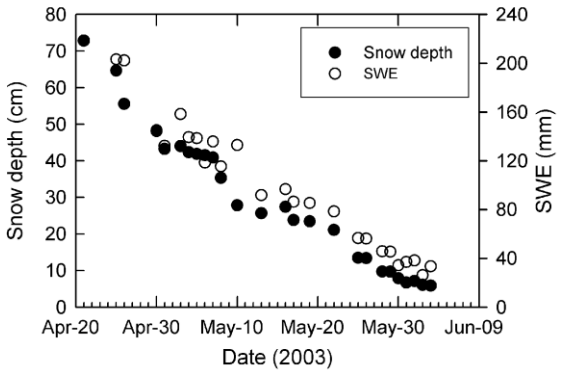

Snow survey VB 2003: SWE values for snow depth points without density measurements were obtained through a linear relationship between observed snow depth and SWE.

date	Snow depth [cm]	Observed SWE [mm]	Corrected SWE [mm]
20-Apr-03	67.3	172.0	172.0
22-Apr-03	65.0	164.9	164.9
23-Apr-03	58.1	167.4	167.4
25-Apr-03	53.2	167.4	167.4
26-Apr-03	44.8	141.6	141.6
28-Apr-03	27.3	100.3	100.3
30-Apr-03	30.2	82.2	82.2
1-May-03	22.6	69.9	69.9
3-May-03	22.9	66.3	66.3
4-May-03	22.2	65.8	65.8
5-May-03	20.8		58.9
6-May-03	19.2		54.4
7-May-03	17.7		50.1
8-May-03	13.8		39.1
10-May-03	5.2		14.7
16-May-03	2.0		5.7
17-May-03	1.8		5.1
19-May-03	1.8		5.1
25-May-03	0.1		0.3
26-May-03	0.0	0.0	0.0

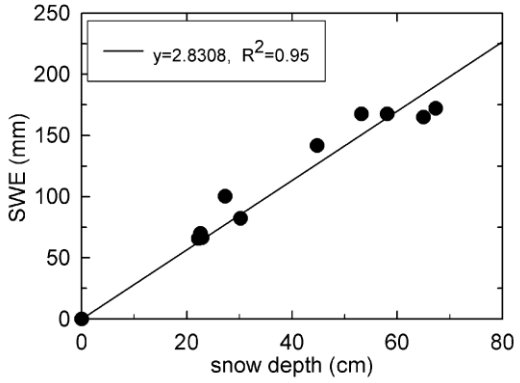

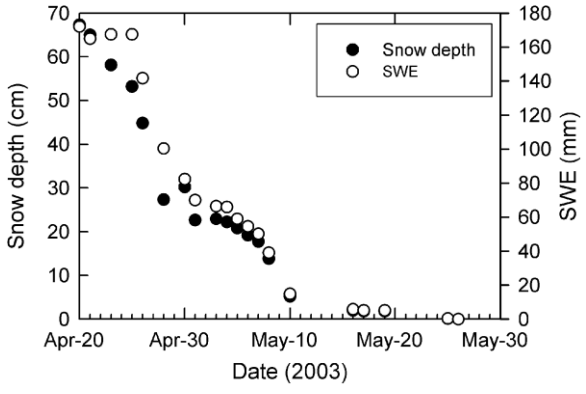

Snow survey NF slope 2004: SWE values for snow depth points without density measurements were obtained through a linear relationship between observed snow depth and SWE.

date	Snow depth [cm]	Observed SWE [mm]	Corrected SWE [mm]
27-Apr-04	105.6	214.1	214.1
1-May-04	89.9		203.7
3-May-04	78.3	179.8	179.8
6-May-04	71.9	179.7	179.7
7-May-04	65.1	174.8	174.8
10-May-04	59.6	155.4	155.4
12-May-04	55.0	157.7	157.7
14-May-04	43.6	129.1	129.1
16-May-04	34.1	110.7	110.7
18-May-04	19.8	64.4	64.4

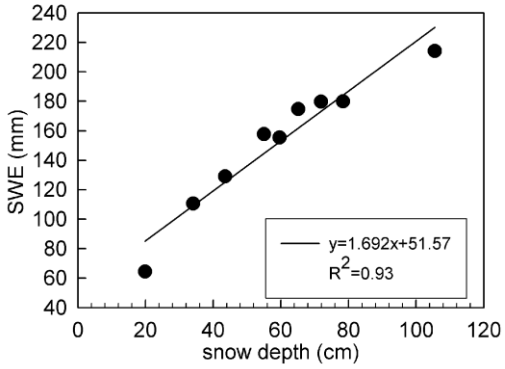

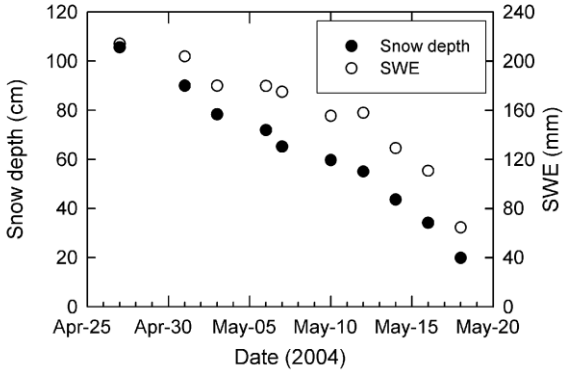

APPENDIX B: MESH HYDROLOGICAL AND VEGETATION PARAMETERS WOLF CREEK BASIN

```
Wolf Creek 2002
P. Dornes
NHRC in Saskatoon
   60.31    224.89     10.00     10.00     50.00   -1.0    1  147   13
 1.000   0.000   0.000   0.000   0.000   2.756   0.000   0.000   0.000
-1.767   0.000   0.000   0.000   0.000   0.713   0.000   0.000   0.000
 0.088   0.000   0.000   0.000   0.000   7.393   0.000   0.000   0.000
 0.321   0.000   0.000   0.000   0.000   0.150   0.000   0.000   0.000
  51.2   0.000   0.000   000.0           20.1   0.000   0.000    00.0
 1.008   0.000   0.000   0.000           1.085   0.000   0.000   0.000
63.361   0.000   0.000   0.000           2.339   0.000   0.000   0.000
 0.500   4.100   1.000  2.765
1.5E-2  2.2E-1  3.4E-2  5.9E-8       1
   -2.00     75.00     20.00
   18.00     10.00     10.00
    1.00      0.00      0.00
  -6.00     -4.50     -3.00    -12.40   -11.00      0.00
   0.040     0.040     0.040     0.040     0.060     0.110     0.000
  0.0000    0.0000     20.20     0.850  200.0000     0.000
 1.000   0.000   0.000   0.000   0.000   2.756   0.000   0.000   0.000
-1.767   0.000   0.000   0.000   0.000   0.713   0.000   0.000   0.000
 0.088   0.000   0.000   0.000   0.000   7.393   0.000   0.000   0.000
 0.321   0.000   0.000   0.000   0.000   0.150   0.000   0.000   0.000
  51.2   0.000   0.000   000.0           20.1   0.000   0.000    00.0
 1.008   0.000   0.000   0.000           1.085   0.000   0.000   0.000
63.361   0.000   0.000   0.000           2.339   0.000   0.000   0.000
 0.500   4.100   1.000  2.765
1.5E-2  2.2E-1  3.4E-2  5.9E-8       2
   -2.00     75.00     20.00
   18.00     10.00     10.00
    1.00      0.00      0.00
  -6.00     -4.50     -3.00    -12.40   -11.00      0.00
   0.040     0.040     0.040     0.040     0.060     0.110     0.000
  0.0000    0.0000     20.20     0.850  200.0000     0.000
 1.000   0.000   0.000   0.000   0.000   2.756   0.000   0.000   0.000
-1.767   0.000   0.000   0.000   0.000   0.713   0.000   0.000   0.000
 0.088   0.000   0.000   0.000   0.000   7.393   0.000   0.000   0.000
 0.321   0.000   0.000   0.000   0.000   0.150   0.000   0.000   0.000
  51.2   0.000   0.000   000.0           20.1   0.000   0.000    00.0
 1.008   0.000   0.000   0.000           1.085   0.000   0.000   0.000
63.361   0.000   0.000   0.000           2.339   0.000   0.000   0.000
 0.500   4.100   1.000  2.765
1.5E-2  2.2E-1  3.4E-2  5.9E-8       3
   -2.00     75.00     20.00
   18.00     10.00     10.00
    1.00      0.00      0.00
  -6.00     -4.50     -3.00    -12.40   -11.00      0.00
   0.040     0.040     0.040     0.040     0.060     0.110     0.000
  0.0000    0.0000     20.20     0.850  200.0000     0.000
 1.000   0.000   0.000   0.000   0.000   2.756   0.000   0.000   0.000
-1.767   0.000   0.000   0.000   0.000   0.713   0.000   0.000   0.000
 0.088   0.000   0.000   0.000   0.000   7.393   0.000   0.000   0.000
 0.321   0.000   0.000   0.000   0.000   0.150   0.000   0.000   0.000
  51.2   0.000   0.000   000.0           20.1   0.000   0.000    00.0
 1.008   0.000   0.000   0.000           1.085   0.000   0.000   0.000
63.361   0.000   0.000   0.000           2.339   0.000   0.000   0.000
 0.500   4.100   1.000  2.765
1.5E-2  2.2E-1  3.4E-2  5.9E-8       4
   -2.00     75.00     20.00
   18.00     10.00     10.00
    1.00      0.00      0.00
  -6.00     -4.50     -3.00    -12.40   -11.00      0.00
   0.040     0.040     0.040     0.040     0.060     0.110     0.000
  0.0000    0.0000     20.20     0.850  200.0000     0.000
```

```
 0.000   1.000   0.000   0.000   0.000   0.000   2.756   0.000   0.000
 0.000  -1.767   0.000   0.000   0.000   0.000   0.713   0.000   0.000
 0.000   0.088   0.000   0.000   0.000   0.000   7.393   0.000   0.000
 0.000   0.321   0.000   0.000   0.000   0.000   0.150   0.000   0.000
 0.000    51.2   0.000   000.0           0.000    20.1   0.000    00.0
 0.000   1.008   0.000   0.000           0.000   1.085   0.000   0.000
 0.000  63.361   0.000   0.000           0.000   2.339   0.000   0.000
 0.615   4.100   1.000  2.3242
4.7E-2  3.7E-1  4.0E-2  2.7E-6       5
   -2.00      -2.00      55.00
   10.00      10.00      10.00
    2.00       1.00       0.00
  -5.20      -2.500      -1.00    - 9.40   -9.00       0.00
   0.040      0.040      0.040      0.21    0.18       0.14      0.000
  0.0000     0.0000     310.00     0.850  300.0000      0.000
 0.000   1.000   0.000   0.000   0.000   0.000   2.756   0.000   0.000
 0.000  -1.767   0.000   0.000   0.000   0.000   0.713   0.000   0.000
 0.000   0.088   0.000   0.000   0.000   0.000   7.393   0.000   0.000
 0.000   0.321   0.000   0.000   0.000   0.000   0.150   0.000   0.000
 0.000    51.2   0.000   000.0           0.000    20.1   0.000    00.0
 0.000   1.008   0.000   0.000           0.000   1.085   0.000   0.000
 0.000  63.361   0.000   0.000           0.000   2.339   0.000   0.000
 0.615   4.100   1.000  2.3242
4.7E-2  3.7E-1  4.0E-2  4.1E-6       6
   -2.00      20.00      55.00
   10.00      10.00      10.00
    1.00      00.00       0.00
  -3.20      -2.500      -1.00    - 9.40   -9.00       0.00
   0.040      0.040      0.040      0.21    0.18       0.14      0.000
  0.0000     0.0000     115.00     0.850  240.0000      0.000
 0.000   1.000   0.000   0.000   0.000   0.000   2.756   0.000   0.000
 0.000  -1.767   0.000   0.000   0.000   0.000   0.713   0.000   0.000
 0.000   0.088   0.000   0.000   0.000   0.000   7.393   0.000   0.000
 0.000   0.321   0.000   0.000   0.000   0.000   0.150   0.000   0.000
 0.000    51.2   0.000   000.0           0.000    20.1   0.000    00.0
 0.000   1.008   0.000   0.000           0.000   1.085   0.000   0.000
 0.000  63.361   0.000   0.000           0.000   2.339   0.000   0.000
 0.615   4.100   1.000  2.3242
4.7E-2  3.7E-1  4.0E-2  4.1E-6       7
   -2.00      20.00      55.00
   10.00      10.00      10.00
    1.00      00.00       0.00
  -3.20      -2.500      -1.00    - 9.40   -9.00       0.00
   0.040      0.040      0.040      0.21    0.18       0.14      0.000
  0.0000     0.0000     310.00     0.850  240.0000      0.000
 0.000   1.000   0.000   0.000   0.000   0.000   2.756   0.000   0.000
 0.000  -1.767   0.000   0.000   0.000   0.000   0.713   0.000   0.000
 0.000   0.088   0.000   0.000   0.000   0.000   7.393   0.000   0.000
 0.000   0.321   0.000   0.000   0.000   0.000   0.150   0.000   0.000
 0.000    51.2   0.000   000.0           0.000    20.1   0.000    00.0
 0.000   1.008   0.000   0.000           0.000   1.085   0.000   0.000
 0.000  63.361   0.000   0.000           0.000   2.339   0.000   0.000
 0.615   4.100   1.000  2.3242
4.7E-2  3.7E-1  4.0E-2  4.1E-6       8
   -2.00      20.00      55.00
   10.00      10.00      10.00
    1.00      00.00       0.00
  -3.20      -2.500      -1.00    - 9.40   -9.00       0.00
   0.040      0.040      0.040      0.21    0.18       0.14      0.000
  0.0000     0.0000     150.00     0.850  240.0000      0.000
 0.000   0.000   0.000   1.000   0.000   0.000   0.000   0.000   1.500
 0.000   0.000   0.000  -4.610   0.000   0.000   0.000   0.000   1.500
 0.000   0.000   0.000   0.050   0.000   0.000   0.000   0.000   0.200
 0.000   0.000   0.000   0.290   0.000   0.000   0.000   0.000   0.090
 0.000   0.000   0.000   100.0           0.000    00.0   0.000    30.0
 0.000   0.000   0.000   0.500           0.000   0.000   0.000   1.000
 0.000 000.000   0.000   0.000           0.000   0.000   0.000   5.000
 0.817   4.100   1.000  3.3592
5.0E-2  9.2E-1  4.6E-2  9.9E-6       9
   20.00      20.00      20.00
   10.00      10.00      10.00
    1.00      00.00       0.00
  -5.00      -3.000      -1.00    -17.20   -17.00       0.00
   0.040      0.040      0.040      0.041    0.041      0.087     0.000
  0.0000     0.0000     310.00     0.850  220.0000      0.000
```

```
 0.000   0.000   0.000   1.000   0.000   0.000   0.000   0.000   1.500
 0.000   0.000   0.000  -4.610   0.000   0.000   0.000   0.000   1.500
 0.000   0.000   0.000   0.050   0.000   0.000   0.000   0.000   0.200
 0.000   0.000   0.000   0.290   0.000   0.000   0.000   0.000   0.090
 0.000   0.000   0.000   100.0           0.000    00.0   0.000    30.0
 0.000   0.000   0.000   0.500           0.000   0.000   0.000   1.000
 0.000 000.000   0.000  30.000           0.000   0.000   0.000   5.000
 0.817   4.100   1.000  3.3592
5.0E-2  9.2E-1  4.6E-2  9.9E-6      10
   20.00     20.00     20.00
   10.00     10.00     10.00
    1.00     00.00      0.00
  -12.00    -10.00     -7.00    -17.20   -17.00      0.00
   0.040     0.040     0.040     0.041     0.041     0.087     0.000
  0.0000    0.0000    120.00     0.850  220.0000     0.000
 0.000   0.000   0.000   1.000   0.000   0.000   0.000   0.000   1.500
 0.000   0.000   0.000  -4.610   0.000   0.000   0.000   0.000   1.500
 0.000   0.000   0.000   0.050   0.000   0.000   0.000   0.000   0.200
 0.000   0.000   0.000   0.290   0.000   0.000   0.000   0.000   0.090
 0.000   0.000   0.000   100.0           0.000    00.0   0.000    30.0
 0.000   0.000   0.000   0.500           0.000   0.000   0.000   1.000
 0.000 000.000   0.000  30.000           0.000   0.000   0.000   5.000
 0.817   4.100   1.000  3.3592
5.0E-2  9.2E-1  4.6E-2  9.9E-6      11
   20.00     20.00     20.00
   10.00     10.00     10.00
    1.00     00.00      0.00
  -12.00    -10.00     -7.00    -17.20   -17.00      0.00
   0.040     0.040     0.040     0.041     0.041     0.087     0.000
  0.0000    0.0000    310.00     0.850  220.0000     0.000
 0.000   0.000   0.000   1.000   0.000   0.000   0.000   0.000   2.970
 0.000   0.000   0.000  -3.665   0.000   0.000   0.000   0.000   2.143
 0.000   0.000   0.000   0.173   0.000   0.000   0.000   0.000   0.066
 0.000   0.000   0.000   0.450   0.000   0.000   0.000   0.000   0.090
 0.000   0.000   0.000   162.6           0.000    00.0   0.000    55.4
 0.000   0.000   0.000   1.434           0.000   0.000   0.000   0.754
 0.000 000.000   0.000  30.000           0.000   0.000   0.000   1.825
 0.817   4.100   1.000  3.3592
5.0E-2  9.2E-1  4.6E-2  9.9E-6      12
   20.00     20.00     20.00
   10.00     10.00     10.00
    1.00     00.00      0.00
  -12.00    -10.00     -7.00    -17.20   -17.00      0.00
   0.040     0.040     0.040     0.041     0.041     0.087     0.000
  0.0000    0.0000    160.00     0.850  220.0000     0.000
```